THE UNIVERSITY OF
SYDNEY

Integrative function in rat visual system

A thesis submitted for the degree of Doctor of Philosophy (Medicine) at the

University of Sydney.

August 2015

Saba Gharaei

Supervisor: Dr. Sam Solomon

Discipline of Physiology

Bosch Institute

The University of Sydney

Declaration by student

I hereby declare that this thesis contains no material that has been submitted, whether in part or full, for the award of another degree at this university or any other institution. To the best of my knowledge, this thesis contains no material previously published or written by another person except where due reference is made.

Saba Gharaei

12 August 2015

Preface

The anaesthetised recording experiments in this thesis were performed at the University of Sydney. Procedures conformed to the Australian National Health and Medical Research Council (NHMRC) and Australian Research Council (ARC) codes of practice for the use and care of animals, and institutional animal care and ethics committees at the University of Sydney. The behavioural experiments in this thesis were performed at the Australian National University. Procedures conformed to the Australian NHMRC and were approved by the animal care and ethics committee at the Australian National University.

During my PhD candidature, I was the first author of one publication and contributed to three other publications that do not involve work reported in this thesis:

Harris JA, Patterson AE & **Gharaei S** (2015) Pavlovian conditioning and cumulative reinforcement rate. Journal of Experimental Psychology: Animal Learning and Cognition. 41(2), 137-151. http://dx.doi.org/10.1037/xan0000054

Gharaei S, Tailby C, Solomon SS, Solomon SG (2013) Texture-dependent motion signals in primate area MT. Journal of Physiology. *591(Pt 22):5671-90. doi: 10.1113/jphysiol.2013.257568. Epub 2013 Sep 2*

Solomon SS, Tailby C, **Gharaei S**, Camp AJ, Bourne JA, Solomon SG (2011) Visual motion integration by neurons in the middle temporal area of a New World monkey, the marmoset. Journal of Physiology. 589(Pt 23):5741-58. PMID: 21946851

Harris JA, **Gharaei S**, Pincham HL (2011) Response rates track the history of reinforcement times. Journal of Experimental Psychology: Animal Behavior Processes. 37(3):277-86. PMID: 21500934

Some of the results described in this thesis have appeared in the following abstracts:

Gharaei S, Arabzadeh E and Solomon SG (2015). Are rats capable of selective, spatial attention? Annual Meeting of the Australian Neuroscience Society, Cairns, Australia

Gharaei S, Arabzadeh E and Solomon SG (2014). Distribution of visual and somatosensory signals in superior colliculus of rat. Kioloa neuroscience meeting, Newcastle, Australia

Gharaei S, Arabzadeh E and Solomon SG (2014). Distribution of visual and somatosensory signals in superior colliculus of rat. Annual Meeting of the Australian Neuroscience Society, Adelaide, Australia

Acknowledgements

Foremost, I would like to thank Sam – it has been a great privilege having him as my supervisor.

I am grateful to my friends Conrad and Mehdi for all the useful discussions.

Finally, I would like to thank Ehsan for his incredible support and Alborz for his lovely drawings that decorated my office desk.

Abstract

A vital function of the brain is to acquire information about the events in the environment and to respond appropriately. The brain needs to integrate the incoming information from multiple senses to improve the quality of the sensory signal. It also needs to be able to distribute the processing resources to optimise the integration across modalities based on the reliability and salience of the incoming signals. This thesis aimed to investigate two aspects of the way in which the brain integrates information from the external environment: multisensory integration and selective attention. The hooded rat was used as the experimental animal model.

In Chapter 2 of this thesis, I investigate the multisensory properties of neurons in superior colliculus (SC), a midbrain structure involved in attentive and orienting behaviours. I first establish that in rat SC, spiking activity is elevated by whisker or visual stimuli, but rarely both, when those stimuli are presented in isolation. I then show that visually responsive sites are mainly found in superficial layers whereas whisker responsive sites were in intermediate layers. Finally I show that there are robust suppressive interactions between these two modalities.

In Chapter 3, I develop a rodent behavioural paradigm that can easily be paired with electrophysiological measurements. The design is adaptable to a variety of detection and discrimination tasks. Head position is restricted in the central nose-poke without head-fixation and the eyes can be constantly monitored via video camera.

In Chapter 4, I ask whether selective spatial visual attention can be demonstrated in rats utilising the paradigms developed in Chapter 3. Selective attention is the process by which brain focuses on significant external events. Does being able to predict the likely side of the stimulus modulate the speed and accuracy of stimulus detection? To address this question, I varied the probability with which the signal was presented on left or right screen. My results suggest that rats have the capacity for spatial attention engaged by top-down mechanisms that have access to the predictability of stimulus location.

In summary, my thesis presents a paradigm to study visual behaviour, multisensory integration and selective spatial attention in rats. Over the last decade, rats have gained popularity as a viable animal model in sensory systems neuroscience because of the access to the array of genetic tools and in vivo electrophysiology and imaging techniques. As such the paradigms developed here provide a useful preparation to complement the existing well-established primate models.

Contents

List of figures

List of Tables

List of equations

List of abbreviations

2AFC	two-alternative forced choice
5-CSRTT	5-choice serial reaction time test
ADHD	attention-deficit hyperactivity disorder
AES	anterior ectosylvian sulcus
AIC	akaike information criterion
ALLS	anterolateral lateral suprasylvian area
AMLS	anterolateral medial suprasylvian area
ASD	autism spectrum disorder
CSD	current source density
DLS	dorsal lateral suprasylvian area
EEG	electroencephalogram
fMRI	functional magnetic resonance imaging
FEF	frontal eye field
FOF	frontal orienting field
LGN	lateral geniculate nucleus
IOR	inhibition of return

MT	middle temporal area
NF	narrow-field cells
PBg	parabigeminal nucleus
PLLS	posterolateral lateral suprasylvian area
PMLS	posteromedial lateral suprasylvian area
Ps	posterior suprasylvian area
PSTH	peristimulus time histograms
ROC	receiver operating characteristic
RT	reaction time
SC	superior colliculus
SOA	stimulus-onset asynchrony
S V	fifth somatosensory cortical area
S IV	fourth somatosensory cortical area
V1	primary visual cortex
V2	secondary visual cortex
V4	fourth visual area
WF	wide-field cells

1.0 General Introduction

An important function of the nervous system is to extract information from events in the environment and to convert that information to bodily movements. This ability of an organism to acquire information about the external world and to respond appropriately is critical for its survival. But the environment often contains a variety of signals about prey, predator, mate or shelter. For an efficient interaction with the environment, the brain needs to (1) integrate the incoming information from multiple senses to improve the quality of the sensory signal and speed up the detection of the biologically significant events and (2) be able to distribute the processing resources to optimise the integration across modalities and different features within a single modality based on the reliability and salience of the incoming signals. The latter ability allows the brain to "attend" to events that can offer the organism survival advantages - for example, to integrate different inputs about an external stimulus that signal the presence of a predator. This thesis aims to investigate selective attention and multisensory integration as paradigmatic examples of the way the brain integrates information from the external environment. In the following I briefly explain what I mean by selective attention and multisensory integration.

Selective attention is the process by which the brain focuses on significant external events. Selective attention is required because the brain does not have the resources to process all possible information from the outside world and must select those events that are likely to be important. Non-human primates are currently the major animal model of selective attention. To acquire a mechanistic understanding of how selective attention is deployed, it would be useful to develop rodent models where specific, reproducible

experiments can be conducted exploiting the ease of behavioural experimentation and the availability of genetic tools. In Chapter 4 of this thesis, I introduce a behavioural paradigm to investigate selective attention in rats.

Multisensory integration refers to the process by which information from different sensory modalities is combined to influence perception and behaviour. We know a great deal about how individual senses including vision, audition and somatosensation process information separately. However less is known about how the brain integrates information across sensory modalities to generate a coherent percept of the world. In Chapter 2, I investigate the multisensory properties of neurons in Superior colliculus (SC), a midbrain structure involved in attentive and orienting behaviours. SC contains neurons that exhibit both sensory and motor related properties and is therefore often served as an excellent model for understanding multisensory integration.

In this introductory chapter, I review what we know of two of these major integrative functions in sensory pathways, selective attention, and multisensory integration, to motivate the experimental work that is described in subsequent chapters. First, I will briefly describe what we know about the emergence and influence of selective attention in the brain. Much of what is known about the mechanisms of attention comes from both human and non-human-primate research. I will first provide an overview of the studies on selective attention in primates (Section 1.3 and Section 1.4) and then in rodents (Section 1.5). I will then describe what we know of multisensory and task integration in different areas of the brain (Sections 1.6-1.8). Both attention and multisensory integration are likely to involve superior colliculus, and the final sections of this chapter introduce SC as a model

system for understanding integrative function, outline the similarities and differences between species, and motivate the use of rodents in the experiments that I will describe.

1.1 Selective attention

Attention is an important function for perception: goal-driven perception and action depend on attention to direct limited resources towards a subset of relevant items (Treisman, 1960; Neisser, 1967). Attending to relevant items allows processing resources to be selectively devoted to part of the input rather than ineffectually dispersed across the entire scene (Lennie, 2003). Disorders of attention are among the most common and most devastating neurological conditions (Robbins & Arnsten, 2009). Attention-deficit hyperactivity disorder (ADHD) and autism spectrum disorder (ASD) are two of the most frequently occurring neuropsychiatric disorders. Attentional disorder is also strongly linked to confusional states, one of the most common mental disorders (Mesulam, 2010), and includes rarer syndromes such as hemi-spatial neglect. Attention is therefore an increasingly important target of scientific research.

Selective attention is the process that allows us to filter out irrelevant locations or features of our environment in favour of the relevant. Attention therefore guides our behaviour by enhancing relevant sensory information while diminishing the less relevant (reviewed in: Beck & Kastner, 2009; Desimone & Duncan, 1995). Allocation of attention can be achieved by several modes and within several domains as illustrated in Table 1.1.

It is important to explain what exogenous and endogenous modes of attention are. Exogenous modes of allocation are relatively involuntary and are driven by bottom-up

stimulation (Posner, 2012). Endogenous modes of allocation are usually voluntary through top-down mechanisms and are specifically tuned to immediate behavioural goals of the individual (Jonides & Irwin, 1981; Müller & Rabbitt, 1989; Folk *et al.*, 1992; Corbetta & Shulman, 2002; Berger *et al.*, 2005; Jack *et al.*, 2006). Framework of attentional allocation also describes four domains: space (with subdomains for covert and overt visual attention which I will explain below), time, sensory modality and task. Below, I will only focus on the domains that are relevant to the current thesis.

Table 1.1: A framework of attention. *Adapted from Posner (2012)*.

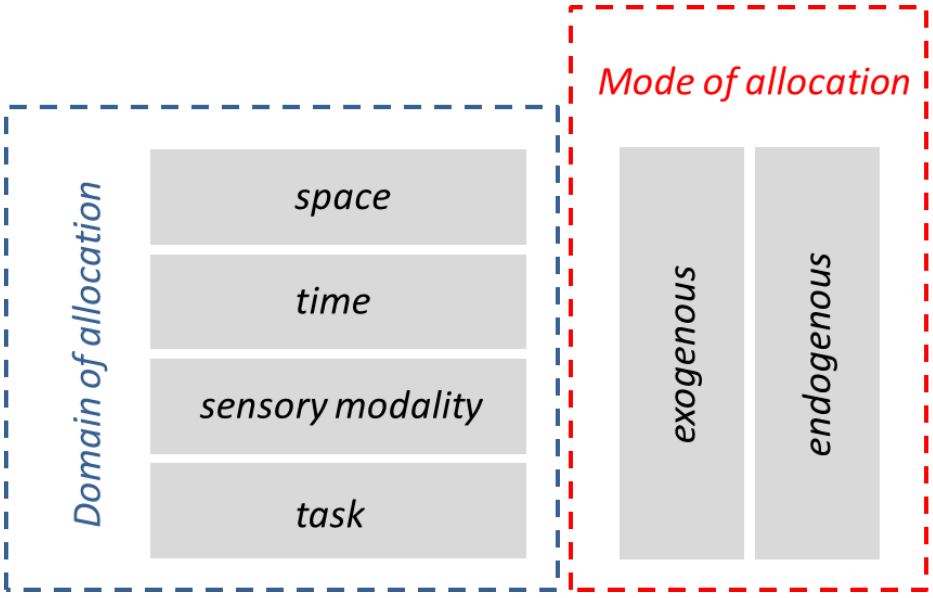

Attention can be towards a particular location in space, often called spatial attention. Attention to space has been mainly studied in the context of vision with two subdomains for covert and overt allocations. Humans or other animals often orient their eyes, head or body to improve sensory perception through overt shifts of attention.

However allocation of spatial attention can also be covert where the brain can focus on aspects of the external world without orientating movements. This covert orienting by the brain is provided by selective attention. While overt spatial attention can be directly observed, covert spatial attention must be inferred from changes in performance in well-designed situations where eye movements are monitored and maintained at fixation. Covert spatial attention is the focus of chapter 4 of my thesis, I will therefore return to paradigms attempting to measure covert spatial attention in later sections.

A main paradigm for quantifying the effects of attention to sensory modality is the temporal order judgment experiment (Spence & Parise, 2010). In this task, participants are presented with two stimuli from different sensory modalities with varying presentation times and are asked to report which stimulus was presented first. In a task with visual and tactile stimuli, it is usually reported that visual stimulus has to lead the tactile stimulus to generate a simultaneous percept (Posner, 2012). This finding is mainly attributed to the peripheral processing time differences between the two modalities. It is important to mention that temporal simultaneity judgments are rarely confusing in real life even though visual stimuli are commonly perceived as occurring at a different time to simultaneously presented tactile stimulation in laboratory environments, and visual neurons have longer response latencies (at least in rodent sensory pathways). Spence and colleagues (2001) explored the effect of exogenous and endogenous attention to different modalities and reported that exogenous attention to a modality generates reaction time (RT) benefits regardless of the target modality. Endogenous attention to a modality produces RT costs for the unattended modalities without benefits for the attended modality (Spence *et al.*, 2001).

Understanding how the brain implements selective attention is a necessary aspect of understanding brain function. However, to date, we know very little about the mechanisms through which attention is deployed. Much of what is known so far about the mechanisms of attention comes from both human and non-human-primate research. Extensive behavioural research in humans has explored the effect of selective attention on performance in both simple and complex tasks. The neural basis of attention has been mainly studied in the visual system of macaque monkeys.

In the following, I will briefly describe neuronal basis of attention as mainly revealed in primate work. I will then explain seminal behavioural experiments studying human attention and the variations on these human studies to study selective attention in non-human primates. I will then describe the limited attempts so far to study selective attention in rodents.

1.2 Neuronal impacts and sources of attention

Understanding the neuronal machinery of attention is important for various reasons such as increasing our knowledge about attention disorders. The focus of this thesis is not the neuronal impact of attention so I only briefly describe some of the main findings. Understanding the neurophysiological foundation of attention requires research on animals. Non-human primates are currently the major animal models of selective attention. The effect of attention has been most widely studied in the visual cortex and SC of monkeys.

Attention is accompanied by an increased responsivity of nerve cells whose receptive fields overlap the location that attention is directed to, as first shown by Goldberg & Wurtz, (1972). The increased stimulus-evoked firing rate has been shown in various visual

areas including V1 (Herrero *et al.*, 2008), V2 (Buffalo *et al.*, 2010), V4 (Moran & Desimone, 1985; McAdams & Maunsell, 1999) and MT (Treue & Trujillo, 1999; Busse *et al.*, 2008; Niebergall *et al.*, 2011). Attention to the area of visual space overlying the receptive fields of the recorded neurons, has also been shown to reduce noise correlations across neurons (Mitchell *et al.*, 2009; Cohen & Maunsell, 2009) and to induce synchrony across a neuronal population (Fries *et al.*, 2002, 2008; Buschman & Miller, 2007; Gregoriou *et al.*, 2009). Attentional selection of a spatial location can also narrow and shift the neuronal receptive field centres towards the focus of attention (Anton-Erxleben *et al.*, 2007; Womelsdorf *et al.*, 2008). Monkey's frontal eye field (FEF; a region located in the frontal cortex) is a key structure involved in primate oculomotor control and critical in the voluntary control of visual attention. Single unit recordings from monkey FEF has identified separate types of neurons mediating covert and overt attention (Sato & Schall, 2003; Thompson *et al.*, 2005).

Most of the studies particularly those aimed at identifying neurophysiological of controlling attention have focused mainly on exogenous, spatial attention. However, the neurophysiological effects of feature-based attention and endogenous attention are less well understood (Noudoost *et al.*, 2010). Feature-based attention (Bichot *et al.*, 2005; Mirabella *et al.*, 2007; Katzner *et al.*, 2009; Ernst *et al.*, 2010) and endogenous attention (Buschman & Miller, 2007; Katyal & Ress, 2014) can also control neuronal responses within the visual system.

Correlates of visual attention are not limited to the cortical areas (refer to the following for the neuronal mechanisms of selective attention in cortex: Desimone and Duncan, 1995; Reynolds and Chelazzi, 2004; Petersen and Posner, 2012) and have also been shown in subcortical structures such as the thalamus (Robinson & Petersen, 1992; Bender & Youakim, 2001; O'Connor *et al.*, 2002; McAlonan *et al.*, 2008) and SC (Goldberg & Wurtz,

1972; Ignashchenkova *et al.*, 2004; Shipp, 2004; Zénon & Krauzlis, 2012; Ngan *et al.*, 2015). I will return to the involvement of SC in selective attention in Section 1.14.

Human fMRI work appears to confirm the effect of attention shown in monkey experiments, but has not been able to shed light on how attention is generated. Acquiring a deeper understanding of how selective attention is controlled and deployed, requires the development of animal models other than monkeys, where specific, reproducible experiments can be conducted. Although studying attention has been traditionally performed in primates, it appears increasingly promising to follow it in rodents. I will return to the behavioural experiments in rodents in Section 1.5.

Primates and rodents share fundamental similarities in the organisation of brain such as common plan for the cortex (Krubitzer, 2007; Carandini & Churchland, 2013). In rodents, Frontal Orienting Field (FOF), a homologues area to FEF in primates (Leonard, 1969), is a candidate area for selective attention. In the literature, FOF is also known as primary whisker motor cortex or the premotor area. Similar to primate FEF, the FOF in rat projects to SC (Reep *et al.*, 1987). It also has strong reciprocal projections to prefrontal cortex (Condé *et al.*, 1995) and brainstem areas involving orienting behaviours (Stuesse & Newman, 1990). Unilateral reversible inactivation in FOF has been found to produce contralateral neglect in rats (Erlich *et al.*, 2011).

1.3 Measuring covert spatial attention in humans

The possibility that spatial attention could be covert without eye movements was shown phenomenologically by Wundt and Helmholtz in the mid -19th century. However, it was not until 100 years later that cognitive psychologists started to develop paradigms that

could measure the properties of covet spatial attention under sufficient experimental controls. Here we focus on the Posner cueing paradigm because it has been effectively applied to the explanation of these properties and to the distinction between endogenous and exogenous spatial attention.

The Posner cueing paradigm is an influential procedure in the study of human attention. In this task, a cue is used to attract participant's attention to a location in space that may contain a target (Posner, 1980). A standard paradigm resembles the following: A participant sits in front of a computer screen and is instructed to fixate at a central fixation point. A cue is then briefly presented on the screen. The cue may either be presented centrally close to the fixation point (an arbitrary symbol indicating to where the participant has to orient attention covertly), or peripherally close to the target location (Figure 1.1). The cue is then removed and after an interval (stimulus onset asynchrony) has passed a target appears. The participant must then respond quickly to the target (usually by a key press). The cue correctly indicates the target location on high proportion of trials; on the remainder of trials the target is presented at an uncued location (predictive cueing; for example, 80% valid and 20% invalid). The cueing can also be in a non-predictive manner (50% valid and 50% invalid). This paradigm allows the comparison of performance in conditions where attention is directed to a location (attended; valid cue), or away from that location (unattended; uncued or invalid cue). Performance in detecting or discriminating a target typically benefits in trials in which the target appears at the cued location than at uncued locations, measured either by accuracy or reaction time (Posner, 1980; Carrasco, 2011). The improvement in accuracy and shorter reaction times are evidence of attention. It is important to note that the cue in the deployment of attention can be exogenous (involuntary or bottom-up) or endogenous (voluntary or top-down) (Jonides & Irwin, 1981;

Müller & Rabbitt, 1989; Folk *et al.*, 1992; Corbetta & Shulman, 2002; Berger *et al.*, 2005; Jack *et al.*, 2006). An endogenous cue is according to internal, behavioural goals. One such example of an endogenous cue is when it relies on inputs from the central visual field and is presented in the same location as the fixation point in the centre of the screen. An exogenous cue, however, is presented in the periphery near where the target will be presented (Figure 1.1).

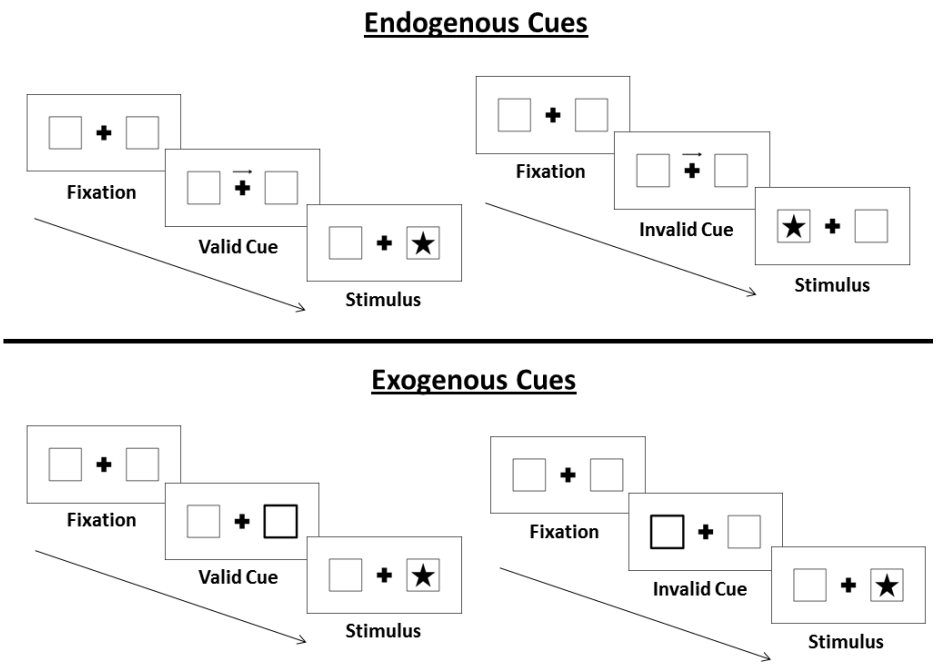

Figure 1.1: An example of a paradigm that modulates spatial attention.
On some trials the cue validly indicates the stimulus location and on the remainder of the trials, the stimulus is presented at an uncued location (invalid cue). Top panel shows a case that the cue was presented centrally close to the fixation point (endogenous). Bottom panel shows when a peripheral cue presented close to the stimulus location (exogenous).

In covert attention tasks involving humans, participants are asked not to move their eyes by looking at a fixation point. Thus, during target presentation, the same sensory information is provided in valid and invalid trials. Likewise, the same motor response is required in valid and invalid trials. Therefore, differences between RTs in invalid and valid trials reflect both the benefit achieved by the prior orienting of attention towards the expected target location and the costs of prior orienting of attention towards an incorrect target location (Posner and Cohen, 1984). The shorter RT and better performance for validly cued targets are only revealed for certain combinations of variables including Stimulus-Onset Asynchrony (SOA), cue predictability, and cue type (peripheral or central) suggesting that different processes underlie orienting of attention (Klein, 2000; Milliken *et al.*, 2003). In humans, RTs to validly cued targets are usually faster for SOAs of up to about 250 ms; this is termed facilitation. In contrast, for SOAs of greater than 300 ms, invalidly cued targets show shorter RTs, and this effect is termed inhibition of return (IOR; Klein, 2000). Therefore the pattern of RTs in the cueing paradigm seems be to biphasic, with facilitation at short SOAs followed by IOR (see Samuel & Kat, 2003, for a review).

The Posner paradigm has been widely used across different populations of participants, for example children and neuropsychological patients and has greatly contributed to the current knowledge of attentional processes (for example Posner, 1988; RAFAL et al., 1988; Brodeur and Pond, 1997; Bartolomeo and Chokron, 2002; Bayliss and Tipper, 2006; Ristic and Kingstone, 2009; Hayward and Ristic, 2013). Furthermore, this paradigm served as the basis for the development of the difference between exogenous and endogenous attentional processes (Jonides & Irwin, 1981; Berger *et al.*, 2005).

1.4 Studies of attention in non-human primates

Because it is so simple in concept and execution, variations of the Posner paradigm have been widely employed in studying neural circuits of attention of non-human primates. A standard paradigm resembles the following. A monkey sits in a chair immobilised via head post and views a screen on which two stimuli are presented. The stimuli remain present for several seconds while the monkey keeps its eyes directed to a central fixation point. The monkey's task is to detect a brief change in one of the stimuli (target), and indicate this by a rapid response (eye movement or lever press) as soon as possible after the target. The time of the target is chosen randomly on each trial. The change is more likely to occur in one of the two stimuli than the other: this bias can be cued endogenously by grouping trials into blocks, or by providing a spatial cue shortly before each trial. That the monkey was attending to one of the locations is established by greater accuracy (hit-rate) and shorter RT for changes at the cued location, compared to the uncued location. The near-threshold stimulus changes show the strongest improvements in the performance and RT (Dosher & Lu, 2000; Reynolds *et al.*, 2000; Herrmann *et al.*, 2010; Nandy *et al.*, 2013).

1.5 Studies of attention in rodents

Selective attention is frequently thought of as a high level mechanism and to exist only in primates with elaborate cerebral cortex. However, rodents have long being used as a

model of sustained attention (for example: Carli et al., 1983; Bunsey and Strupp, 1995; Bushnell, 1998; Humby et al., 1999; Bushnell and Strupp, 2009; Jaramillo and Zador, 2011; Rodgers and DeWeese, 2014; Zhang et al., 2014). A widely used method for assessing sustained attention in rodents is 5-choice serial reaction time test (5-CSRTT) which is employed to explore the whether rodents can maintain attention to five opening ports to detect a flash (Carli *et al.*, 1983; Bari *et al.*, 2008). A standard paradigm resembles the following. A rodent is placed in a chamber with five ports where a small and brief flash of light is presented in one of the ports after a short delay. The task requires the animal to indicate the location of the visual flash via a nose poke. A 3-choice alternative of the 5-CSRTT has also been developed which tests similar function (Bunsey & Strupp, 1995; Morgan *et al.*, 2001; Gendle *et al.*, 2004). These tasks are well suited to measuring sustained attention as the animal must maintain attention to all of the ports to detect the flash and respond quickly and accurately.

While the 3-choice and 5-CSRTT are suitable for measuring sustained visual attention, they are less suited to measuring covert selective attention as the animals can orient body and head towards a particular port. The Posner paradigm has not been widely deployed in work on rodent attention. Limited attempts have explored whether rats can use cues to spatial location, and can show reduced reaction time or improved accuracy at cued locations (Weese *et al.*, 1999; Bushnell & Strupp, 2009; Marote & Xavier, 2011). Marote and Xavier (2011) utilised a 3-choice nose-poke task in rats to investigate the effects of non-predictive and predictive peripheral visual cues to a target using SOAs of 200-1200 ms. They observed faster RT for some of the SOAs. Rats in both predictive and non-predictive conditions performed faster in valid trials than invalid trials for SOAs of 200 and 400 ms. The rats in the predictive conditions also showed faster RT for the SOA of 800 ms. My

experiments seek to confirm or extend their study. Wagner and colleagues (2014) used a similar attention task to investigate whether IOR could be demonstrated in rats. However, they could not robustly show IOR in all of the rats using the 3-holed wall operant chambers. A caveat of these studies is that unlike the work in primates, they have not measured or constrained the position of the head or eyes during the task. Therefore, these studies do not tell us whether improved performance seen in some of the conditions reflects changes in position of the body with respect to the stimuli, or whether it reflects the allocation of selective attention.

1.6 Multisensory integration

An organism's sensitivity to environmental events and hence its survival is increased by combining information from multiple senses. Most environmental events stimulate multiple senses and then each sense independently delivers a unique perspective on the event. A multisensory stimulus is therefore an event which produces several independent energies that are simultaneously detectable by different senses. The brain has developed the capacity to integrate information across different senses (Figure 1.2). This process of utilising different available information is called multisensory integration (Rowland *et al.*, 2007*a*; Stein *et al.*, 2009*a*, 2009*b*). A hypothesis for multisensory integration to happen is that information must first converge from different senses onto individual neurons as shown in Figure 1.2 (Meredith, 2002).

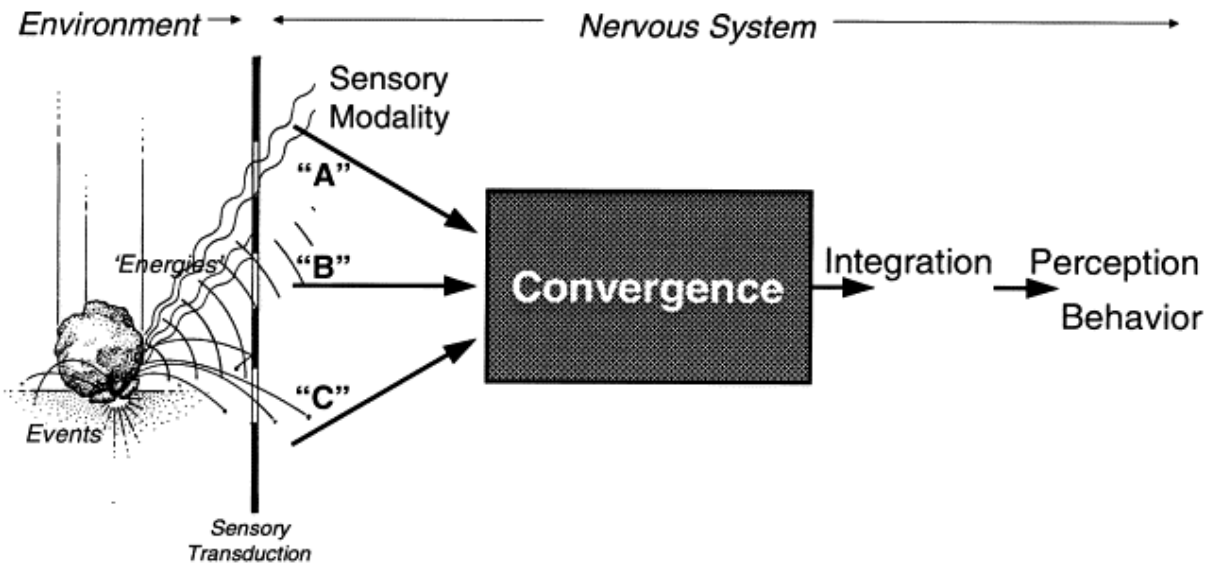

Figure 1.2: The sequence of multisensory processing.

Environmental events usually produce several physical energies. These energies are simultaneous but do not influence the physical properties of each other. In the nervous system, these energies are detected by receptors (gaps in vertical black bar) specifically tuned for a particular stimulus modality. Nevertheless, in many areas of the brain, modality-specific projections converge onto individual neurons. These individual neurons are influenced by two to more sensory modalities. Multisensory integration can occur due to this convergence of multiple inputs which changes perception and behaviour. *Adapted from Meredith (2002).*

Multisensory integration has obvious survival advantages for an organism and species and has been shown to facilitate and speed the detection, localisation, and identification of an evolutionary significant event (Wallace *et al.*, 1993; Hughes *et al.*, 1994; Frens & Van Opstal, 1995; Corneil & Munoz, 1996; Stein *et al.*, 2009*a*; Fetsch *et al.*, 2010;

Hirokawa *et al.*, 2011; Clery *et al.*, 2015). Further benefits of multisensory integration include strong effect in reduction of signal ambiguity, for example in human language perception (Grant *et al.*, 2000; Shams *et al.*, 2000; Calvert *et al.*, 2004; Massaro, 2004; Sathian, 2005).

1.7 Multisensory response

At the neuronal level, a multisensory stimulus often produces a response that differs from that expected from the response to the component unisensory stimuli. A neuron can increase its response under the multisensory condition compared to the unisensory conditions. This is referred to as enhancement (Figure 1.3A). Nevertheless, enhancement of the response during multisensory condition is insufficient to account for a number of perceptual phenomena. For instance, suppression of responses to an unattended stimulus during selective attention cannot be attributed to spatial enhancement effects (Meredith, 2002). This suppression of responses to a non-attended stimulus is observed in both cross-modal selective attention (Wallace *et al.*, 1993; Foxe *et al.*, 1998; Hillyard & Anllo-Vento, 1998) and stimuli within the same modality (Moran & Desimone, 1985; Reynolds *et al.*, 1999; Worden *et al.*, 2000). A response can therefore also be depressed under the multisensory condition (Figure 1.3B).

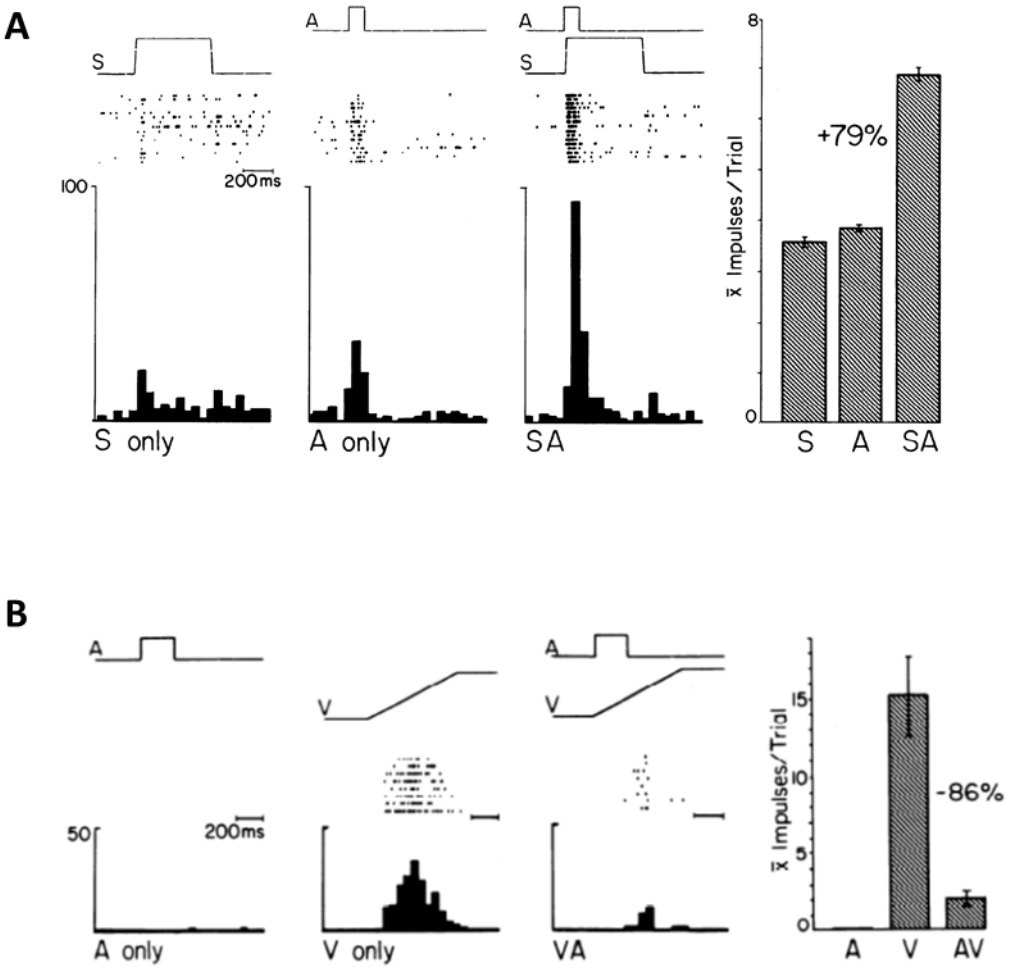

Figure 1.3: Extracellular recordings from two example neurons in cat SC.

The response of the neurons is shown for individual stimulus presentations (rasters) and peristimulus time histograms (PSTH; bin width 10 ms). **A.** Example neuron showing response enhancement during multisensory condition. This neuron responds to presentation of a somatosensory stimulus and an auditory stimulus when presented in isolation. When the two stimuli are combined, the resultant multisensory response is more than individual responses. **B.** Example neuron showing response depression during multisensory condition. The auditory stimulus failed to activate this neuron. A moving visual stimulus, however, evoked strong responses. The response of the neuron was significantly reduced during multisensory condition. *Adapted from Meredith and Stein (1986).*

The resultant form of multisensory integration (which can be either response enhancement or depression) is determined by physical parameters of the component stimuli and their spatial and temporal relationship (Meredith & Stein, 1986, 1996; Meredith *et al.*, 1987; Calvert *et al.*, 2004). Early studies in cat SC mainly utilised visual and auditory stimuli to investigate the multisensory integration (Rowland *et al.*, 2007*b*; Rowland & Stein, 2008). These studies have yielded three general rules for multisensory integration (Meredith, 2002). The first two involve space and time: a spatial rule predicting higher efficiency of interaction for spatially congruent stimuli (visual and auditory); a temporal rule postulating the same for temporal alignment. The third is the rule of inverse effectiveness. It predicts stronger modulations of neuronal activities by the multisensory stimulus when at least one of the individual stimuli (visual or auditory) is weakly effective. Thus, the magnitude of multisensory integration is inversely related to the efficacy of the stimuli being integrated. Generally, studies in cats and primates have shown that multisensory stimuli that are in close spatial and temporal register enhance the responses of multisensory neurons in SC (Wilkinson *et al.*, 1996; Frens & Van Opstal, 1998; Jiang *et al.*, 2001, 2002; Perrault *et al.*, 2003; Burnett *et al.*, 2004; Bell *et al.*, 2005; Stanford *et al.*, 2005; Stanford & Stein, 2007). However as shown before in Figure 1.3B, a multisensory stimulus can also depress neuronal responses in the SC (Meredith & Stein, 1986; Kadunce *et al.*, 1997; Mysore *et al.*, 2010; Hirokawa *et al.*, 2011). Meredith and stein (1986) investigated the visual, auditory, and somatosensory convergence in cat SC and showed that 20% of the neurons in the deep layers produced significantly fewer responses to the multisensory stimulus than elicited by uni-sensory stimuli presented in isolation. The majority of the neurons exhibiting

response depression to multisensory stimulus appeared to be influenced by stimuli from only one modality during uni-sensory presentations. Therefore the inhibitory or suppressive influence of a seemingly ineffective stimulus only becomes evident during multisensory presentation.

1.8 Different areas of the brain involved in multisensory integration

Many areas of the brain contain individual neurons that show multisensory responses. In the mammalian brain a key area responsible for multisensory integration is the Superior Colliculus (SC), a midbrain structure often served as a model for understanding multisensory processing (Wallace *et al.*, 1993; Jiang *et al.*, 2001; Perrault *et al.*, 2003; Stanford *et al.*, 2005; Rowland *et al.*, 2007*b*, 2007*a*; Rowland & Stein, 2008). The model system I have chosen for the current thesis is also the SC and I will explain SC in detail in later sections. In addition to the SC, various brain areas ranging from other midbrain structures, thalamus and cortical areas have been demonstrated to contain neurons that are capable of integrating cross-modal cues and many of these areas have connection to the SC. Studies in cats and primates have shown multisensory influences on neuronal activity within classically defined uni-sensory regions including low-order areas of sensory cortices (Wallace *et al.*, 1993; Calvert, 2001; Ghazanfar & Schroeder, 2006; Ghazanfar & Chandrasekaran, 2007; Kayser & Logothetis, 2007). This conflicts with the classical view of sensory organisation where multisensory responses are confined to highly specialised regions of the brain (Ghazanfar and Schroeder, 2006; Stein and Stanford, 2008).

Evidence has emerged of multisensory convergence in cortical pathways previously considered as being exclusively devoted to the processing of uni-sensory inputs (Schroeder & Foxe, 2005; Ghazanfar & Schroeder, 2006). The main evidence demonstrating that multisensory integration occurs early in cortical sensory processing came from studies of the auditory cortex of primates (Cahill *et al.*, 1996; Lakatos *et al.*, 2007; Kayser *et al.*, 2008, 2010; Bizley & King, 2009). Brosch and colleagues (2005) found that non-auditory stimuli (visual or somatosensory stimulation and movements) could activate and affect processing within the auditory cortex of the monkeys. Other research indicated that auditory cortical neurons responded to somatosensory stimulation (Fu *et al.*, 2003). Even eye position or direction of gaze could affect neuronal activity within the primary auditory cortex (Werner-Reiss *et al.*, 2003). The effects observed in the study by Werner-Reiss and colleagues (2003) where the modulation of auditory cortical neurons occurred as a function of eye position can be produced by some other factors that are correlated with eye position such as spatial attention. In another study, field potential multisensory responses of dynamic visual facial stimuli paired with voices were demonstrated within the primate auditory cortex (Ghazanfar *et al.*, 2005).

Although primary sensory regions show subtle responses that are influenced via stimulation of other sensory modalities, higher association regions show a higher occurrence of multisensory neurons compared to primary regions (Sugihara *et al.*, 2006; Gu *et al.*, 2008; Dahl *et al.*, 2009). These insights into multisensory involvement of higher association regions came from functional imaging studies in humans (Beauchamp *et al.*, 2004; Driver & Noesselt, 2008; Lewis & Noppeney, 2010) and microelectrode recording studies in other primates (Gu *et al.*, 2008; Dahl *et al.*, 2009).

Attention and multisensory integration are both important for integration of information in the environment. Selective attention can modify multisensory integration processes at multiple stages (Talsma & Woldorff, 2005). An individual needs to attend across different modalities to bind the inputs and detect salient events. For example an fMRI study in humans demonstrated that multisensory mechanisms can integrate both endogenous and exogenous spatial information to orient towards the most relevant spatial location (Santangelo *et al.*, 2009).

Above I have described multisensory integration and attention in primates and rodents. An area that appears to be involved in both attention and multisensory integration in both species is SC, a well-known site of sensorimotor integration. It receives inputs from multiple sensory modalities and plays an important role in moving the eyes, head and body towards or away from a biologically significant event. In the following sections I introduce SC as a model system for understanding integrative function.

1.9 Anatomy of SC

The optic tectum is a structure that forms a major part of the vertebrate midbrain. In mammals, this structure is called the Superior Colliculus (SC). It forms part of the roof of the midbrain and appears as a bump on either side of the midline beneath the posterior part of the cerebral cortex. Figure 1.4 shows the location of SC in rat brain.

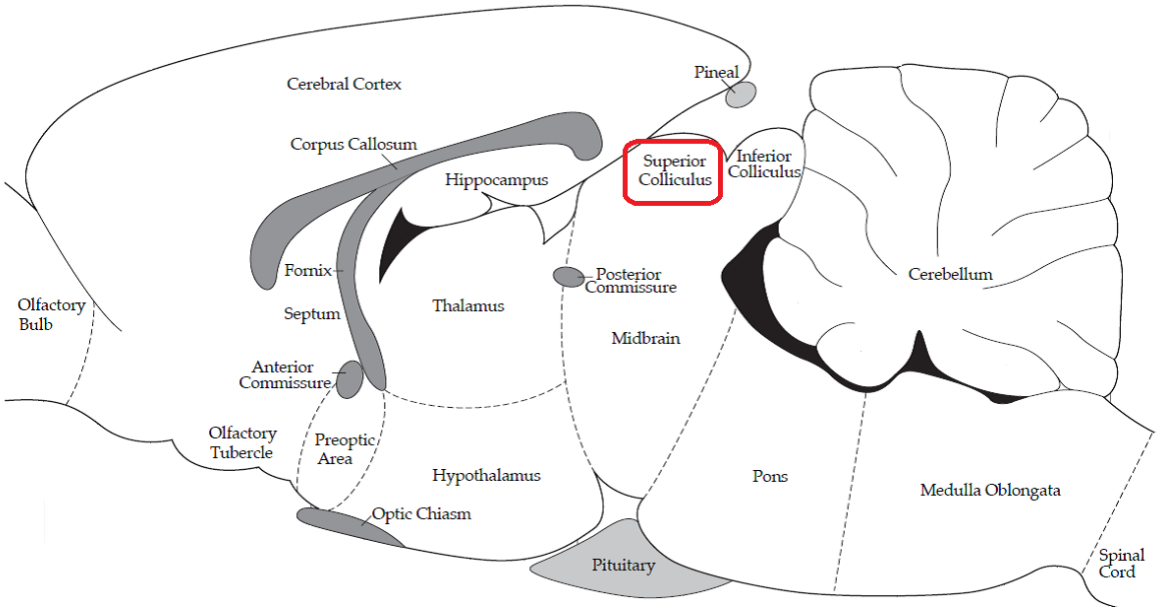

Figure 1.4: Location of SC in rat brain.

SC is ideally located in a central position of the rat brain in order to receive and process sensory inputs from differing modalities and to coordinate motor responds. *Adapted from Paxinos and Watson (1986).*

The anatomical structure and input/output architecture of the mammalian SC is conserved across species (Huber & Crosby, 1943; Harting *et al.*, 1973; Gaither & Stein, 1979; Sahibzada *et al.*, 1986; Ozen *et al.*, 2000; Sefton *et al.*, 2004; May, 2006; Isa & Hall, 2009).

The SC is articulated as having seven lamina or independently identifiable layers, as outlined in Table 1.2 (Huerta & Harting, 1984).

Table 1.2: Lamina of the SC. From the surface the layers are stratum zonale, stratum griseum superficiale, stratum opticum, stratum griseum intermediale, stratum album intermediale, stratum griseum profundum and stratum album profundum. *Table based on original information from Lund and Lund (1972) and Huerta and Harting (1984).*

	Name	Abbreviation	Popular nomenclature
Lamina 1	Stratum Zonale	SZ	Surface
Lamina 2	Stratum Griseum Superficiale	SGS	Superficial grey
Lamina 3	Stratum Opticum	SO	Optic layer
Lamina 4	Stratum Griseum Intermediale	SGI	Intermediate grey
Lamina 5	Stratum Album Intermediale	SAI	Intermediate white
Lamina 6	Stratum Griseum Profundum	SGP	Deep grey
Lamina 7	Stratum Album Profundum	SAP	Deep white

The seven layers alternate between lamina composed of fibre connections and lamina largely constituted by soma of the neurons. These lamina were initially considered as being partitioned into two separate regions on the basis of their differing functionality; the

superficial layers comprised the top three lamina while the four remaining lamina were ascribed as the deeper layers (Stein, 1984; Sparks & Hartwich-Young, 1989; Stein & Meredith, 1993). The division was roughly based on differences in uni-sensory versus multisensory functionality, cell morphology, physiology and the variations in afferent-efferent connections (Stein, 1984; Stein *et al.*, 2009*b*). It has also been established that there are connectional and physiological differences between the individual layers (Huerta & Harting, 1984). The three superficial layers are innervated by retinal axons. Neurons in these superficial layers project to intermediate and deep layers, which also receive auditory and somatosensory inputs. Lee and colleagues (1997) demonstrated that brief electrical stimulation of the superficial layers evokes a strong and prolonged excitation in premotor neurons of the intermediate layers. This led to further experimentation that found that sensory inputs from the retina and visual cortex are received by cells in the superficial layers, and then transmitted to premotor neurons in the intermediate layers. The premotor neurons, in turn, issue command signals to the midbrain and gaze centres to initiate saccade and body movements (May, 2006; Isa & Hall, 2009).

1.10 Cellular architecture of SC

SC is an elaborate multilayered structure which contains various cell types. Ramón y Cajal identified and illustrated cell types and arrangements in the rabbit SC by Golgi method (Figure 1.5A). In a recent study, Gale and Murphy (2014) distinguished different classes of neurons in the superficial layers of mouse SC on the basis of their morphology and electrophysiological characteristics (Figure 1.5B). Briefly, Narrow-field cells (NF) are often direction selective and prefer small stimuli. They project to deeper layers of the SC and to the parabigeminal nucleus (PBg) which is a brainstem nucleus that provides cholinergic

feedback to the superficial SC and is thought to be involved in attention. Apart from PBg, the brainstem parabrachial region is another source of cholinergic activity (Sooksawate & Isa, 2006). Wide-field cells (WF) respond to small moving stimuli anywhere within a large region of space and project to pulvinars. Horizontal cells are inhibitory GABAergic (Mize, 1992) and respond to large stationary or fast moving stimuli and project to PBg and to dorsal and ventral LGN. Stellate cells prefer small stimuli and project to both PBg and LGN.

The circuitry of SC is complex involving broad connectivity with various brain areas and the interaction of multiple neurotransmitters. Inhibition occurs through abundant presence of GABA receptors on the superficial grey densities (Binns, 1999; Endo & Isa, 2001). Activation of inhibitory GABAc receptors on interneurons can increase outputs of SC *via* dis-inhibition and there is evidence for cholinergic modulation of these efferent path-ways (Lee & Nguyen, 2001; Schmidt *et al.*, 2001; Sefton *et al.*, 2015).

Except the WF cell type, other superficial SC neurons project to PBg which is thought to involve in attention (Mufson *et al.*, 1986; Illing *et al.*, 1990; Mysore *et al.*, 2011). Cholinergic activity is implicated in mechanisms involving attention, and is high in both superficial layers and the intermediate grey layer of SC (Tan & Harvey, 1989). NF neurons project to deeper layers of SC and therefore provide visual inputs to the layers that are thought to be more involved in spatial attention and orienting movements (Gale & Murphy, 2014). Unlike the superficial layers where acetylcholine is distributed homogeneously, it occurs in clusters or patches in deeper layers (Graybiel, 1978; Illing & Graybiel, 1986).

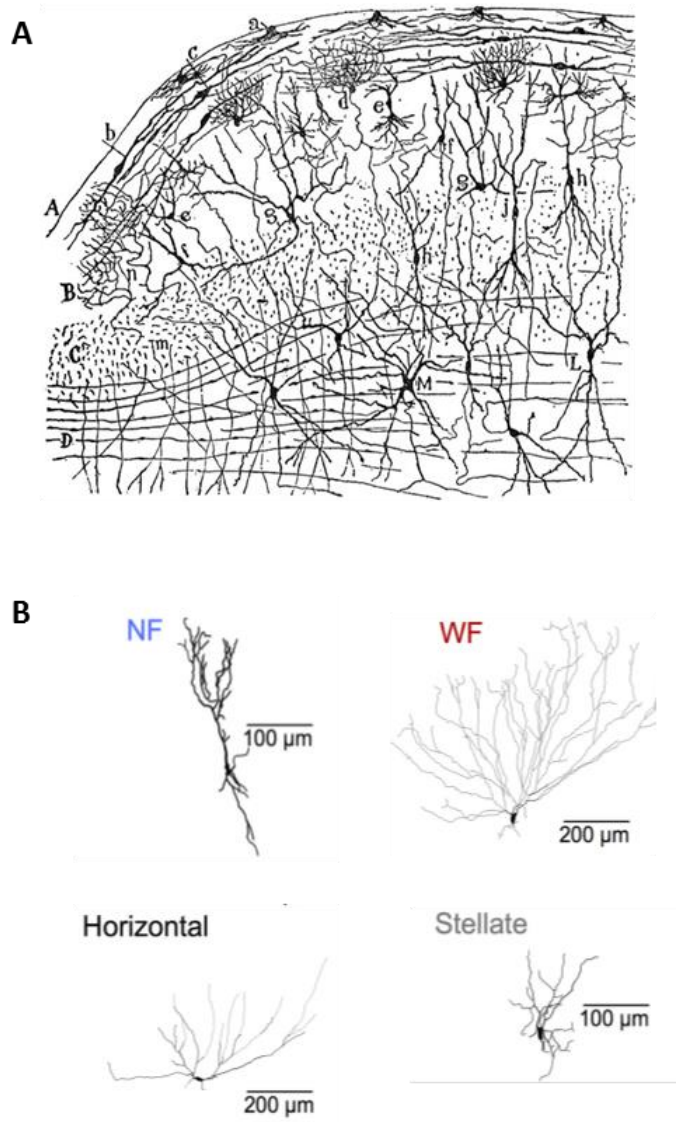

Figure 1.5: Different cells in SC

A. Ramón y Cajal's drawing of collicular cells of the rabbit. The letters indicate cell types revealed by Golgi-stained material. **B.** Identification of four superficial SC cell types on the basis of their somato-dendritic morphology visualised either by filling cells with fluorescent dye during whole cell recordings performed in vitro or by Neurobiotin electroporation during cell attached recordings performed in vivo. Narrow-field cells (NF) have thick primary dendrites that extend ventrally into the Stratum Opticum (deepest portion of the superficial SC) and dorsally to the surface of superficial SC. Wide-field cells (WF) have somas in the Stratum Opticum and extend elaborately branched thin dendrites to the dorsal surface of the superficial SC. Horizontal cells have horizontally extending long dendrites. Stellate cells have a small field of thin dendrites extending in numerous directions. *Adapted from Ramón y Cajal (1995) and Gale and Murphy (2014).*

1.11 Topographic organisation

The brain has developed well-defined topographic sensory maps. The topographic maps facilitate spatially guided behaviours by providing interactive informational representations of the space (White & Munoz, 2011). Much of the knowledge about the topographic organisation in the SC comes from research in cats. Each of the three sensory representations for visual, auditory and somatosensory is laid out in topographic maps with different maps in overlapping spatial register with one another (Stein *et al.*, 1976, 2009*b*, 2014; Stein, 1981; Middlebrooks & Knudsen, 1984; Meredith & Stein, 1990; Stein & Meredith, 1993). These topographic maps extend vertically through the layers of the SC. The neurons in a vertical column of SC represent the same general region of visual, auditory and somatosensory space. The visual and somatosensory topographical maps within the SC develop very early in mammals, and only become aligned with the auditory maps as they slowly develop over a longer postnatal period (King *et al.*, 1996, 1998). A topographic map of auditory space exists in the SC of most mammals (King & Palmer, 1985; Gaese & Johnen, 2000). Neurons within the deeper layers of the SC are tuned directionally with auditory receptive fields that vary depending on the origin point of the audition (Vachon-Presseau *et al.*, 2009).

The sensory maps, in turn, overlap with a common premotor map where movement of the eyes, head and limbs can be initiated (Wurtz & Goldberg, 1971; Sparks, 1986; Jay & Sparks, 1987*a*, 1987*b*; Groh & Sparks, 1996*a*, 1996*b*; White & Munoz, 2011). It is through this arrangement that incoming sensory information from a biologically significant event match with the outgoing motor signals. Therefore a coordinated overt response such as eye

movement is initiated regardless of which sense or combination of senses was activated (Stein *et al.*, 2009*b*, 2014).

As mentioned above, much of the knowledge about multisensory integration and the topographic organisations comes from the research in cats. Given that the focus of a chapter of this thesis is to study spatial and temporal overlap of visual and somatosensory signals in SC of rats, I will now review thoroughly a few experiments on the topographic organisation of these two maps in rodents. Dräger and Hubel (1975; 1976) showed that the topographic representation of the mouse visual field is similar to what had been found in other mammals (Feldon *et al.*, 1970; Hughes, 1971; Lane *et al.*, 1973; Stein *et al.*, 1975), with the temporal part of the contralateral visual field projecting posteriorly and the inferior visual field laterally (Figure 1.6). There exists an area of central vision with higher magnification in the mice, however the difference in magnification is small compared to those found in primates and cats (Dräger and Hubel, 1975; 1976). The magnification in this central area is anisotropic with only an increase for the vertical direction in the visual field.

As evident from Figure 1.7, representation of whiskers covers the major part of the SC somatosensory receptive fields. The projections of whiskers and the other body parts follow spatial rules given by the visual projection. The paws are visible to the mouse in the lowest part of the visual field and the ears in the temporal field of vision. The A and E rows of the whiskers are respectively associated with the highest and the lowest visual field coordinates. In any successive perpendicular electrode penetration in mouse SC, somatosensory receptive fields recorded in the deeper layers are concerned with that group of whiskers or with those parts of the body that were in alignment with the visual receptive fields recorded in the upper layers (Figure 1.7).

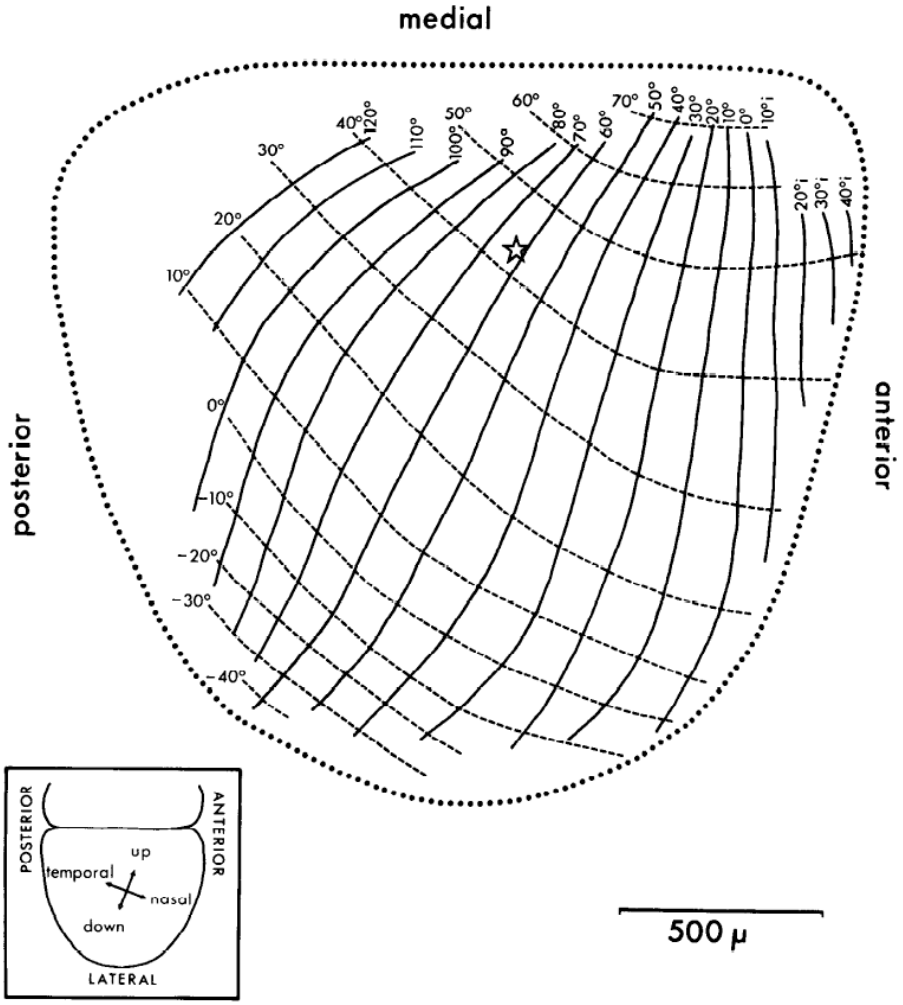

Figure 1.6: Map of visual field onto surface of SC in the mouse.

It shows the projection of the SC onto a horizontal plane with the interrupted curves representing lines of constant elevation and solid curves representing lines of constant azimuth. Star indicates the position of the disc of the contralateral eye. Inset represents the general plan of visual-field representation onto SC. *Adapted from Dräger and Hubel (1976).*

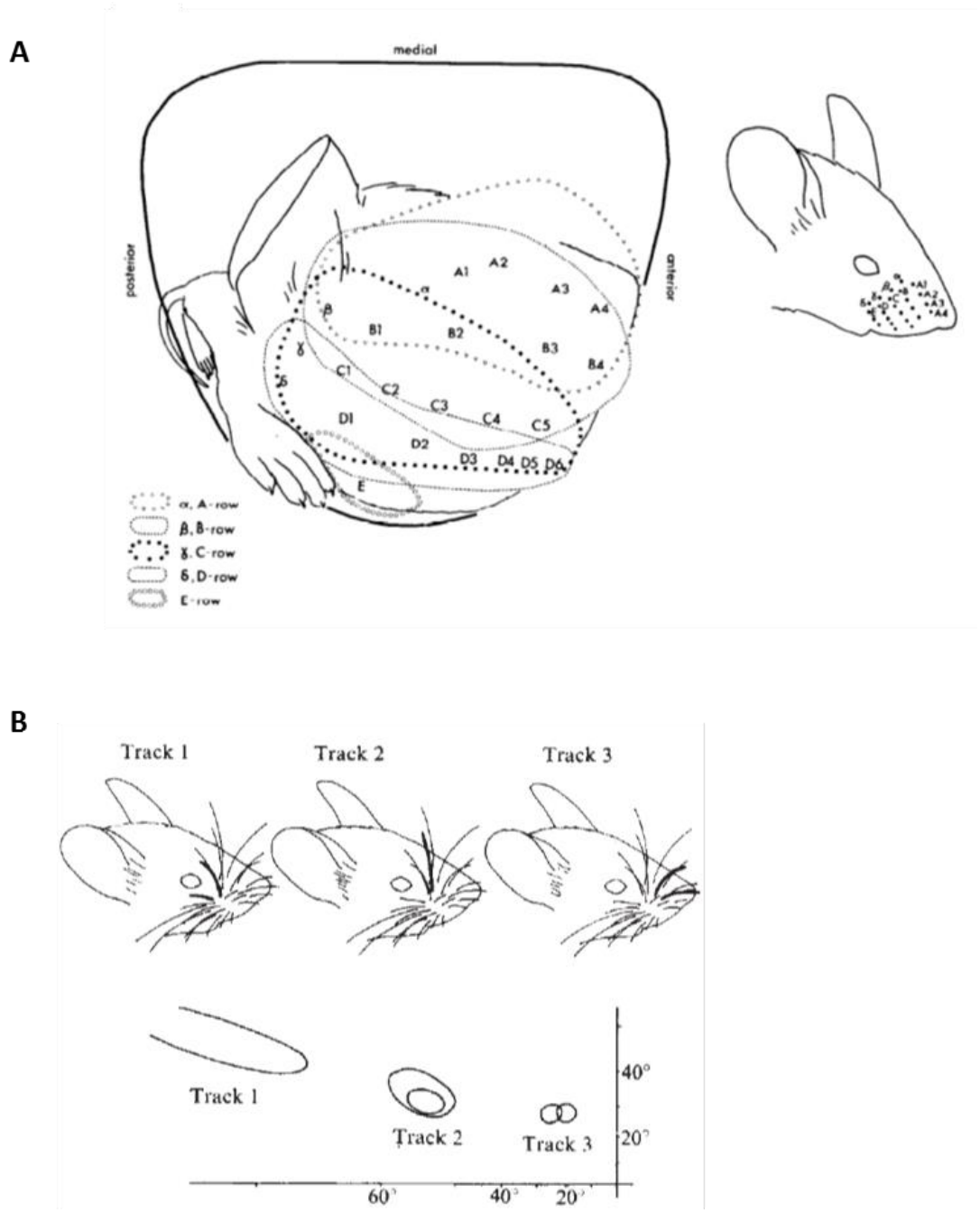

Figure 1.7: Correlation between visual and somatosensory receptive fields.

A. Map of somatosensory projection onto SC. Letters and numbers refer to different whiskers, using terminology shown on the side figure. **B.** The visual field regions and whiskers from which responses could be evoked in three successive electrode tracks perpendicular to the surface of SC. In the upper panels, whiskers from which maximum responses could be evoked are drawn as thicker lines. *Adapted from Dräger and Hubel (1975) and Dräger and Hubel (1976)*.

1.12 Many areas of the brain are connected to SC

Harting and colleagues (1992) utilised anterograde auto-radiographic method to reveal the distribution of projections from 25 cortical areas to cat SC. The remarkable finding was that all of these cortical areas project to SC (Figure 1.8). The superficial layers receive projections from 17 of the areas studied and all of the cortical areas, except areas 17 and 18, project to intermediate/deep layers. Most of these projections terminate in a non-continuous way and there are elaborate double tier modes of distribution (Kawamura *et al.*, 1982; Segal & Beckstead, 1984; Stechison *et al.*, 1985; Illing & Graybiel, 1986; McHaffie *et al.*, 1988; Hall *et al.*, 1989; Harting *et al.*, 1992). The deeper layers send extensive inputs to brain stem areas involved in the regulation of eye movement and orientation.

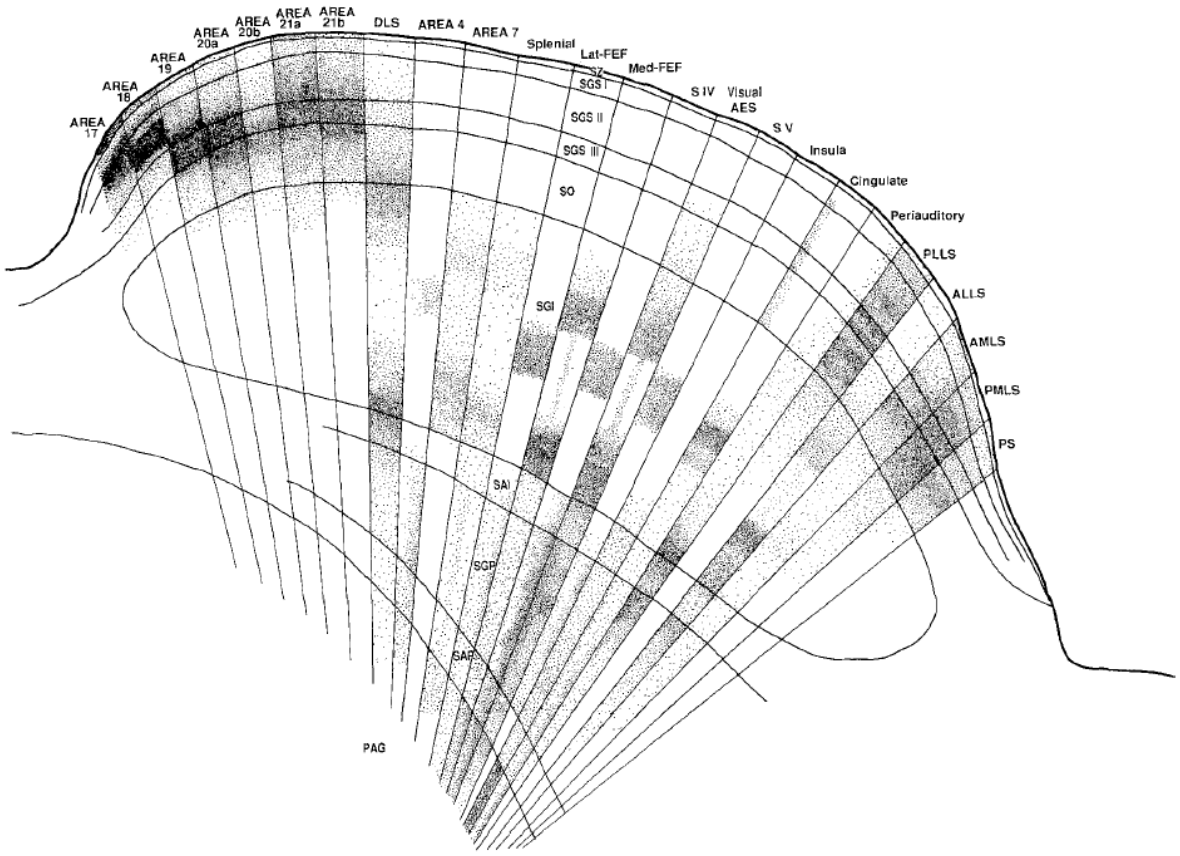

Figure 1.8: Widespread areas of cortex project upon SC.

Anterograde transport studies of twenty-five cortical areas in Cats. Ps, posterior suprasylvian area; PMLS, posteromedial lateral suprasylvian area; AMLS, anterolateral medial suprasylvian area; ALLS, anterolateral lateral suprasylvian area; PLLS, posterolateral lateral suprasylvian area; S V, fifth somatosensory cortical area; AES, anterior ectosylvian sulcus; S IV, fourth somatosensory cortical area; FEF, frontal eye field area; DLS, dorsal lateral suprasylvian area. *Adapted from Harting et al. (1992).*

In rodents, similar to other mammals, the superficial layers receive extensive inputs from the retinal axons, the visual cortex, and the PBg (Sefton *et al.*, 2004, 2015; Skaliora *et al.*, 2004; May, 2006). These superficial layers project to several other areas involved in vision and attention (Malpeli & Schiller, 1978; Mackay-Sim *et al.*, 1983; Sefton *et al.*, 2004; Skaliora *et al.*, 2004; May, 2006; Terjung, 2011). The intermediate and deeper layers receive visual, auditory, and somatosensory (mainly whisker) inputs (Vidyasagar, 1978; Sefton et al., 2004). The inputs to these deeper regions come from multiple cortical and subcortical areas. Some of these inputs come from the barrel cortex (Cohen *et al.*, 2008) as well as visual and other sensory cortices (Wang & Burkhalter, 2013). Cells in deeper layers can also be activated *via* cells in superficial layers and by the contralateral SC (Takemoto *et al.*, 1978; Yamasaki *et al.*, 1984; Isa *et al.*, 1998; Hilbig *et al.*, 2000; Terjung, 2011). This connectivity may provide a mechanism for selective attention to support spatial attention or the competition between right and left hemi-fields. There are two main sources of whisker inputs to SC, a direct input from the trigeminal complex and an indirect input from the barrel cortex (Castro-Alamancos & Keller, 2011; Bezdudnaya & Castro-Alamancos, 2011). The intermediate and deeper layers project extensively to brain stem regions associated with motor control (Sahibzada *et al.*, 1986; Dean *et al.*, 1989; Herbert *et al.*, 1997; Sefton *et al.*, 2004; Terjung, 2011). Table 1.3 outlines main inputs and outputs of SC in mammals as provided by Schiller (2011).

Table 1.3. Inputs and outputs of mammalian SC. *Adapted from Schiller (2011).*

Inputs	**Outputs**
Retina	Pulvinar
Ventral lateral geniculate nucleus	Lateral geniculate nucleus
Occipital cortex	Pretectum
Parietal cortex	Posterior nuclear group
Temporal cortex	Suprageniculate nucleus
Frontal cortex	Intralaminar thalamic nuclei
Parabigeminal nucleus	Reticular formation
Reticular formation	Pontine nuclei
Substantia nigra	Parabigeminal nucleus
Cerebellum	Inferior olive
Periaquiductal grey	Oculomotor complex
Inferior colliculus	Central gray
Spinal cord	Spinal cord

1.13 SC involvement in approach or avoidance behaviours

An unexpected prominent event can either signal the presence of a prey or a predator, therefore it is important for an organism to decide whether to approach or avoid (Sahibzada *et al.*, 1986; Dean *et al.*, 1989; Furigo *et al.*, 2010; Favaro *et al.*, 2011). Consequently, there are two kinds of behaviours both gated by SC. The orienting approach behaviours are primarily mediated by the crossed descending projections from the deeper layers (Castro-Alamancos & Keller, 2011). The ability of SC to move the head (Dean *et al.*, 1986), to guide eye movement's speed and direction (McHaffie & Stein, 1982) and to control whisker movements (Hemelt & Keller, 2008) is mainly relevant in this approach behaviour. SC is also involved in aspects of spatial navigation and spatially guided movements (Felsen & Mainen, 2008). The connection between whisker responsive cells in SC and the pre-dorsal bundle mediates approach (Dean *et al.*, 1989; Westby *et al.*, 1990; Cohen & Castro-Alamancos, 2010*a*, 2010*b*). In an odour discrimination task, Stubblefield and colleagues (2013) manipulated SC activity of mice by optogenetic techniques and found that the direction of orienting movements was affected. In rats, SC cells show an increased response associated with reward retrieval which is not caused by sensory or motor influences (Weldon *et al.*, 2007).

Avoidance or defensive responses evoked by threatening stimuli are also associated with SC (Dean *et al.*, 1989; Wei *et al.*, 2015). For example, it has been shown that potentially harmful looming stimuli initiate responses in the SC of many species including mice and humans (Westby *et al.*, 1990; Liu *et al.*, 2011; Billington *et al.*, 2011; Wei *et al.*, 2015). Microstimulation of SC can cause defensive reactions including freezing and escape

(Sahibzada *et al.*, 1986; Brandão *et al.*, 2003). Escape responses caused by fear have also been shown to involve SC (Cohen & Castro-Alamancos, 2007, 2010*a*, 2010*b*; Churchland *et al.*, 2010). Liang and colleages (2015) showed that a flash of light induces a transient arrest of locomotion which is directly dependent on SC activity. Using optogenetic manipulations they show that visual cortex directly drives this arrest locomotion via cortico-tectal projections (Liang *et al.*, 2015).

For many species such as fish, primates and birds, the prey and predators could appear from many directions. By contrast, in rodents escape and avoidance behaviours are associated with the upper visual field as predators are often detected as movements in the upper visual field (Westby *et al.*, 1990; Comoli *et al.*, 2012). However, approach behaviours are associated with the lower visual field where prey is often found. These ecological factors are therefore compatible with the idea that escape and avoidance behaviours are represented in the medial SC whereas approach behaviours are represented in the lateral SC (Comoli *et al.*, 2012). Indeed, stimulation of rat lateral SC induces approach behaviours, whereas stimulation of medial SC produces defence responses (Sahibzada *et al.*, 1986; Dean *et al.*, 1986; Comoli *et al.*, 2012). Furthermore, modulation of neuronal activity in lateral SC is observed during hunting in the rats, whereas activity of medial SC enhances in the presence of a predator (Favaro *et al.*, 2011; Comoli *et al.*, 2012).

Neurons in deep layers of SC respond to noxious stimuli (Stein & Dixon, 1979; McHaffie *et al.*, 1989; Redgrave *et al.*, 1996). SC is involved in autonomic orienting reflexes and cardiovascular changes in response to a sudden aversive stimulus such as the appearance of a predator (Dean *et al.*, 1989; Netser *et al.*, 2010). Keay and colleagues (1988)

showed that stimulation of the rat SC produces cardiovascular responses and these modulations depend on the location of the stimulation within SC.

1.14 Involvement of SC in attention

The main evidence to show the importance of SC in spatial attention and attentional shifts comes from primate research (Goldberg & Wurtz, 1972; Ignashchenkova *et al.*, 2004; Shipp, 2004; Zénon & Krauzlis, 2012; Ngan *et al.*, 2015). These attentional shifts in SC include both overt shifts through moving the body, head and the eyes and covert allocation of attention in the absence of any movements (Sparks, 1999; Gandhi & Katnani, 2011; Krauzlis *et al.*, 2013). Cells in the intermediate and deep layers of SC are likely to be involved in selecting which stimuli will guide behaviour. Neuronal responses are more for visual targets that will be selected as the end point of saccades compared with those that are ignored (Krauzlis & Dill, 2002; McPeek & Keller, 2002; Krauzlis *et al.*, 2013). For some of these cells, this modulation is related to the selected visual target rather than to the movement of upcoming saccade (McPeek & Keller, 2002; Horwitz *et al.*, 2004). Micro-stimulation of SC causes saccades to the target location of the activated area and inactivation of SC causes saccades to the distractor area (Carello & Krauzlis, 2004; Nummela & Krauzlis, 2010). SC is also essential in covert attention in the absence of any orienting movements (Ignashchenkova *et al.*, 2004). Neurons in the superficial layers of primate SC increase their responses when an attended test stimulus is within their receptive field relative to a distractor within the receptive field (Gattass & Desimone, 2014). Lovejoy and Krauzlis (2010) showed that inactivating intermediate layers of SC leads to deficits in covert

spatial attention. Interestingly, these deficits are not accompanied by corresponding attentional modulations in the visual cortex (Zénon & Krauzlis, 2012).

There is limited research in rats investigating the involvement of SC in attention. Similar to guiding saccades in primates, SC in rats has been shown to involve in guiding licking behaviours (Ngan *et al.*, 2015). Mathis and colleagues (2015) showed that structural abnormalities in SC of genetically modified mice can cause problems with response inhibition. This defect in response inhibition was specific to attentional problems and was not due motor abilities or visually driven behaviour (Mathis *et al.*, 2015).

1.15 Differences and similarities of SC between species

As is made clear throughout this chapter, the sensory and motor organisation of the SC is fundamentally similar between different mammalian species (Stein, 1981). These similarities are in spite of the differences in their phyletic levels and ecological niches. Multisensory properties of the SC have mainly been studied in cats whereas its role in attentional modulation has mainly been investigated in primates. However recent studies in rodents show similar anatomical, physiological and functional organisation of SC. Below, I point out some of the differences observed between species that may be due to different ecological stresses.

There are key differences in the general organisation and neuronal circuitry of the visual system across species (Dräger & Hubel, 1975*b*; Stein, 1981; Ngan *et al.*, 2015). Compared to rodents, the primate and cat visual system is more specialised to central and binocular vision. Unlike rodent SC, in primates and cats there are marked differences

between the representation of the central region of retina and the rest of the retina (Dräger & Hubel, 1976). In our experiments, these differences should not be a problem as we utilise large visual flashes. The primate SC gets information from the hemi-retina of both eyes which are dedicated to the contralateral visual field whereas in rodent, information mainly comes from the retina in the contralateral eye (Stein, 1981; Heesy, 2009) with a sparse ipsilateral projections (Lemke & Reber, 2005; Dhande & Huberman, 2014). Additionally, rodents have laterally placed eyes and their eye movements are usually non-conjugate to maintain an overhead continuous binocular field instead of fixating on a target (Wallace *et al.*, 2013).

There are also species differences in the modalities emphasised in the deeper layers of SC. In rodents, the somatosensory system is prominent with extensive whisker representations (Dräger & Hubel, 1976). However, in cats the auditory inputs seem to be more significant than the somatosensory (Gordon, 1973). Compared to cats, rodents use their whiskers much more for navigation and the prominent whisker representation in rodent SC could reflect its adaptation to specific environmental pressures. The somatosensory topographic map in the cat SC is mainly dedicated to the face and other body parts than whiskers (Gordon, 1973; Stein *et al.*, 1975). In cats and primates who have well-developed eye and head movements, the relationship between body parts and visual fields is not constant. Therefore, it is not expected to see a very close relationship between the SC representations of the visual and somatosensory systems (Stein, 1981). By contrast, in rodents there is an elaborate topographical register between whiskers and visual fields (Dräger & Hubel, 1976). This may be due to the facts that rodents tend to orient their whole body instead of moving the eyes and also because their whiskers cover a large part of the

visual fields. Therefore, instead of utilising auditory and visual stimuli which are mainly used for research in cats' SC, I investigate the overlap in visual and whisker representations in rat SC (Chapter 2).

Many neurons in SC of different species are orientation or direction selective meaning that they respond preferentially to lines of a certain orientation or movement axis. There are species differences in the proportion of these cells and the specific direction most often preferred. In cats nasal-temporal movements along the horizontal meridian is the frequent preferred direction (Sterling & Wickelgren, 1969; Stein & Arigbede, 1972; Palmer & Rosenquist, 1974) and they seems to be as the result of inputs from the visual cortex (Palmer & Rosenquist, 1974; Stein *et al.*, 1975). In primates, the distribution of preferred directions is random (Goldberg & Wurtz, 1972). In rats, superior and temporal movements are often preferred (Fukuda & Iwama, 1978; Girman & Lund, 2007), while in mouse inferior-superior movements are usually preferred (Dräger & Hubel, 1975*b*). In my experiments, the species difference in preferred direction is not a potential issue as I use stationary visual stimuli.

Three very recent studies investigated the orientation and direction selectivity of superficial layers of SC in mice (Feinberg & Meister, 2014; Ahmadlou & Heimel, 2015; Inayat *et al.*, 2015). Although these studies are not directly relevant to my research, they point out the potentially important role of SC in rodent vision. Feinberg and Meister (2014) used 2-photon microscopy and intrinsic imaging in awake mice and showed that neurons with similar orientation preferences form large patches of vertical columns. In a concurrent study, Ahmadlou and Heimel (2015) also confirmed the existence of these orientation columns by extracellular recordings and calcium imaging. Interestingly, the columnar

organisation in the mouse SC is different from the randomly spread ("salt and pepper") orientation preferences in V1 (Ohki *et al.*, 2005; Van Hooser *et al.*, 2005) which may suggest a more important role for the SC in rodent vision. These orientation columns in SC of mice are reminiscent of the orientation columns observed in the visual cortex of primates (Hubel & Wiesel, 1968; Blasdel & Salama, 1986).

1.16 Why I choose to study rats

Whilst rodents have a simpler visual system than primates, with lower spatial acuity and simpler cortical architecture (Chalupa & Williams, 2008), they are gaining popularity as a viable animal model in visual neuroscience because of the access to molecular and genetic tools and in vivo optical imaging techniques. These tools allow cell-type-specific neurophysiology (Sohya *et al.*, 2007; Kerlin *et al.*, 2010; Runyan *et al.*, 2010; Bock *et al.*, 2011) and exquisite control of neuronal activity (Huber *et al.*, 2008; Cardin *et al.*, 2009). Rodents are widely used as models for human diseases, and their behaviour is studied in laboratories to find new drugs for psychiatric and neurologic disorders. Furthermore, the behavioural phenotype of transgenic rodents is used as a read-out in the search for the genetic basis of brain disorders and to reveal the underlying functional role of proteins and genes. Other advantages of using rodents for behavioural experiments are that they are cheaper and generally can be trained more rapidly than monkeys. Therefore, we aimed to develop a simple behavioural paradigm to study rodents' visual behaviour.

The main differences between rodents and primates' vision to consider while developing a behavioural model are the lack of a high acuity central vision, lack of binocular overlap and low spatial acuity. The spatial acuity in hooded rats is 1.2 cycles/degree (Lashley, 1938; Wiesenfeld & Branchek, 1976; Birch & Jacobs, 1979; Dean, 1981; Fagiolini *et*

al., 1994; Seymoure & Juraska, 1997; Girman *et al.*, 1999; Sefton *et al.*, 2004). Unlike rodents, primates have central vision fovea and thus move their eyes to bring high acuity vision to the area of interest. One needs to consider the low spatial acuity and lack of central vison when studying rodent vision and make the stimuli ecologically relevant to the animal. In our experiments, these differences should not be a problem as we use large visual stimuli and the gratings have low spatial frequency.

We have chosen to develop a rodent model in rats, rather than mice, because there is a much richer history in behavioural training in rats and thus a higher likelihood of success.

1.17 Aims and objectives

The current thesis aims to investigate selective attention and multisensory integration in rats. Both attention and multisensory integration involve SC and are aspects of the way the brain integrates information from the external environment. As mentioned before in the introduction, SC is an excellent model for understanding multisensory integration. Little is known about multisensory integration and the areas involved in rodents. Rats are capable of combining information across senses and show performance benefits to cross modal stimuli. The SC of rodents has a laminar organisation that is strikingly similar to primates (Girman *et al.*, 1999; May, 2006; Isa & Hall, 2009). We have therefore aimed to study multisensory integration in the SC of rats. In chapter 2 of the current thesis, we first investigate the spatial and temporal overlap between responses of

neurons in the rat SC to visual and whisker inputs. We then characterise the nature of multisensory interaction between these two modalities.

In chapter 3, we seek to develop a rat model of visual behaviour. Our criteria for the paradigm development are to be able to achieve multiple trials in a restricted period of time with restriction of head movements and the ability to know eye positions. Adaptability of our paradigm to wide range of tasks is another factor that we have considered. In this chapter, I provide an overview of the apparatus development, basic task structure and how we utilised learning theories to help us shape the rats.

To acquire a deeper understanding of how selective attention is controlled and deployed requires the development of animal models other than monkeys, where specific, reproducible experiments can be conducted. Chapter 4 aims to develop a rodent model of selective attention. The work here will complement a general model of sustained attention in rodents (5-CSRTT) and the 3-choice task. These models are well suited to measuring sustained visual attention, but are less suited to measuring selective attention. They are also ill suited to exploring the neural mechanisms of attention, or attention's impact on the signals of nerve cells, because careful control of the sensory stimuli is required to characterise these nerve cells. Our aim is therefore to develop a behavioural model of selective visual attention in rats.

2.0 Distribution of visual and somatosensory signals in superior colliculus of rat

2.1 Introduction

Evolutionarily significant events in the environment are often simultaneously detected by more than one sense, and the brain has evolved the capacity to integrate information across the senses. Since each sense can independently convey a given event, a more accurate perceptual evaluation and decision may be made through the combination of different sensory signals (Meredith, 2002; Stein *et al.*, 2014). Combining signals from different senses facilitates detection, localisation and identification of the event, and has obvious survival advantages. Multisensory integration is therefore a process by which information from different sensory modalities is combined to influence perception and behaviour (Stein et al., 2009b).

Multisensory integration can be quantified using different models. In the current chapter, I quantify multisensory integration employing a few of these models and introduce another. One common way to quantify the effects of multisensory integration is to compare the multisensory response with the response elicited by a uni-sensory stimulus when presented in isolation (usually this is the most effective stimulus that produces the largest response (Meredith & Stein, 1986; Wallace *et al.*, 1993; Rowland & Stein, 2008; Stein *et al.*,

2009*a*; Ghose *et al.*, 2014). An alternative approach is the summation model, where the uni-sensory responses are summed to give a prediction of the expected multisensory response (Populin & Yin, 2002). In this model, multisensory response can be sub-additive, additive or super-additive. Although comparison with summed uni-sensory responses is useful when examining the underlying computation engaged during multisensory integration, it is problematic as a criterion for identifying multisensory integration because it faces substantial empirical and theoretical challenges (Stein *et al.*, 2009*a*). These models are basic and descriptive but limited in capturing multisensory integration and there is room for development as multisensory integration is thought to be nonlinear. In this chapter, I introduce a broader model to capture integration over a range of stimulus intensities.

Understanding the neuronal machinery of multisensory integration is important and many regions of the brain contain individual neurons that show multisensory responses. A number of brain areas such as parietal cortex, secondary somatosensory cortex, insula, caudate nucleus and globus pallidus utilise multisensory integration to facilitate and speed the reaction to a stimulus of interest (Hughes *et al.*, 1994; Chudler *et al.*, 1995; Frens & Van Opstal, 1995; Corneil & Munoz, 1996; Brett-Green *et al.*, 2004; Nagy *et al.*, 2006; Lemus *et al.*, 2010; Hirokawa *et al.*, 2011; Lippert *et al.*, 2013). An excellent example is the superior colliculus (SC), a midbrain structure which has often served as a model for understanding multisensory integration as it receives inputs from multiple sensory modalities (Wallace *et al.*, 1993; Jiang *et al.*, 2001; Perrault *et al.*, 2003; Sefton *et al.*, 2004; Skaliora *et al.*, 2004; Stanford *et al.*, 2005; May, 2006; Rowland *et al.*, 2007*b*, 2007*a*; Rowland & Stein, 2008). The multimodal integration shown in SC is also consistent with a SC's well-known role in

orienting the animal towards appetitive stimuli such as prey and away from threatening stimuli such as predator.

The anatomical structure and input/output architecture of the mammalian SC is substantially conserved across species, presumably reflecting the common need to transform sensory signals into appropriate orientation responses (Sahibzada *et al.*, 1986; Sefton *et al.*, 2004). The SC is a laminated structure traditionally divided into superficial layers and intermediate/deep layers with the complexity of sensory integration increasing with depth (May, 2006; Girman & Lund, 2007). Superficial lamina in the SC are primarily oriented to the reception and organisation of afferent sensory inputs from the retina and the visual cortex (Huerta & Harting, 1984). Topographically, a retinal visual projection is mapped onto the surface of the SC with descending columns into the superficial layers (Lund & Lund, 1972). Projections from the superficial layers then descend into the intermediate and deeper layers where sensory inputs from different modalities are combined (Edwards *et al.*, 1979). Each of the three sensory representations for visual, auditory and somatosensory in SC is laid out in topographic maps with different maps in overlapping spatial register with one another (Stein *et al.*, 1976, 2009*b*, 2014; Stein & Gallagher, 1981; Middlebrooks & Knudsen, 1984; Meredith & Stein, 1990; Stein & Meredith, 1993). The topographical sensory maps are also synchronised with a premotor map, which allows the matching of inbound afferent sensory information originating from an external environmental stimulus to be coordinated with an outbound efferent motor signal where movement of the eyes, head and body can be initiated (Guitton & Munoz, 1991; Groh & Sparks, 1996*a*; Stein *et al.*, 2009*b*). It is through this arrangement that a coordinated

response is initiated regardless of which sense or combination of senses was activated (Stein *et al.*, 2009*b*, 2014).

Multisensory integration in SC has mostly been investigated in cats, and to a lesser extent in primates. Early studies in cat SC have shown that when multisensory stimuli (visual and auditory) are in close spatial and temporal register, they enhance the responses of multisensory neurons in SC (Wallace *et al.*, 1993; Wilkinson *et al.*, 1996; Frens & Van Opstal, 1998; Jiang *et al.*, 2001, 2002; Perrault *et al.*, 2003; Burnett *et al.*, 2004; Bell *et al.*, 2005; Stanford *et al.*, 2005; Rowland *et al.*, 2007*b*, 2007*a*; Stanford & Stein, 2007; Rowland & Stein, 2008; Hirokawa *et al.*, 2011). However a multisensory stimulus can also depress neuronal responses in the SC (Meredith & Stein, 1986; Kadunce *et al.*, 1997; Mysore *et al.*, 2010; Hirokawa *et al.*, 2011). Meredith and Stein (1986) investigated the visual, auditory, and somatosensory convergence in cat SC and showed that 45% of the neurons in the deep layers showed more response to a multisensory stimulus than a uni-sensory stimulus presented in isolation while 20% showed response depression. The majority of the neurons exhibiting response depression to multisensory stimulus appeared to be influenced by stimuli from only one modality in uni-sensory presentations. Therefore the inhibitory influence of a seemingly ineffective stimulus may only become evident during multisensory presentation.

Much less is known about multisensory integration in rodents. Rats are capable of combining information across senses and show performance benefits to cross modal stimuli (Tees, 1999; Pinto-Hamuy *et al.*, 2004; Winters & Reid, 2010; Gleiss & Kayser, 2012; Raposo *et al.*, 2012; Lippert *et al.*, 2013; Sheppard *et al.*, 2013). Given the current advances in genetic techniques and behavioural neuroscience, rodents provide a good model system for

studying multisensory integration. In rodents, similar to other mammals, the superficial layers of SC process visual information. They receive extensive inputs from the retinal axons, the visual cortex, and the parabigeminal nucleus (Sefton *et al.*, 2004; Skaliora *et al.*, 2004; May, 2006). These superficial layers project to several other areas involved in vision (Malpeli & Schiller, 1978; Mackay-Sim *et al.*, 1983; Sefton *et al.*, 2004; Skaliora *et al.*, 2004; May, 2006; Terjung, 2011). The intermediate and deeper layers receive visual, auditory, and somatosensory (whisker) inputs (Vidyasagar, 1978; Sefton *et al.*, 2004). The inputs to these deeper regions come from multiple cortical and subcortical areas. Cells in deeper layers can also be activated *via* cells in superficial layers and by the contralateral SC (Takemoto *et al.*, 1978; Yamasaki *et al.*, 1984; Isa *et al.*, 1998; Hilbig *et al.*, 2000; Terjung, 2011). The intermediate and deeper layers project extensively to brain stem regions associated with motor control (Sahibzada *et al.*, 1986; Dean *et al.*, 1989; Herbert *et al.*, 1997; Sefton *et al.*, 2004; Terjung, 2011).

In rodents, the whiskers cross in front of a large part of the visual fields. Of particular interest to the current study is the spatial and temporal overlap between responses of neurons in the rodent SC to visual and whisker inputs. Dräger and Hubel (1975; 1976) investigated the relationship between the topographic representations of these two sensory systems in rodent SC. They showed that the topographic representation of the mouse visual field is similar to what had been found in other mammals, with the temporal part of the contralateral visual field projecting posteriorly and the inferior visual field laterally. A major part of somatosensory representation is dedicated to whiskers. The most striking feature of the somatosensory projection was its topographic organisation relative to the visual field. In any electrode penetration, somatosensory receptive fields recorded in the deeper SC were

concerned with that group of whiskers or with those parts of the body that were in alignment with the position of the visual receptive fields recorded in the upper layers. Therefore, the somatosensory organisation, represented in deeper layers, appeared topographically arranged so as to be in spatial registration with the visual input. However, a quantitative evaluation of the distribution of visual and whisker inputs in rodent SC has not been done and that is what we are aiming to establish in the current study.

In this chapter, I first investigate the spatial and temporal overlap between responses of neurons in the rat SC to visual and somatosensory (whisker) inputs. I then use a generalised model framework to characterise the interaction between the two modalities. Neurons in the intermediate layers of SC strongly respond to simultaneous multi-whisker vibrations (Hemelt & Keller, 2007; Cohen *et al.*, 2008; Bezdudnaya & Castro-Alamancos, 2014), and in order to maximise the chance for interactions between the two modalities, I used full-field visual flashes and multi-whisker vibrations (Wallace *et al.*, 2004; Lippert *et al.*, 2013). To explore the laminar organisation of functional responses in SC, I use multichannel linear probes that allowed rapid characterisation of visual and whisker response properties within individual animals.

2.2 Methods

2.2.1 Ethical approval

Adult male hooded rats (Long Evans, n = 11, weighing between 243 and 447 g) were obtained from Monash Animal Research Platform and University of Adelaide. Procedures were approved by institutional (University of Sydney) Animal Ethics Committee, and

conform to the Society for Neuroscience and NHMRC policies on the use of animals in neuroscience research.

2.2.2 Experimental preparation

Each animal was initially sedated with an intramuscular (I.M.) injection of a combination of ketamine (80 mg/kg) and xylazil (6 mg/kg). I then gave preoperative intramuscular injections of dexamethasone (0.3 mg/kg; Maine Pharmaceuticals, VIC, AUS) to reduce inflammation. The trachea was then exposed and an endotracheal tube was inserted to control the breathing of the animal artificially and the head was placed in a stereotaxic frame.

Post-surgical anaesthesia was maintained by isoflurane (0.5–1% in a mixture of 1:1 nitrous oxide and oxygen) for the duration of the experiment. The electrocardiogram (ECG) and SpO2 were monitored continuously. The animal was artificially ventilated, with a 60:40 mix of N_2O and Carbogen, so as to keep end-tidal CO_2 near 33 mmHg. ECG signals were monitored to ensure adequate depth of anaesthesia. Dominance of low frequencies (1–5 Hz) in the EEG recording, and absence of EEG changes under noxious stimulus (paw-pinch) were taken as the chief sign of an adequate level of anaesthesia. Rectal temperature was kept near 37°C with the use of a heating blanket.

At the end of the experiment the animal was euthanased with intravenous 500 mg/kg sodium pentobarbitone (Lethobarb; Verbac Australia, NSW, AUS) and was perfused transcardially with 0.9% sodium chloride and then 4% paraformaldehyde in 0.1 m phosphate

buffer. The brain was then removed and post-fixed for 24 h. The tissue was then transferred to a 30% sucrose solution in 0.1 m phosphate buffer.

2.2.3 Recordings

A craniotomy of ca. 3 mm was made over SC within the following coordinates: 6.8 mm from Bregma, 1.5mm lateral from midline. These coordinates routinely yielded visual and whisker responsive cells. In 7 animals, extracellular recordings were obtained using high-impedance single electrodes (3-5 MOhm, Thomas Recordings). The analogue signals from the electrodes were amplified, band-pass filtered (0.3–10 kHz) and sampled at 48 kHz by the same computer that generated stimuli. Multiple neurons recorded simultaneously were isolated using real time principal components analysis. Off-line analysis was used to confirm and refine the identification of spike waveforms. The timing of waveforms was recorded with an accuracy of 0.1 ms.

In 4 other animals, a 2 × 16 dual-shank linear silicon probe (Neuronexus; A2x16-10mm-50-500-177-A32), with an inter-contact distance of 50 µm and inter-shank distance of 500 µm, was inserted perpendicular to the cortical surface (Figure 2.1A). I recorded multi-unit activity from a total of 672 electrode contacts at 21 recording sites (21 penetrations, at 2x16 depths per penetrations). Signals from each contact point were amplified, bandpass-filtered (0.3–5 kHz), and digitized at a rate of 24 kHz by an RZ2 real-time processor (Tucker-Davis Technologies, FL, USA). The function *findpeaks* in the Matlab environment (MathWorks, Natick, MA, USA) was used to identify candidate waveforms with peak amplitude that exceeded 4 standard deviations (SDs) of the raw signal on the relevant channel. All the analyses were performed using Matlab.

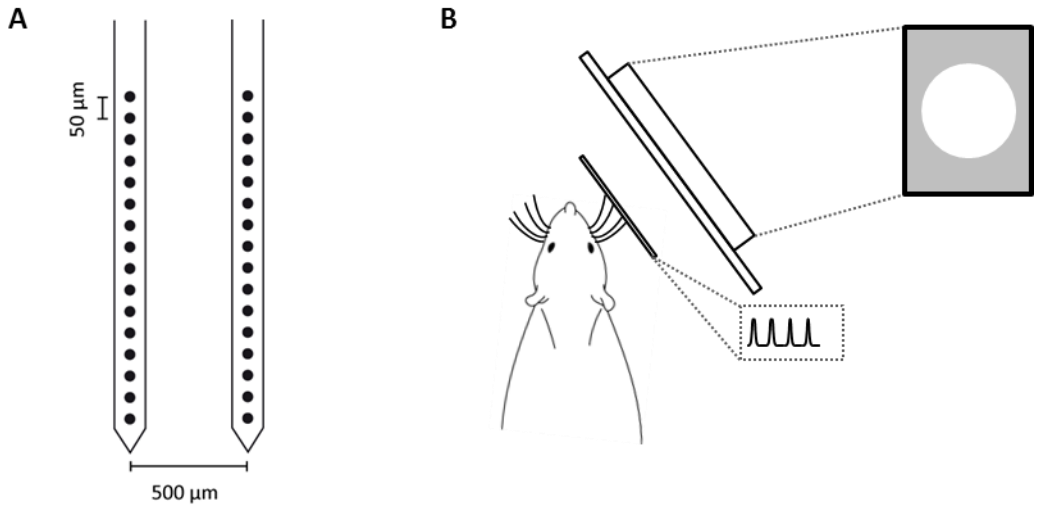

C

Figure 2.1: A. Schematic representation of the dual-shank electrode array. **B.** Schematic representation of the experimental set-up **C.** A picture of the experiment set-up.

2.2.4 Sensory Stimulation

Measurements were carried out in a dim room. Visual stimuli were generated by a G5 Power Macintosh computer using custom software (EXPO; P. Lennie, Brain & Cognitive Sciences, University of Rochester, USA); they were drawn with eight-bit resolution using commands to OpenGL. Visual stimuli were displayed on a calibrated LCD monitor (viewSonic703b; refresh rate 85 Hz, mean luminance ~ 45 cd/m2) viewed directly at a distance of 30 cm in a dimly lit room, and centred on the grand mean of multiunit activity from recording electrodes. The visual stimulus was a circle with an increment or decrement in light from the mean luminance background. Somatosensory stimuli were generated through a sound card of the same G5 Power Macintosh computer using custom software EXPO. Whisker vibrations were provided by a vibrating metal mesh, attached to a mini-shaker (Brüel & Kjær; vibration exciter 4810 and amplifier 2718). The mesh, placed at a distance of 0.5 cm from the base, contacted most whiskers of the contralateral whisker pad and moved along the vertical axis with position modulated by a sine wave with a frequency of 10 Hz. As schematically represented in Figure 2.1B, I used full-field visual flashes and multi-whisker vibrations, in order to maximise the chance for interactions between the two modalities (Wallace *et al.*, 2004; Lippert *et al.*, 2013).

For each neuron, I first obtained response to full contrast visual or multi-whisker stimuli, at maximum intensity (visual contrast = 1; whisker vibration amplitude = 2.43 mm) as described below. In each case the set of stimuli were presented in a pseudo-random sequence for 0.5 s, with inter-stimulus interval of 0.5 s. The stimulus set always included presentation of a blank screen with no whisker vibrations. Responses were obtained for a median 100 repetitions of each stimulus (mean 93, SD 17.9, range 34–100).

In another stimulus set, the 25 combinations of 5 visual contrast levels (0, 0.12, 0.25, 0.5, 1.0) and 5 somatosensory vibration amplitudes (mm) (0, 0.297, 0. 595, 1.351, 2.432) were presented in pseudorandom order. The inter-stimulus interval was 0.3 s. Responses were obtained for 50 repetitions of each stimulus. We presented the visual stimulus 0.08 s before the whisker stimulus. The duration of the visual stimulus was 0.2 s and the duration of whisker stimulus was 0.12 s (both stimuli turned off together). This interval was chosen based on our previous data collection and prior data suggesting that the stimulus onset asynchrony optimises the opportunity for multisensory interactions (Meredith *et al.*, 1987; Stein & Meredith, 1993; Ghose *et al.*, 2012, 2014).

2.2.5 Analysis

Peristimulus time histograms (PSTH, binwidth 10 ms) were generated for each stimulus. Mean spike count was calculated for the duration of the stimulus and for most analysis the baseline activity over the same duration was subtracted from the mean spike count. Response latency was defined as the occurrence of two consecutive post-stimulus bins displaying significant responses (t-test; $p< 0.05$).

2.2.6 Classification of neuronal responses

To characterise neuronal responses to visual and whisker stimuli, we used a nonparametric method based on the signal detection theory: a receiver operating characteristics (ROC) analysis (Green & Swets, 1966). The ROC quantifies stimulus detection based on single trial observations by taking into account the trial-by-trial variability in

neuronal response. The ROC provides a criterion-free method for deciding whether neurons are responsive to sensory stimulation. Formally, the ROC estimates whether an ideal observer could classify whether a given spike density was recorded under one of two conditions. For any stimulus type, the spike counts pre and post stimulus were compared (for a time window of 500ms). The overlap between the two spike count distributions was quantified by applying multiple criterion levels, ranging from the minimum to the maximum observed spike count. Each criterion yielded a hit (stimulus present condition) and false-alarm (stimulus absent condition) rate. Plotting hits and false-alarm rates against each other for every criterion led to an ROC curve. The area under the ROC curve was then calculated by summing of the trapezoids between two consecutive criteria (connected by straight lines).

The area under ROC necessarily falls within the range of 0 to 1, where 0.5 reflects no difference between the distributions (and thus no sensory response). An area of 1 indicates no overlap between the two distributions. Statistical significance of this area was determined as follows: the two spike count distributions were rearranged 1000 times (that is, the trial labels of the two distributions were shuffled 1000 times). For each iteration the area under ROC for the pair of shuffled distributions was calculated and subtracted from the observed area under ROC. The fraction of shuffled area under ROC greater than the observed area under ROC was calculated. This fraction value gave the significance (the neurons with this fraction less than 0.05 are the ones that responded significantly to the stimulus).

2.2.7 Quantifying multisensory integration

Following prior work on multisensory integration (Meredith & Stein, 1986; Wallace *et al.*, 1993; Perrault *et al.*, 2005; Ghose *et al.*, 2014), we characterised multisensory interactions using the "interactive index" (ii):

$$ii = \frac{CM - SM_{max}}{SM_{max}} \times 100$$

Equation 2.1

where *CM* is the mean response evoked by the multisensory stimulus (visual plus whisker), and SM_{max} is the mean response evoked by the preferred single modality stimulus (visual or whisker). The interaction index characterises how the multisensory response differs from the largest evoked uni-sensory response. A positive *ii* value indicates increased response in the multisensory condition, whereas a negative *ii* indicates a reduction of response in the multisensory condition. Statistical comparisons between these conditions were performed using a nonparametric Wilcoxon rank sum test, as the data was not normally distributed, according to the Kolmogorov-Smirnov normality test.

2.2.8 A simple model of multisensory integration

The intensity response function of sensory neurons can often be characterised by a sigmoidal function. Parameters of the sigmoidal function, such as baseline, inflection point, response range and saturation quantify key aspects of the neuron's response profile. These features are also quantifiable by classes of normalisation models (e.g. Carandini & Heeger, 2012) that form the computational framework for sensory integration. Normalisation at the stage of multisensory integration provides a simple description of how neurons weigh inputs from each modality, across a range of stimulus strengths. For example, the normalisation

model makes explicit predictions regarding cross-modal suppression. Ohshiro and colleagues (2011) proposed that divisive normalisation which acts at the stage of multisensory integration accounts for key features of integration such as the principle of inverse effectiveness and the spatial principle. To characterise neuronal responses to a range of stimulation amplitudes across two modalities, we used the following normalisation equation, based on Naka-Rushton function (Naka & Rushton, 1966):

$$R(V,S) = R_{max}\frac{(w_1V + (1-w_1)S)^n}{(w_2V + (1-w_2)S)^n + {M_{50}}^n} + \mathrm{b}$$

Equation 2.2

where *V* is the strength of the visual input and *S* is the strength of the somatosensory input each in the range 0 to 1; The numerator is weighted linear sum of these inputs, with the parameter w_1 controlling the relative excitatory drive assigned to each modality. The denominator contains two terms: one is again a weighted sum of visual and whisker inputs, the relative strength is controlled by the parameter w_2 (controlling the relative suppressive drive assigned to each modality); the second (M_{50}) is a constant that defines the weighted suppressive strength at which half the maximal response is attained. Additional parameters provide an expansive nonlinearity (*n*), scale the response (R_{max}) and provide a maintained discharge (*b*). In total there are 6 free parameters; for each site we found the combination of parameters that best predicted response (minimised the square error between the model predictions and observed responses), using the function "fit" in the Matlab environment. There are separate weights in the numerator and denominator because the normalization pool may weigh contributions differently. The visual and somatosensory input strengths are expressed in linear units.

For each site we found the best predictions of the model described above, as well as a reduced model that did not contain the normalisation term (the denominator). The reduced model has 4 free parameters (it does not have the free parameters w_2 and M_{50}). To establish the improvement in model predictions gained by adding the normalisation term (and thus adding two extra free parameters), we utilised the Akaike Information Criterion (AIC) to compare the full and the reduced model (Akaike, 1973). The selection of the model is important, as under-fitting a model may not capture the true nature of the response variability, while an over-fitted model loses generality (Snipes & Taylor, 2014). AIC is therefore a method to select the model that best balances these problems.

Akaike (1973) showed that the selection of the best model is determined by an AIC score:

$$AIC = n \times \ln\frac{RSS}{n} + 2k \qquad \textbf{Equation 2.3}$$

where K is the number of free parameters, n is the number of data samples and RSS is the residual sums of squares.

Hurvich and Tsai (1989) further refined this estimate to correct for small data samples; If ratio of n/K < 40, then AICc is calculated using the following bias adjustment:

$$AICc = AIC + \frac{2k(k+1)}{n-k-1}$$

Equation 2.4

The best model is the model with the lowest AICc (or AIC) score. It is important to note that the AIC and AICc scores are ordinal and do not convey any information on their own. They are merely a way of ranking different models.

2.3 Results

Here, I first show that we achieved robust responses from both visual and whisker stimulations in the rat SC. Following that, I will characterise the overlap between representation of visual and whisker inputs in terms of location and time. I will then characterise the interaction between these two modalities.

Our first aim is to characterise the overlap in responses of neurons in rat SC to visual and whisker inputs, in time and location. To do this we measured spiking activity simultaneously from different layers with multichannel linear probes, during presentation of either full-field visual or multi-whisker stimuli. We used these large stimuli to elicit response from multiple neurons instead of tailoring the stimulus for one neuron's RF. In order to reveal the physiological correlates underlying the laminar organisation of the SC, we first

presented the visual and whisker stimuli separately. The stimulus duration was 0.5 s for both types of stimuli, with an inter-stimulus interval of 0.5 s.

Figure 2.2 shows the response of example sites, recorded at different depths within the SC, to visual and whisker stimuli. To assess the visual and whisker responses, we used an objective method to categorise the response types using an ROC analysis (Section 2.2.6). This method will be described in the next section. Robust responses were obtained for both visual (red) and whisker (blue) stimuli. Each column shows a simultaneously recorded set of neurons. The dashed vertical gray lines indicate the onset and offset of the stimulus. The left two columns show the responses of neurons on a representative electrode shank placed such that the most superficial recording site was at a depth of 2.75 mm (distance between each recording site is 0.05mm). Based on atlas of Paxinos and Watson (1986), the SC is expected to start at the depth of 3mm from the surface of the brain. The 3 most superficial sites do not show stimulus related activity (grey). Deeper sites show clear visual responses (mainly responding to both ON and OFF phases of the stimulus). The two right columns show a representative example of a deeper penetration into SC. In this case, we observe robust visual and whisker responses in the intermediate sites. In summary, visually responsive electrodes are in the superficial and intermediate layers. Whisker responsive electrodes are in intermediate layers. We also observed individual sites that responded to both visual and whisker (black) stimulations when presented in isolation. These sites were observed across the different layers of SC.

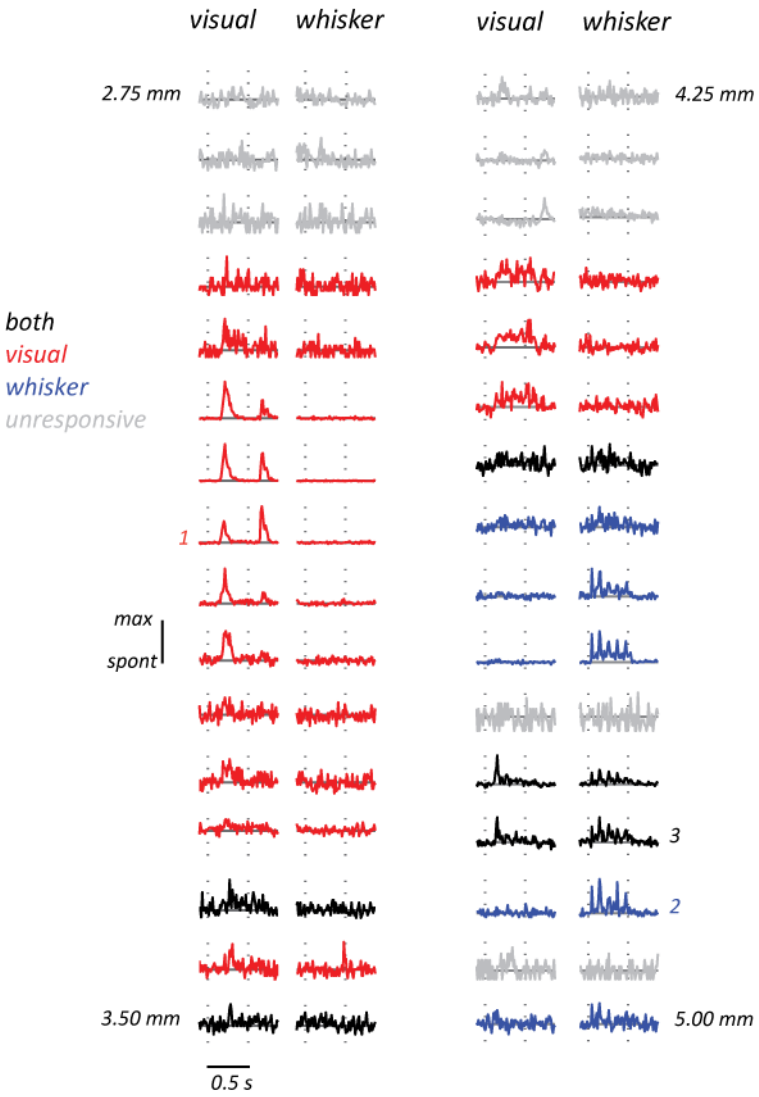

Figure 2.2: Response of example sites in SC to visual and whisker stimuli

Example peristimulus time histograms (PSTH; bin width 10ms) to visual or whisker stimulation as recorded at different depths. Each column shows a simultaneously recorded set of neurons. The left two columns show a representative electrode shank placed at the depth of 2.75 mm for the most superficial site (the distance between each site is 0.05mm). The two right columns represent an example deeper penetration in SC. The dashed vertical grey lines indicate the onset and offset of the stimulus (stimulus duration = 500ms). The response of each site has been normalised to the maximum of PSTH for that site. Visually responsive electrodes (red) are in the superficial and intermediate layers. Whisker responsive electrodes (blue) are in intermediate layers. Response to both visual and whisker stimulation (black) are also observed across layers of SC. The same colour coding used in this figure, will be used throughout the chapter.

2.3.1 Spatial overlap between visual and whisker representations

To assess the distribution of visual and whisker responses at different depths within SC, we used an objective method to categorise the response types. We quantified the trial-to-trial response variability using an ROC analysis (Figure 2.3), which quantifies the overlap in spike rate during stimulus present condition and stimulus absent condition. Figure 2.3A shows example ROC curves, for three example neurons, for visual or whisker stimulation. The dashed line shows what is expected by chance, and the area under the dashed line is 0.5. By contrast, for the whisker responding neuron, the area under the ROC curve for the whisker stimulation (i.e. AUC (Whisker)) is 0.68, indicating that activity during whisker stimulation is generally higher than spontaneous activity. For the visual stimulation of the whisker neuron, the same analysis provides an ROC value of 0.49, indicating activity is not different to spontaneous activity (the corresponding values for the visual responsive neuron are as follows: AUC (Visual) = 0.95 and AUC (Whisker) = 0.48; and for the example neuron that responded significantly to both visual and whisker stimulation: AUC (Visual) = 0.73 and AUC (Whisker) = 0.58). The same characterisation was performed for all recorded units. In the following analysis I include measurements from 672 electrode contacts at 21 recording sites obtained using multi-electrode arrays.

We expected that visual and whisker responses should be concentrated at different depths within SC. Figure 2.3B shows the distribution of ROC values, during visual or whisker

stimulation, as a function of depth below the surface of SC. Individual sites are colour coded according to criteria that will be described below – sites where multiunit activity showed no response to either stimulus (grey symbols), showed response to visual stimulation only (red symbols), whisker stimulation only (blue symbols), or both (black symbols). Figure 2.3B shows that visually responsive sites are mainly found in superficial layers whereas whisker responsive sites are in intermediate layers. There is a region of overlap, ca. 0.6-1.3 mm where sites could show substantial ROC for whisker or visual stimulation. In addition, we observed sites with significant multisensory responses throughout the SC; however, even these multisensory sites generally showed strong preference for one of the modalities.

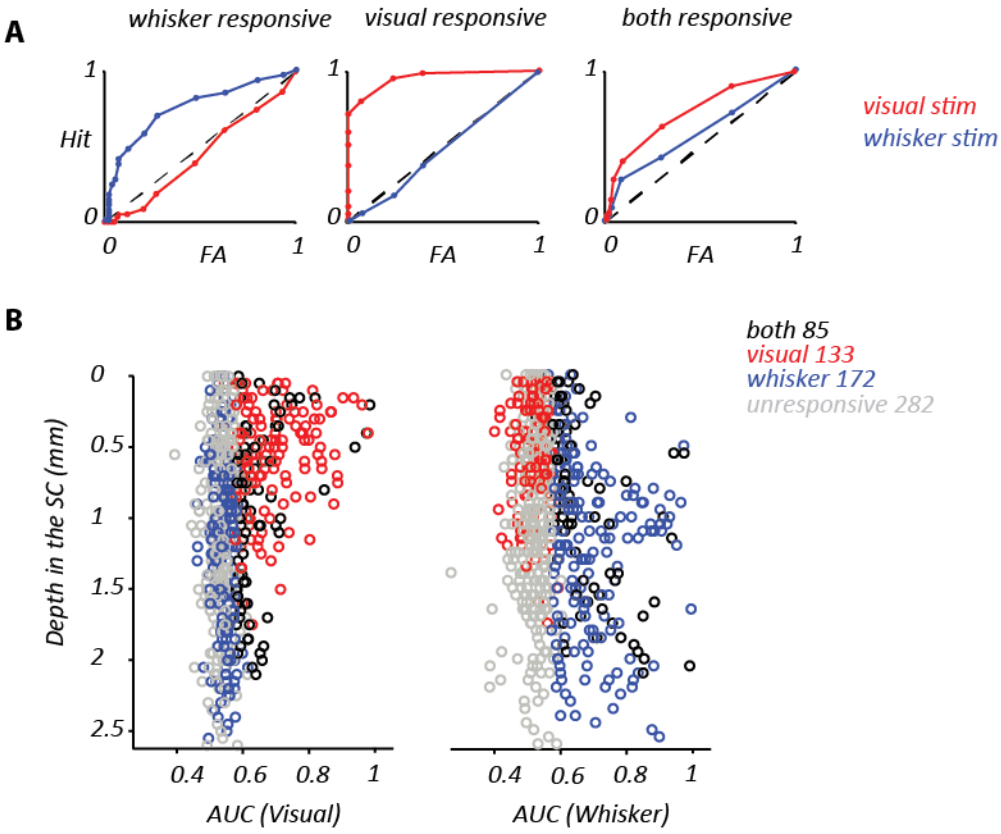

Figure 2.3: Response characterization of SC neurons using ROC analysis

A. Receiver operating characteristic (ROC) curves corresponding to a whisker neuron, a visual neuron and a neuron that responded significantly to both visual and whisker stimuli. It quantifies the response overlap between stimulus present and absent conditions. Every dot in this inset indicates hit and false-alarm rates for one response criterion. The empirical dots are connected by straight lines to estimate the area under the curve with a trapezoid method. The area under ROC curve values are calculated for visual and whisker stimulation. The value of area under ROC curve falls within the range of 0 to 1; area of 0.5 indicates that the hit rate is equal to the false-alarm rate, reflecting complete overlap between stimulus absent and stimulus present distributions. Area of 1, on the other hand, indicates no overlap between the two distributions and thus perfect discriminability. **B.** For each unit, depth from the surface of the SC is plotted against the area under ROC for visual (right) and whisker (left). The units with significant response to both visual and whisker stimulation were plotted on both sides (black circles). The visually responsive electrodes with high response rate (higher ROC values) were mainly in superficial layers. Whisker responsive electrodes with high response rate were mainly in intermediate layers.

2.3.2 Comparison of visual and whisker responses at individual sites

The analyses above show that visual and whisker responses are concentrated at different levels of the SC, with a limited region of overlap. To compare the visual and

whisker responses at individual sites, I compared the area under ROC curve for visual and whisker stimulation (Figure 2.4A). In addition to the multiunit measurements described above I include additional single-unit measurements, made using single electrodes, from 65 neurons (Figure 2.4A; filled symbols). An area under ROC of 0.5 indicates neural activity is not responsive to the sensory stimulus. Neurons that do not respond significantly to either visual or whisker stimulation would therefore lie at the lower left of the figure, where both ROC values are around 0.5 (grey symbols). Sites that respond significantly to visual stimulation but not to whisker stimulation would have an area under ROC value of around 0.5 for whisker stimulation and higher ROC values for visual stimulation ($p < 0.05$; red symbols). By contrast, sites that respond significantly to whisker stimulation but not to visual stimulation would have an area under ROC value of around 0.5 for visual stimulation and higher ROC values for whisker stimulation ($p < 0.05$; blue symbols). Sites that respond significantly to both visual and whisker stimulations ($p < 0.05$; black symbols) are also present. These sites generally showed strong preference for one of the modalities. This is apparent by the lack of any site with high visual and whisker area under ROC (i.e. no sites appear at the upper right of the figure). Figure 2.4B shows example PSTHs for a visual site (1), a whisker site (2) and a site that responded to both (3). These example sites are also indicated in Figure 2.2.

We used the comparison in Figure 2.4A to classify units as visual, whisker or both. Figure 2.4C shows the distribution of sites using this classification. To factor out differences in encounter rates, at each depth we calculated the proportion of sites that could be activated by one or both stimuli. Figure 2.4C reinforces the impression that there is overall segregation of visual and whisker responses in SC.

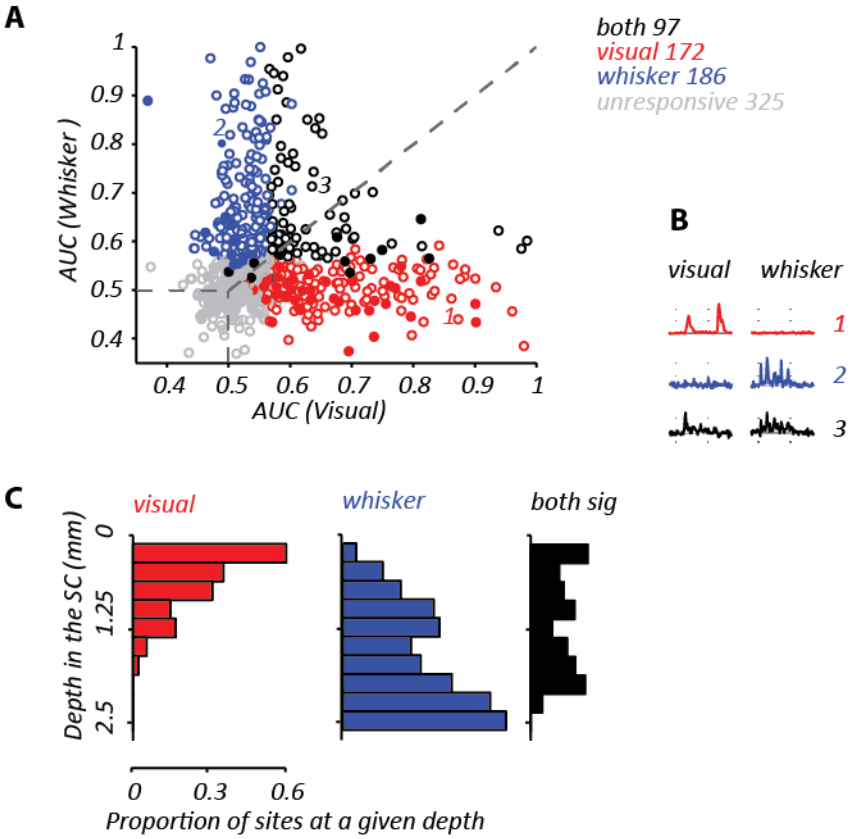

Figure 2.4: A. The area under ROC curve values are calculated for visual and whisker stimulation for all the sites and plotted against each other. Filled symbols represent the single units recorded using single electrodes (both n = 12; visual n = 39; whisker n = 14; unresponsive n = 43). There is limited convergence of the visual (red) and whisker (blue) inputs. **B.** PSTHs for the 3 example numbered sites (from Figure 2.2) are shown. **C.** Depth distributions of 672 electrode contacts at 21 recording penetration. Y axis shows the depth from the surface of SC. X axis shows the proportion of all the recording sites at that depth. Visually responsive electrodes (red bars on the left; n = 133) were mainly in superficial layers. Whisker responsive electrodes (blue bars in the middle; n = 172) were mainly in intermediate layers. Significant response to both visual and whisker stimulation was observed scattered across layers of SC (black bars on the right; n = 85).

In summary, spiking activity is elevated by whisker or visual stimuli, but rarely both, when those stimuli are presented in isolation. The distribution of sites that prefer visual or whisker stimulation is distinct, but does show overlap at depths between 0.6 and 1.3 mm.

2.3.3 Temporal overlap between visual and whisker representations

The analyses above show limited spatial overlap between visual and whisker representations in rat SC. To characterise the overlap between responses of neurons to visual and whisker inputs in terms of time, we calculated the response latency to each stimulus when presented in isolation. From PSTHs (binwidth 12 ms) generated for each stimulus, response latency was defined as the first occurrence of consecutive post-stimulus bins displaying significant responses ($p < 0.05$). Figure 2.5 shows the response latency distribution for the visual (left) and whisker (right) stimulations. The latency distribution of visual and whisker stimulation is distinct: the median visual response latency was 111ms, and the median whisker response latency was 35ms. These response latencies are slightly larger than reported in the literature for SC and extrastriate areas (Cohen *et al.*, 2008; Bezdudnaya & Castro-Alamancos, 2011; Vermaercke & Op de Beeck, 2012; Ghose *et al.*, 2014). This can be due to the fact that we used long (500ms) and large stimuli to elicit response from multiple neurons instead of tailoring the stimulus for one neuron's RF. Indeed the visual latency that we obtained in our experiment seems consistent with a previous experiment when using large flashes of 500ms (Girman & Lund, 2007).

In summary, there is limited temporal overlap between visual and whisker representations in rat SC.

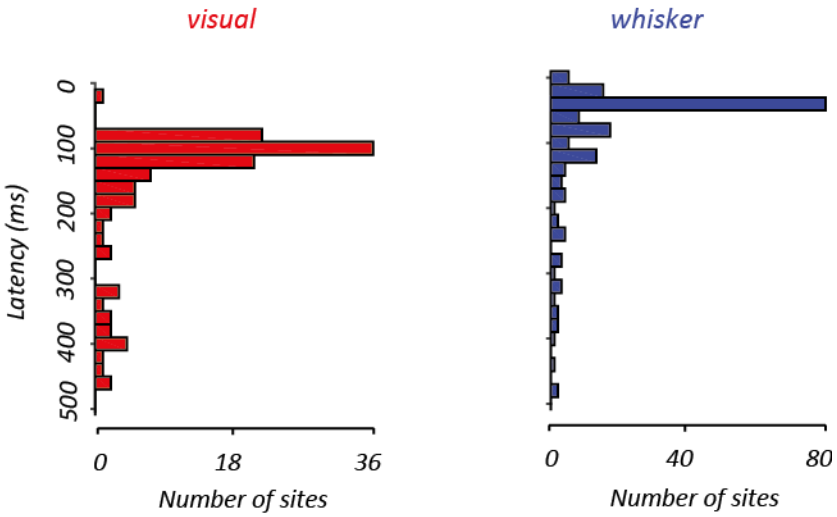

Figure 2.5: Response latency of visual and whisker sites in SC

The histograms of the response latency are given for visual (n = 118) and whisker stimulation (n = 176). Stimulus-evoked response latency was defined as the first of two consecutive significant PSTH bins compared to the baseline. The median visual latency (111ms) was longer than whisker latency (35ms).

2.3.4 Combined visual and whisker stimuli supresses the response

So far we have considered responses to visual and whisker stimuli presented in isolation, and find little evidence for convergent representations. Stimuli presented to one modality may nevertheless modulate the responsivity of neurons to stimuli presented to the other modality, and we now assess whether and how joint presentation of whisker and visual stimuli affects spiking responses. These measurements are from recordings made in a subset of the sessions that were also used in the analyses above. Preliminary analyses suggested that the visual responses lagged whisker responses by ca. 80 ms (similar to that obtained by subsequent analysis of the full data set – Figure 2.5). We therefore sought to maximise opportunity for multisensory interactions by presenting visual stimulus 80 ms

before the whisker stimulus. In the following analyses I include responses from 105 neurons, recorded at 352 electrode contacts from 11 recording sites.

Figure 2.6 compares the responses of the multisensory and the uni-sensory stimuli. Figure 2.6A shows average of normalised PSTHs obtained at maximum visual contrast (left), maximum whisker vibration (middle) or the corresponding multisensory condition (right). I plot separately the visual sites (top row), whisker sites (middle row) and sites that responded to both (bottom row). To compare the observed and the predicted multisensory response, the predicted response (sum of the uni-sensory conditions; grey line) is superimposed over the observed response. The observed responses appear lower than the sum of the respective uni-sensory responses. Across neurons (n = 105), the magnitude of the observed response to multisensory stimulus is compared against the response magnitude to the preferred stimulus (visual or whisker) when presented alone (Figure 2.6B). Overall observed responses to multisensory stimuli were consistently lower than the response to the preferred stimulus. Next, I quantified the multisensory response based on the summation model where the uni-sensory responses are summed to give a prediction of the expected multisensory response. Across neurons (n = 105), the magnitude of the observed response to multisensory stimulus is compared against the predicted response (Figure 2.6C). The dashed line shows what is expected if the response of the neurons to the multisensory stimulus was additive. Overall, observed responses to multisensory stimuli were mainly sub-additive (lie below the line of unity). In summary, our results show that observed responses to multisensory stimuli were consistently lower than the sum of the respective uni-sensory responses.

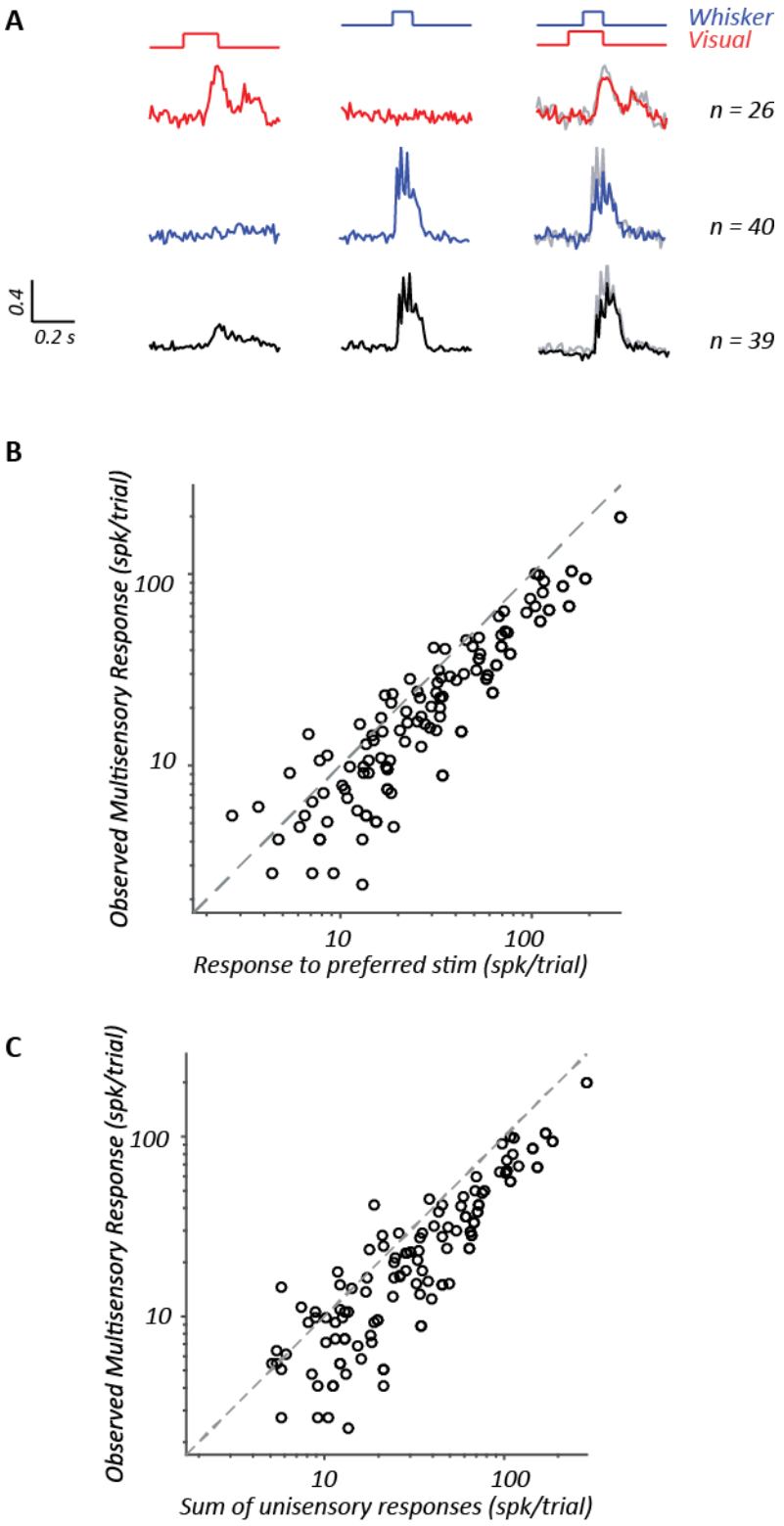

Figure 2.6: Spiking responses to visual, whisker, and combined stimulation in SC

A. The top row shows normalised mean PSTH of the sites that responded significantly to visual stimulus but not to the whisker stimulation. The normalised average PSTHs are

plotted for maximum visual (left), whisker (middle) and multisensory (right) stimulations. Onset and offset of visual and whisker stimuli are represented by blue and red square waves on top of the PSTH plots for each condition. The duration of visual stimulation was 200ms and whisker stimulation was 120ms. In multisensory condition, grey is the predicted response by summing of visual and whisker stimuli when presented alone. Background activity has been subtracted from all the conditions. The middle row shows the responses of whisker only sites to maximum visual, whisker and maximum multisensory stimulations. Bottom row shows normalised mean PSTH of the sites that responded significantly to both visual and whisker stimuli. **B.** Each point (n = 105) plots the observed magnitude of response evoked by multisensory stimulus against the response magnitude to the preferred stimulus (visual or whisker) when presented alone. Overall observed responses to multisensory stimuli were consistently lower than the response to the preferred stimulus (negative deviation from the line of unity). This plot is log-log-transformed for better visibility. **C.** Each point (n = 105) plots the observed magnitude of response evoked by multisensory stimulus against the predicted response by summing of visual and whisker stimuli when presented alone. Overall observed responses to multisensory stimuli were consistently lower than the sum of the respective uni-sensory responses (negative deviation from the line of unity). This plot is log-log-transformed for better visibility.

A common metric for assessing multisensory integration, is the interactive index ("*ii*"; Equation 2.1), which relates the multisensory response to the preferred stimulus response (the larger of the two uni-sensory responses). Figure 2.7 shows the distribution of the interactive index across the population of neurons. For clarity, individual points are not categorised by the preferred sensory stimulus; I return to this below. Figure 2.7 shows negative interactive indexes in majority of the cells, that is, suppression of response during multisensory stimulation. Average interaction index for whisker preferring sites was –11% (n = 40), for visual preferring sites was -6.1% (n = 26) and for sites responsive to both stimuli was -15.7% (n= 39). Statistical comparisons between multisensory response and the response to the preferred stimulus was significant at 21/105 sites ($p < 0.05$; nonparametric

Wilcoxon rank test; black symbols in Figure 2.7); all of these showed negative interaction indices; 6 were whisker preferring, 2 were visual preferring, and 13 responded to both stimuli. Note that all 13 sites that respond to both stimuli show strong preference for whisker stimulation (mean whisker ROC = 0.84; mean visual ROC = 0.53).

We considered the possibility that facilitatory interactions are found in neurons with weak responses to the preferred stimulus, and suppressive interactions are found in those with strong responses, or vice versa. Figure 2.7B compares interaction index with response amplitude for the preferred stimulus: there is a small yet significant negative relationship such that in neurons with weak responses to the preferred modality, the interaction tends to be slightly more facilitatory (correlation coefficient = -0.24, $p < 0.01$). We also considered the possibility that interaction indices were found in neurons that show relatively strong responses to the non-preferred stimulus in isolation. Figure 2.7A shows that the relative response to the non-preferred stimulus, which is always low, does not predict the interaction index.

In summary, we show that there are robust interactions between sensory modalities, even though under uni-sensory conditions the non-preferred stimulus elicits very weak or no response from those neurons. These interactions are primarily suppressive.

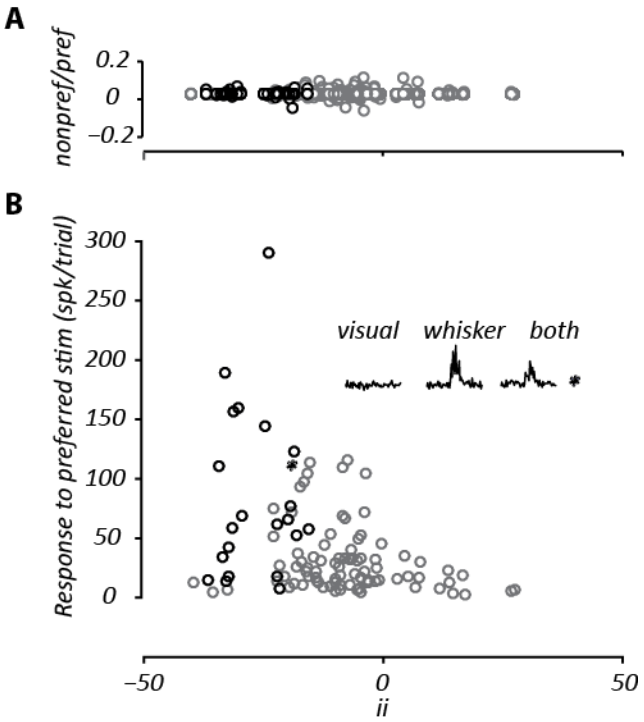

Figure 2.7: Quantification of multisensory interactions

For every unit (n = 105), response magnitude to the preferred stimulus (visual or whisker) is plotted as the function of interactive index (ii). Statistically significant ii values are plotted in black. Most of the observations evidence multisensory depression (negative ii values). The inset shows the response of a representative example neuron (star) that showed significant response depression under multisensory condition. The top panel plots the response to non-preferred stimulus over the response to preferred stimulus as the function of ii. Background activity has been subtracted. It shows that even though under uni-sensory conditions the non-preferred stimulus did not elicit any responses from the cells, it still reduced the responses under multisensory conditions.

2.3.5 Response surfaces for multisensory stimulation

Above we characterised neuronal response to the most intense visual or whisker stimulus, alone or in combination. These responses are drawn from a larger set of responses, to a matrix of stimuli that included all combinations of visual stimulation at each of 5 contrast levels and whisker stimulation at each of 5 vibration amplitudes.

In the following we characterise response across the joint surface. To do this we compared response to the predictions of a simple normalisation model of sensory combination (Equation 2.2 in Section 2.2.8):

$$R(V,S) = R_{max}\frac{(w_1V + (1-w_1)S)^n}{(w_2V + (1-w_2)S)^n + {M_{50}}^n} + \mathrm{b}$$

Where *V* and *S* are the strength of visual and whisker inputs respectively, each in the range 0 to 1. The numerator is weighted linear sum of these inputs, with the parameter w_1 controlling the relative excitatory drive assigned to each modality. The denominator contains two terms: one is again a weighted sum of visual and whisker inputs, the relative strength is controlled by the parameter w_2; the second is a constant that defines the input strength at which half the maximal response is attained. Additional parameters provide an expansive nonlinearity (*n*), scale the response (R_{max}) and provide a maintained discharge (*b*). In total there are 6 free parameters; for each site we found the combination of parameters that best predicted response (minimised the square error between the model predictions and observed responses). We included for analysis 88 sites where the model provided good predictions (r^2>0.6). These included 15/26 (58%) of visually responsive sites, 30/40 (75%) of whisker responsive sites and 29/39 (74%) for sites that responded to both stimuli. Most of

the excluded sites responded only to stimuli of the highest intensity, or showed low and variable response across the joint surface. For these excluded sites, even response to the highest intensity stimulus was relatively small (mean whisker ROC = 0.587; mean visual ROC = 0.594).

Figure 2.8 shows the response of an example whisker neuron (A) and an example visual neuron (B) with good model fits. The response (z axis) is plotted against whisker intensity levels (y axis) and visual intensity levels (x axis). Every point is the response to one of the 25 possible visual and whisker combinations. The surface is the fitted model with lighter colours indicating more evoked responses. The response of both these example neurons increased with the intensity of their preferred stimulus (whisker for the neuron in A and visual for the neuron in B). A suppressive impact of the less preferred stimulus modality (although modest in magnitude) is observable at the largest values of its intensity (the curves slightly bend downward at such extreme intensity values of the non-preferred modality).

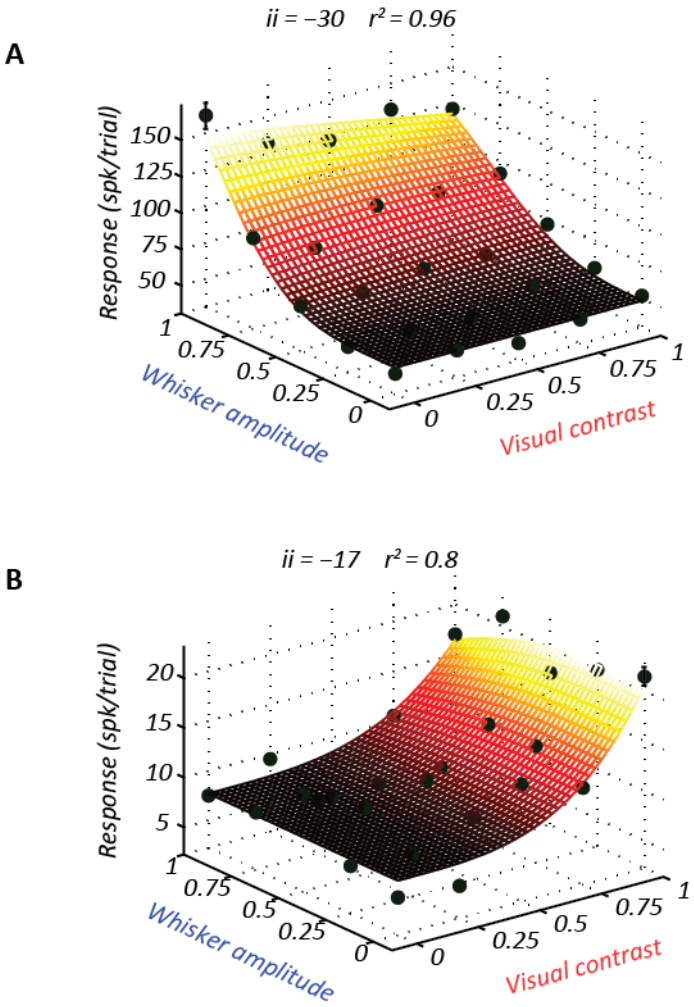

Figure 2.8: The response of example neurons across a range of stimulation amplitudes

The response of each neuron to all 25 stimulus conditions was fitted by a model (described in Section 2.2.8) to quantify the whole matrix of responses. The base line activity has been subtracted. For clarity, only mean response is plotted (the SEM is shown for one response condition).The average response of the neuron (z axis) is plotted against different levels of visual contrast (x axis) and different levels of whisker vibration (y axis) for **A.** an example whisker neuron (W1 = 0.0933; W2 = 0.2786) and **B.** an example visual neuron (W1 = 1; W2 = 0).

We are primarily interested in the weight parameters w_1 and w_2, which respectively describe the contribution of each sensory modality to the excitatory and suppressive mechanisms in the receptive field. Figures 2.9 and 2.10 summarise these parameters. To allow comparison with the analyses above, the symbol colour in Figure 2.9 and 2.10 shows the category (visual, whisker, both) obtained from the ROC analyses. Figure 2.9A shows the distribution of w_1, which ranges from 0 to 1: higher values indicate predominantly visual input and lower values indicate predominantly whisker input. Consistent with the ROC analyses, the sites with lower w_1 are whisker preferred sites and the ones with higher w_1 are visual. Nevertheless, one cell stands out and shows strange behaviour; the cell is classified as a whisker cell using ROC analyses (blue circle) but it has a high w_1 value from the model which indicates predominantly visual inputs. Further examination revealed that the cell was indeed a whisker cell. While the r^2 of the fit was high (r^2>0.6), in close inspection the fit exhibited an irregular surface profile producing a misleading high w_1 value. It is important to note that it was only one cell that showed a strange response function.

Sites with lower w_1 (whisker) are located deeper in the SC than sites with higher w_1 (visual). This is consistent with the ROC analysis, which was based on responses to a high intensity stimulus. Also consistent with the above analyses, Figure 2.9B indicates that all but one of the sites with lower w_1 values (whisker, w_1< 0.5) have negative interactive indexes (mean -14.4, n= 59). Sites with higher w_1 values (visual, w_1 > 0.5) show more uniformly distributed interactive indexes nevertheless mainly negative (mean -7.8, n= 29). This suggests that the each modality suppresses the responses to the other modality.

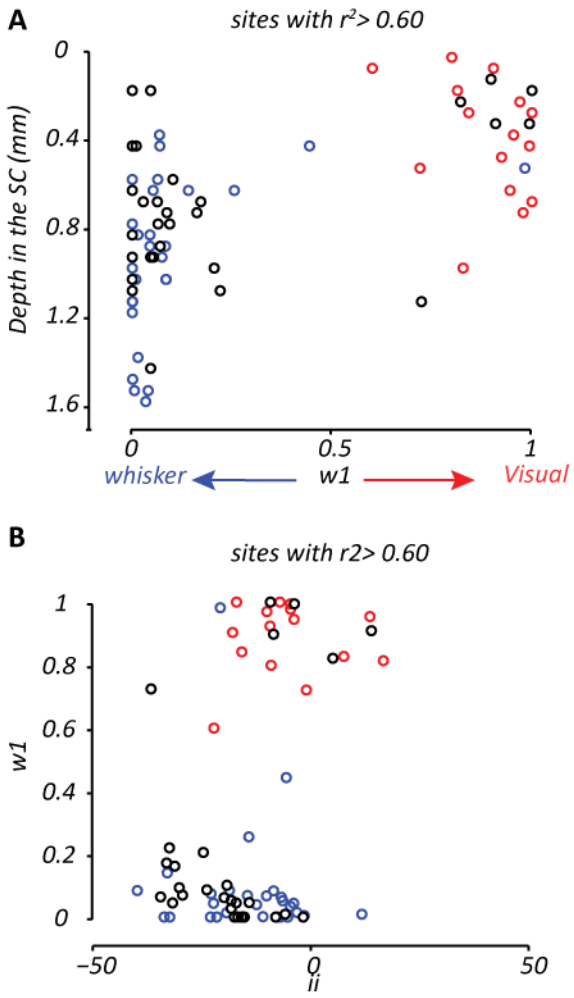

Figure 2.9: Investigating the response across a range of stimulation intensities.

A. The depth from the surface of the SC is plotted against excitatory coefficient (w_1) of the model. In the model, w_1 values range from 0 to 1; higher values indicate predominantly visual input and lower values indicate predominantly whisker input. Neurons with poor model fits (r^2<0.6) were excluded from the analysis. To allow comparison with the previous analyses (Section 2.3.4), the symbol colour in this figure shows the category (visual, whisker, both) obtained from the ROC analyses described before (Section 2.3.6). Sites with lower w_1 (whisker; blue) are located deeper in the brain than the sites with higher w_1 (visual; red). **B.** w_1 values are plotted against the interactive index. Most of the sites with lower w_1 values (whisker) seem to have negative ii whereas the sites with higher w_1 values (visual) seem to have uniformly distributed ii.

Figure 8C compares, for those sites where the full model offered better predictions, the distributions of w_1 and w_2. Most points are clustered to the left of the plot, indicating that sites with predominantly whisker input were more likely to show suppressive interactions. Further, most points lie above the line of unity, indicating relatively stronger contribution of visual input to the suppressive mechanism (denominator) than the excitatory mechanism (numerator).

The model allows us to estimate the relative weight of visual and whisker inputs to suppressive mechanism (w_2) but this will only be meaningful where the model is well constrained. To restrict analyses to informative sites, we calculated the Akaike Information Criterion (AICc; see Section 2.2.8) for the full model, and a reduced model in which the denominator was removed. The best model is the one with the lowest AICc values. Figure 2.10A compares AICc vales for the full and reduced models at individual sites. Most data points are below the unity line (dashed red line in Figure 2.10A), indicating lower AICc scores for the reduced model. For analysis of suppressive mechanisms (w_2, in the denominator), we only included those sites that show added benefit of normalisation term (that is, AICc was lower for the full model than the reduced model; Figure 8B). This restricts the analysis to neurons that are potentially informative about the denominator of the model. Figure 2.10C shows that the inhibitory coefficient (w_2), which also ranges from 0 to 1, has higher values than the w_1 coefficient (i.e. majority of the data points are located above the dashed grey unity line in Figure 2.10C). This indicates that these sites are inhibited by the presence of the other stimulus. The w_2 values do not seem to associate with the M_{50} values of the model (Figure 2.10D). The interaction between w_1 and w_2 further indicates a suppression of responses by the other modality stimulus; when w_1 is low w_2 is above the diagonal line.

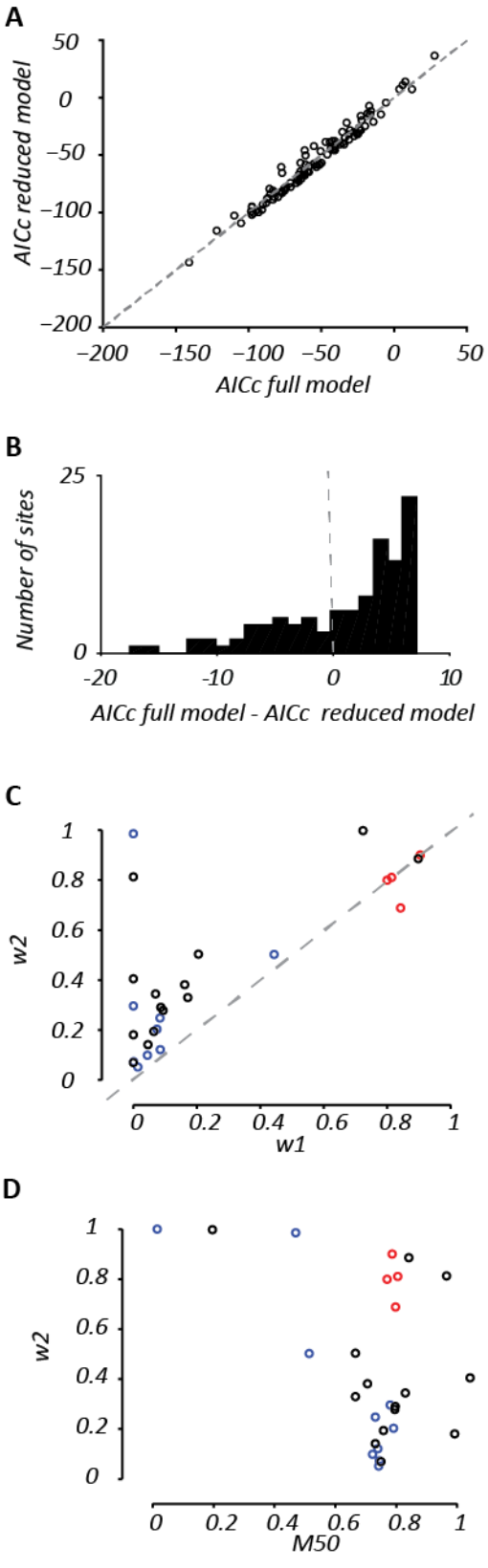

Figure 2.10: Investigating the model parameters

A. AICc values for the full and reduced models are plotted against each other (n = 352 electrode contact points). Most data points are below the dashed unity indicating lower

AICc scores for the reduced model. **B.** The histogram of the difference between AICc values for the full and reduced models are plotted. The best model is that with the lowest AICc values. Therefore, for sites to the right of zero line (dashed gray line), the reduced model is better than the full model. For sites to the left of the zero line, the full model is better. **C.** For sites with good fits (r^2>0.6) and lower full AICc values, inhibitory coefficient (w_2) of the model is plotted against w_1. Similar to w_1, w_2 ranges from 0 to 1. For these sites, w_2 values are higher than w_1 values which indicates a depression of responses by the other modality stimulus. **D.** w_2 values are plotted against the M_{50} value from the model. The value of w_2 does not seem to associate with the M_{50} value.

2.4 Discussion

I have shown that in rat SC, spiking activity is elevated by whisker or visual stimuli, but rarely both, when those stimuli are presented in isolation. As expected visual and whisker responses were concentrated at different levels of the SC but did show an area of overlap. Visually responsive sites were mainly found in superficial layers whereas whisker responsive sites were in intermediate layers. Investigation of response latency revealed that there is limited temporal overlap between visual and whisker representations such that the visual responses lagged whisker responses. I then showed that there are robust suppressive interactions between these two modalities when they are aligned in time, even though under uni-sensory conditions the non-preferred stimulus elicits very weak or no response from those neurons.

Section 2.4.1 Spatial overlap

Dräger and Hubel (1975; 1976) showed that in mouse, whisker topographic organisation in intermediate/deep layers of SC is arranged so as to be in spatial registration

with the representation of the visual field. They found that in any electrode perpendicular penetration, whisker receptive fields recorded in the deeper SC were concerned with that group of whiskers that were in alignment with the position of the visual receptive fields recorded in the upper layers. They did not, however, compare the response to each modality at each site, or the interactions between modalities. We aimed to quantitatively evaluate the distribution of visual and whisker inputs in rat SC. Using multichannel linear probes, I simultaneously recorded neuronal activity from different SC layers to reveal the physiological correlates underlying the laminar organisation. In these simultaneous recordings, to increase the number of responsive neurons, I used full-field visual stimuli and multi-whisker vibrations. We used full-field visual stimuli and multi-whisker vibrations to maximise the chance of observing responses from either modality on the multichannel probes. These large stimuli were capable of producing robust spiking activity, as has also been reported elsewhere (Hemelt & Keller, 2007; Cohen *et al.*, 2008; Hirokawa *et al.*, 2011; Ghose *et al.*, 2014; Bezdudnaya & Castro-Alamancos, 2014). Nevertheless, the sensitivity of neurons in the uppermost layers of SC can decrease using full-field visual flashes. Girman and Lund (2007) showed that increasing the size of flashing spots increased responses of cells in the most superficial sub-lamina, reaching a maximum at diameters between 1.5–10°. The neurons' responses decreased thereafter with increasing the size; the stimuli here were up to 100 degrees diameter (median = 87 deg; mean = 75 deg).

We found that when we presented the visual or whisker stimuli in isolation, the neurons were rarely activated by both. There was limited spatial overlap between the distribution of sites that prefer visual or whisker stimulation and an area of overlap was found at depths between 0.6 and 1.3 mm from the surface of the SC. On individual

recording shanks (e.g. left panel of Figure 2.2) we often saw interdigitation of sites responsive to either modality. These sites on individual shanks were located in the intermediate layers (0.7 ± 0.13 mm from the surface of the SC). The location of responsive whisker and visual sites in our simultaneous recordings is consistent with previous anatomical and functional studies of whisker and visual representations in SC (May, 2006; Hemelt & Keller, 2007; Cohen & Castro-Alamancos, 2010*c*, 2010*b*; Ghose *et al.*, 2014; Bezdudnaya & Castro-Alamancos, 2014; Watson *et al.*, 2015).

Section 2.4.2 Combined visual and whisker stimulation

An advantage of our approach is that we characterised response of neurons to combined visual and whisker stimulation at multiple stimulus intensities. Under these conditions, each modality generally suppressed the responses obtained through the other modality. The suppressive interactions between sensory modalities has previously been observed in SC (Meredith & Stein, 1986; Kadunce *et al.*, 1997; Mysore *et al.*, 2010; Hirokawa *et al.*, 2011) and other areas of the brain (Wallace *et al.*, 1992; Dehner *et al.*, 2004; Meredith *et al.*, 2006). In cat SC, the neurons that exhibit response depression to multisensory stimulus, are often only influenced by stimuli from one modality in uni-sensory presentations (Meredith & Stein, 1986). This observation in cat SC is consistent with our results in rats: the response to the non-preferred stimulus was always low and the suppressive influence of a seemingly ineffective stimulus only became evident during multisensory presentation.

Lippert and colleagues (2013) showed that in the rat parietal cortex, visual and whisker inputs converge and interact. The visual and whisker stimuli were either presented

synchronously or asynchronously with a variety of stimulus sequence delays. For the multi-unit activity, the nature of multisensory interaction was independent of stimulus order and was consistently sub-linear. This is similar to what we found in SC. In our experiments, apart from the asynchronous multisensory presentation described before, we also presented the visual and whisker stimuli synchronously in the multisensory condition and observed similar suppression of responses (data not shown here). As well as multi-unit responses, Lippert and colleagues (2013) measured current source density (CSD) responses in the rat parietal cortex and showed that the sign of multisensory interaction was dependent on stimulus order. When the whisker stimulus preceded the visual, supra-linear summation of CSD was observed, but the reverse stimulus order resulted in sub-linear effects in the CSD. This is in contrast to their multi-unit activity where the interaction was suppressive regardless of stimulus sequence. Local pharmacological silencing abolished these multisensory interactions suggesting that the observed non-linear interactions are due to local intra-cortical and not from collicular or thalamic processes (Lippert *et al.*, 2013).

There is an important inference to make from the experiments like ours where the suppressive influences of one modality onto the other are evident only when the stimuli are combined: it is well possible that the proportion of multisensory neurons in brain is underestimated. When stimuli from different modalities are presented sequentially, they are ineffective in identifying depressive interactions except in the neurons that have an unusually high and regular spontaneous activity (Meredith, 2002).

Section 2.4.3 Multisensory convergence

Events in the environment are often simultaneously detected by more than one sense. The brain has evolved the capacity to integrate information across the senses and this can be of critical importance to survival. There are some challenges regarding multisensory integration that the brain has to overcome. A main problem is whether different sensory information came from the same source (such as prey) or different sources (prey and the wind). And then combine different information if they come from the same source (Ma & Pouget, 2008). Another issue that the brain has to solve is to estimate the reliability of different sensory information. For example visual information is more reliable during the day than in the dark, whereas in the dark the brain can trust whisker or auditory information.

There are multiple ways that inputs from different sensory modalities can converge. They can converge within a particular region without terminating on the same neuron (areal convergence as illustrated in the left side of Figure 2.11). In this form of convergence, individual neurons only respond to one modality and there is no multisensory integration (Meredith, 2002). Alternatively, inputs from different sensory modalities can converge onto the same neuron which responds to either modality and can also show multisensory integration (neuronal convergence in the right side of Figure 2.11). It is however more likely that population of unimodal neurons intermix with one another within an area of the brain where the multisensory functions fall within a continuum between these two forms of convergence (as illustrated in the middle panel of Figure 2.11).

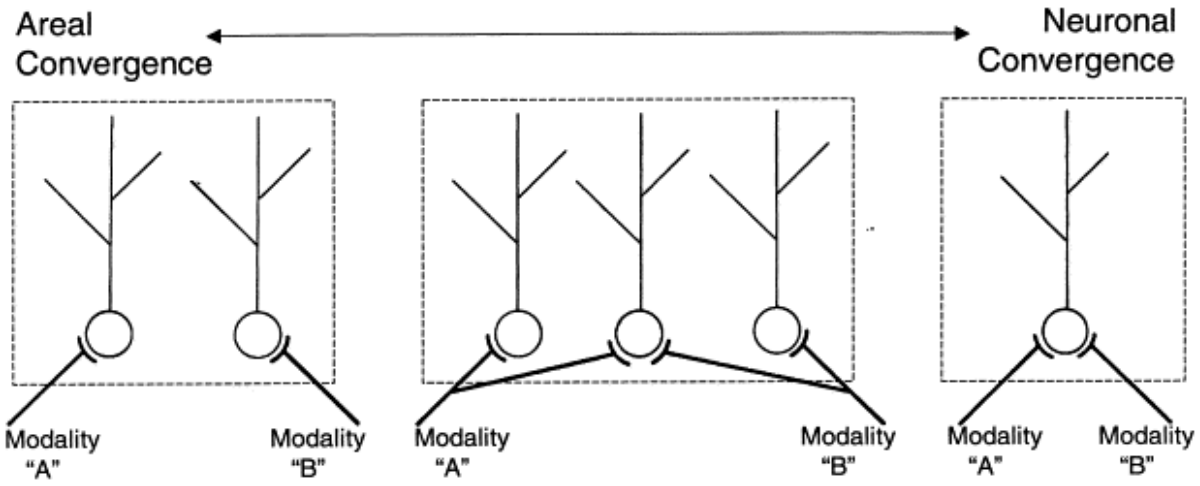

Figure 2.11: Forms of multisensory convergence.

Within a particular region of the brain, inputs from two modalities can converge. In the areal convergence on the left, the inputs from different modalities do not terminate on the same neuron. In the neuronal convergence on the right, inputs from the different sensory modalities converge onto individual neurons. It is also possible that multisensory convergence is a continuum between these two forms and shows properties of both. *Adapted from Meredith (2002)*.

In our experiments, we found an area of overlap within SC where (nearby) neurons responded robustly to visual or whisker stimuli. Therefore the nature of convergence between these two modalities may be areal, with uni-modal visual and whisker neurons are intermingled within the area. Nevertheless, we observed robust suppressive interactions between these two modalities, indicating that these uni-modal neurons are connected to other neurons (either multisensory, or sensitive to the other modality) that can in turn influence the responses. The convergent suppressive component between these two modalities is probably indirect. It is possible that in rat SC, the suppressive interactions arise

from intra-SC connections between otherwise unimodal neurons rather than from direct multimodal input converging on the same neuron from sensory sources outside SC. Indeed, it would be predicted that in the case of convergence, spatially coincident stimuli would depress and not enhance multisensory response (Meredith, 2002). Eventually, these suppressive interactions between the senses may serve to influence the quality of a perception rather than to detect an environmental event.

In general, multisensory integration is important for precise perception and behavioural performance. There are a number of accounts as to how the brain integrates neuronal responses across two or more modalities. It is important to note that there are uncertainties in the information available to our senses, and in their encoding by sensory systems. Optimal integration requires that the summation of information takes the reliability of each source into account (see Angelaki *et al.*, 2009 for a review). The Bayesian account of multisensory integration formulates how the reliability of different sensory signals affects the summation: it has been shown that humans and other primates employ a strategy of placing greater weight on a more reliable sensory cue (Gu *et al.*, 2008; Fetsch *et al.*, 2012). The mathematical combination of different sensory inputs by single neurons is usually in line with optimal probabilistic models of computation in neural circuits (Fetsch *et al.*, 2012). Consistent with the Bayesian ideas, the normalisation framework employed in this thesis incorporates weights that determine the relative contribution of each sensory modality to the overall summation.

Our findings are consistent with complex convergent multisensory circuits in rat SC. The convergent suppressive component between these two modalities is likely to be indirect. These findings open the door to interesting questions about the circuits that

mediate these suppressive interactions between different modalities. These interactions can be as result of dynamics within SC circuity, or there might be a potential role of specific neocortical inputs to the SC in mediating multisensory integration in collicular neurons. Studies of SC of cats and primates have indeed shown that the multisensory integration is mediated by some cortical areas (for example Jiang *et al.*, 2001; Alvarado *et al.*, 2007). It appears likely, that homologous cortical areas are present in the rodents. There are several good candidates for such areas in rat's neocortex (Toldi *et al.*, 1986; Brett-Green *et al.*, 2003; Wallace *et al.*, 2004; Lippert *et al.*, 2013; Ibrahim *et al.*, 2016). This is an important issue in understanding of how and through which neural circuitry multisensory integration works.

As an evolutionary ancient midbrain structure that receives inputs from multiple sensory modalities, SC is expected to play a key role in orienting behaviour to external events (Meredith, 2002; Stein et al., 2014). However, the circuits underlying multisensory integration and the mechanism by which rat SC may facilitate and speed the reaction to a stimulus of interest remain elusive. Our work here reveals the functional arrangement of whisker and visual responsive neurons across rat SC, the suppressive nature of their interaction, and identifies potential differences across species in the physiological properties of SC neurons.

3.0 Visual behaviour in freely moving rats

3.1 Introduction

In order to understand the relationship between neuronal responses and visual perception, we need to be able to measure performance in well controlled behavioural visual tasks. As the visual system of non-human primates closely resembles that of humans, it has been the primary candidate for such measurements during operant conditioning (Newsome *et al.*, 1989; Britten *et al.*, 1992; Hegdé & Van Essen, 2003; Read & Cumming, 2003; Williams & Shapley, 2007; Nienborg & Cumming, 2010; Gattass & Desimone, 2014). There is, however, increasing interest in applying similar methods to rodents. Whilst rodents have a simpler visual system than primates, with lower spatial acuity and simpler cortical architecture (Chalupa & Williams, 2008), they are gaining popularity in visual neuroscience because of the readily available molecular and genetic tools. These tools are more readily applied in mice, but are increasingly available for rats. Here I provide a rodent model of visual behaviour in rats, where a rich history of behavioural training provides a platform for discovering the neurobiology of behaviour.

The analysis of neural-behavioural correlates requires a paradigm that adheres to the following criteria: a) allows multiple observations (trials) in a restricted period of time; b) restricts the range of head movements and allows knowledge of eye position; c) is adaptable to a wide range of tasks. In what follows I evaluate these criteria in the context of existing behavioural methods.

Multiple trials in a restricted period of time

Large number of trials provides statistical power and gives us the opportunity to fully explore relevant stimulus parameters and to resolve even small differences in performance or neural activity across various conditions. Achieving large numbers of trials is particularly important in the context of electrophysiological measurements. An ideal apparatus therefore requires the ability to complete large number of trials in a short period of time which also has the ability to easily be paired with electrophysiological measurements.

A common paradigm used to investigate visually guided behaviour involves training rodents to swim in a water maze towards a submerged platform, indicated by a visual stimulus (Prusky *et al.*, 2000; Prusky & Douglas, 2004; Douglas *et al.*, 2006; MacKinnon *et al.*, 2010). The swimming task, however, yields only a few trials per session. Other tasks have trained rodents in two-alternative forced choice (2AFC) in a self-paced regime, where animals have free access to the home cage at any time (Meier & Reinagel, 2011; Meier *et al.*, 2011; Clark *et al.*, 2011). Whilst these tasks yield large number of trials, they are not within a restricted period of time and therefore not ideal for electrophysiological measurements.

Restriction of head movements and stable eye positions for tracking

It is critical to have control of head and eye motion with respect to visual stimuli for reliable and valid electrophysiological measurements. Assessment of visual receptive fields requires stable head and eye position, and capacity to monitor both. The water-maze method (above) does not allow this. Head-fixation has been used for behavioural research,

particularly in monkeys, to facilitate precise stimulus control, behavioural assessment and neural recording. For example, receptive fields of sensory neurons can be stimulated in precise ways to assess perception (Britten *et al.*, 1992).

More recently, the head-fixed preparation has been applied to rodents (primarily mice) in a variety of visual tasks (Lee *et al.*, 2007; Sawinski *et al.*, 2009; Andermann *et al.*, 2010; Busse *et al.*, 2011; Sriram & Reinagel, 2012; Histed *et al.*, 2012; Carandini & Churchland, 2013; Feinberg & Meister, 2014). Head-fixation offers greater experimental control over sensory inputs and motor outputs compared to the freely moving preparation. However, time is needed to habituate the animal to head-fixation and stress is an unwanted effect of head-fixation that, at the very least, can lead to prolonged training periods needed to condition the animals even to simple tasks—if they do not prevent learning altogether. The head-fixed preparation also makes repeated testing (e.g. months/ years) difficult as the implant needs to be maintained. Finally, the behavioural repertoire of rodents includes many whole-body movements that are impossible to perform under head-fixation (Schwarz *et al.*, 2010).

Adaptability to wide range of tasks

Another criterion to consider is adaptability to a variety of tasks. In the experiments I conduct here we chose to employ a Go/NoGo task. Nevertheless the experimental design is adaptable to a variety of tasks including two-alternative forced choice (2AFC). The 2AFC paradigm has been successfully developed to study complex visual tasks in rats such as shape processing and objection recognition (Zoccolan *et al.*, 2009; Tafazoli *et al.*, 2012; Vermaercke & Op de Beeck, 2012; Alemi-Neissi *et al.*, 2013; Rosselli *et al.*, 2015). The Go/NoGo task is one of the standard paradigms of animal psychology (Blough & Blough,

1977) and is often used in rodent studies (Abraham *et al.*, 2004; Andermann *et al.*, 2010; O'Connor *et al.*, 2010; Smear *et al.*, 2011; Histed *et al.*, 2012). In its simplest form, the Go/NoGo task requires the animal to produce an operantly conditioned response (for example lick a spout) in the presence of one kind of stimulus (CS+) and not to produce this response in the presence of another kind of stimulus (CS−). For detection of a brief signal (visual or auditory), the occurrence of the signal is defined as CS+ and its absence as CS−. One advantage of the Go/NoGo task is that there is one response metric. Therefore observed differential responses are not due to competing motor plans.

In summary, an ideal setup for pairing behaviour with electrophysiological measurements allows a large number of trials in a restricted period of time, restricted range of head movements, the monitoring of eye position, and adaptability to wide range of tasks. My aim here is to develop an operant apparatus that adheres to these. As I will describe, the animal's primary task is to initiate a trial by entering a central nose-poke, and to maintain the nose-poke until a relevant signal indicates availability of reward. Sucrose water reward is then provided at the reward spout if the animal arrives at the reward spout within an allocated time following signal onset. From this I can measure response time and accuracy. The design of the experimental apparatus restricts the range of head motions without head-fixation, allowing eye-position to be monitored via video feed. The rats are free to move, but as I will show they generally keep their head stable at a central nose-poke during visual stimulation. The design is adaptable to a variety of tasks including 2AFC visual detection and discrimination tasks, measurement of attentional modulations in visual tasks and also in tasks employing different sensory modalities.

The current chapter provides an overview of the apparatus development, basic task structure and the learning theories used in shaping the behaviour of the rats. I describe the

platform for establishing passive visual stimulation. This will also form the basis for behavioural tasks that I describe in the next chapter.

3.2 Methods and paradigm development

3.2.1 Subjects

Adult male hooded rats (Long Evans; n = 8; 6-8 weeks at the start of the training) were obtained from the Florey Neuroscience Institute at Melbourne University. All procedures were approved by the Animal Care and Ethics Committee at the Australian National University. Rats were housed in an independently ventilated and air filtered transparent plastic box (two rats per box). The colony room was climate controlled and had a 12 hour light-dark cycle, with lights were turned off at 7pm. In the 3 days prior to commencement of the study, each rat was handled for 15 minutes per day to accustom them to the experimenter and to ease any anxiety.

3.2.2 Food and water regulation

To provide motivation, rats were provided regulated access to food and water, which they were gradually adapted to. Measured rat chow (5g per 100g of body weight) was provided after each daily experiment. Water was removed from the home cage 2-4 hours before the start of the experiment, but was provided ad libitum at all other times. Rats readily adapted to this scheduling of food and water access, showed normal growth

trajectories, and no signs of distress. On weekends and days we did not run the behavioural experiments, we provided rats with measured rat chow (5g per 100g of body weight) and ad libitum access to water. Weight, social behaviour and grooming behaviour were monitored each weekday. We estimated expected weight as 85% of the weight before implementation of food and water regulation, with additional cumulative 3g/wk up to a maximum of 400g. Body weight was always above 85% of the expected weight.

3.2.3 Apparatus

The experimental apparatus was a custom-made Plexiglas chamber (Figure 3.1A). The chamber was framed by a front panel, floor panel, walls and an L-shaped ceiling with posts and rails (Thorlabs, Inc.) formed over a magnetic honey comb base. The floor panel was elevated 9.5 cm from the base using posts, and contained multiple slots for waste to fall through. The side-walls were attached to the floor panel using two Dovetail optical rails (Thorlabs, Inc.). The distance between the side walls was 6.5 cm. The ceiling and back plate were attached, forming an L-shape in cross section, and was held in place via slots in the floor panel. The distance between the front panel and back panel of the ceiling was 18 cm, and it rested 13 cm above the floor plate.

A substantial advantage of the current design is that the front panel has a triangular aperture through which the rat's head can extend, allowing direct viewing of the monitors. The vertex of the triangle was 9 cm above the floor panel and the width was 5cm; these dimensions ensured the animal could not escape, and limited the range of potential head movements. A platform placed below the aperture, 6.5 cm from the floor, formed a step for the animal to rest its front paws on.

As I will describe, rats were trained to interact with sensors and reward port attached to a post outside the chamber, 4 cm from it and accessible only by extending the head through the triangular aperture. The post held a central nose-poke and a reward spout below its, both of which were framed by infra-red sensors. The reward spout delivered 10% sucrose in water solution via a motorized pump (Watson Marlow).

Visual stimuli were presented on two LCD monitors (Dell – Model No. P2012Ht, 60 Hz Refresh rate, width 25 cm and height 44 cm; mean luminance ~ 80 cd/m2) normal to each other and normal to the line of sight from the central nose poke, at a distance of 16 cm from the central nose poke. This is closer than the distance established for maximum behavioral visual acuity in rats (20-30 cm; Wiesenfeld and Branchek, 1976), but allowed a wider field of view. Visual stimuli were generated using Matlab (Mathworks, Natick, MA, USA) and PsychToolbox (Kleiner *et al.*, 2007) to control standard OpenGL capable graphics cards (intel 4000HD).

The behavior of the rat (nose-poke or the response at the reward spout) was continuously registered into a data acquisition card (National Instruments) using a custom-built circuit that measured contact at the spouts or nose-poke through optical sensors. Custom-written code controlled the experiment (presenting visual stimuli, providing auditory signals, registering the behaviour of the rats along with the corresponding time stamp of each behavioral action, and controlling rewards.

3.2.4 Modifications for electrophysiological recording

Modifications of the basic configuration described above were required to allow electrophysiological recordings from animals, obtained by chronic implants of multiple

moveable tetrodes. My primary consideration was to minimise any force applied to the implanted micro-drive (Figure 3.1B), by reducing the likelihood of the implant contacting ceiling or walls of the chamber. The implanted micro-drive, the head-stage preamplifier, and the tether attached to the head-stage all provide potential force points. I note that animals were initially habituated to the basic configuration, described above, which discouraged attempts to exit the chamber. The flexibility of the chamber design allowed transition from the basic to modified design within 1 minute.

In the modified chamber, the distance between the side walls of the chamber was increased (from 6.5 cm to 11 cm) and the ceiling was replaced with another (increasing height from 13 cm to 23 cm). The increase in ceiling height provides an opening in the front panel, above the triangular aperture. Two plexiglass rods were therefore attached to the ceiling to close the potential exit (Figure 3.1C). A slot (width 2.5 cm) through the middle of the ceiling allowed access for the tether.

A

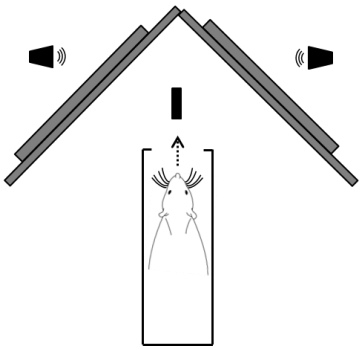

B

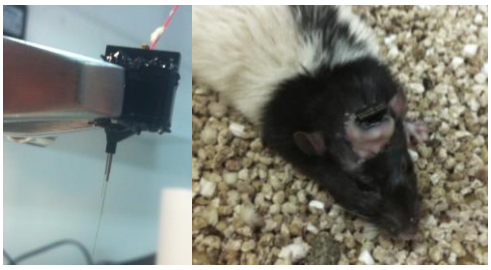

C

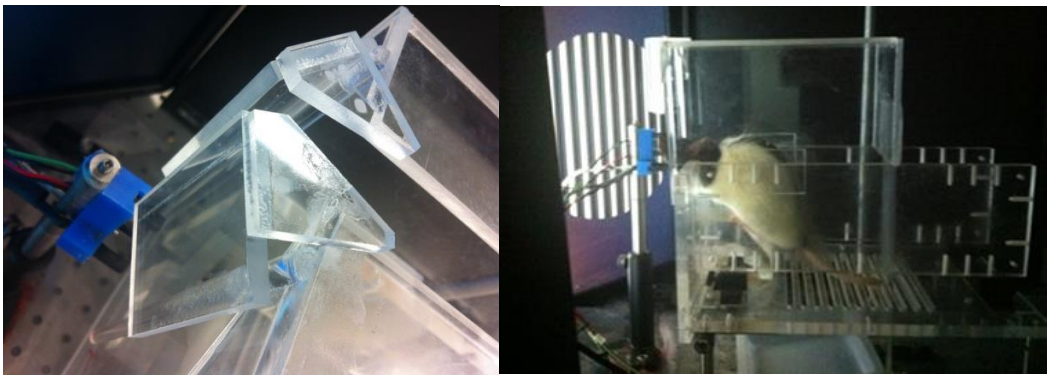

Figure 3.1: A. The behavioural apparatus and its schematic drawing. **B.** A photograph of the micro-drive for electrophysiological recordings along with a photograph of an implanted rat. **C.** The modified apparatus for electrophysiological recordings.

3.2.5 Alternative designs

The designs described above reflect the outcome of several rounds of trial and error. I note three particular deviations from the current design that substantially influenced performance.

First, in initial implementations, the chamber was wider, with 9.5 cm distance between the side walls. This eased capacity of the animals to turn within the apparatus and thus provided greater opportunity for 'distraction': fewer trials per session (rat1: 74 ± 18; rat2: 87 ± 13) and more training sessions were required to achieve criterion performance. Decreasing the distance to 6.5 cm led to faster training and more trials per session from the same rats (rat1: 278 ± 19; rat2: 304 ± 11).

Second, early designs included a metal, T-shaped, step for animals to rest their forepaws. A small metal rod was attached to a threaded metal bolt that in turn was tapped to the floor panel. This type of step was adequate for the behavioural training but brought about two confounds during recording. First, the metal introduced an alternative electrical contact and thus noise. Second, implanted rats could place their head under the platform, providing potential trap and substantial force on the implant. The plexiglass cube, which extends to the floor panel, alleviates both these problems and in addition encourages the animal to stretch to the nose-poke, reducing range of possible head movements.

Third, early designs included a separate back panel which could be adjusted, depending on the size of the rat, to decrease the distance between the front and back panels. This feature was unnecessary, as it became apparent that it was the width of the chamber that influenced turning behaviour. The subsequent L-shaped ceiling/back is substantially easier and faster to place.

3.2.6 Overall task structure and response categories

In the following I provide an overview of the basic task structure; I outline specific modifications to it where necessary in later sections. The animal's primary task was to initiate a trial by entering a central nose-poke, and stay there until a relevant signal indicated availability of reward. Sucrose water reward was provided at the reward spout if the animal arrived at the reward spout within an allocated time following signal onset. To promote faster response, the volume of the sucrose reward was greater for responses within half of the maximum time allowed (Kaneko *et al.*, 2006). Reward was ~ 0.07 mL for faster responses and ~0.05 mL for slower responses.

It is useful to describe some terms that define the structure of the task (Table 3.1).

Table 3.1: Some terminology used in the behavioural tasks throughout the thesis

Nose-poke delay	Time between nose-poke initiation and signal onset, set by the experimenter.
Maximum execution latency	Maximum time between signal onset and arrival to the reward spout for the reward to be available, set by the experimenter.
Inter trial interval	Minimum time between two consecutive nose-poke initiations, set by the experimenter. The central nose-poke sensor was unresponsive if the animals entered it before the inter trial interval had passed. The inter trial interval was 4 sec for most of the experiments.
Reaction time	The time between signal onset and the animal's exit from the nose-poke.
Execution latency	The time between signal onset and animal's arrival at the reward spout.

It is also useful to define the four possible behavioural outcomes (Table 3.2) as also schematically represented in Figure 3.2.

Table 3.2: Possible behavioural outcomes

Hits	Trials in which animals waited in the central nose-poke until signal onset, then left the central nose-poke and entered the reward spout within the maximum execution latency. Animals could then start a new trial provided the inter trial interval had passed.
Misses	Trials in which animals waited in the central nose-poke until signal onset but failed to leave or go to the reward spout within the maximum execution latency. Animals could then start a new trial provided the inter trial interval had passed.
False alarms	Trials in which animals left the central nose-poke before signal onset and yet went to the reward spout. A penalty time (1 sec) was added to the inter trial interval.
Non-valid trials	Trials in which animals left the central nose-poke before signal onset but did not go to the reward spout. We think that in most of these cases the animal has accidentally initiated a trial by for example breaking the sensor beam with their whiskers. The penalty time was not added to these trials and the rats could start a new trial immediately.

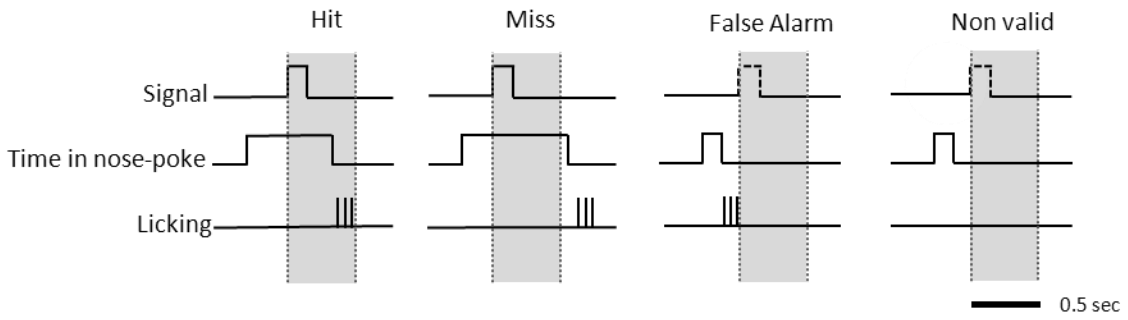

Figure 3.2: Schematic representation of the possible behavioural outcomes. Shaded grey area defines the 0.5 sec maximum execution latency.

In the following I provide the shaping procedure for both active and passive tasks. First I outline the shaping for the passive task where the rats passively observe a visual stimulus and after a fixed nose-poke delay an auditory white noise signals the availability of reward. Second, I outline the shaping procedure for the active task where the rats responded to a change in the visual stimulus. In this case, it is crucial to ensure that the rats perform the task based on the visual signal and not merely based on timing predictions.

3.2.7 Shaping animals for passive observation

The aim of these behavioural tasks was to provide a platform for electrophysiological measurements of visual responses in the brain of awake and unrestrained animals. Assessment of visual receptive fields requires stable head and eye position, and capacity to monitor both. To avoid potential head or eye movements during presentation of visual stimuli, or confound between temporal structure of the stimulus and cues to leave the central nose poke, here the signal to leave is provided by an auditory tone.

Spout shaping: animals learn that reward can be collected. Animals are placed in the experimental chamber for 30 mins to explore the chamber and collect reward from the reward spout. Upon approach to the reward spout an auditory white noise signal (0.1 sec duration) was presented through speakers and sucrose reward was provided. The auditory signal was provided to facilitate development of an association between the signal and the reward. One shaping session was provided. During this session the central nose-poke was removed from the post and the stimulus monitors were turned off.

Nose-poke shaping: animals learn association between central nose-poke and reward spout. The central nose poke was attached and animals were required to enter it to initiate a trial. An auditory white noise signal (duration 0.1 sec) was presented as soon as the central nose-poke was entered. Sucrose reward was provided only if entrance to the central nose-poke was followed by entrance to the reward spout within 3 sec (maximum execution latency = 3 sec). Once animals learned to nose-poke (1 session), I gradually decreased the maximum execution latency to 1 sec (3 sessions). The stimulus monitors remained off in this stage of the shaping.

Delay period shaping: animals learn to stay in central nose-poke during a delay before presentation of auditory white noise signal, which indicated that the rat animal could proceed to the reward spout. The stimulus monitors were turned on and a randomly chosen visual stimulus (gratings or uniform fields, viewed through small apertures) appeared at random locations following entrance to the central nose-poke. The visual stimulus was therefore unrelated to the animal's task. The delay between entering the nose-poke and the presentation of the auditory signal was gradually increased from 0 to 2 sec over 33 sessions, by increasing the mean of a slightly variable (uniform distribution) delay time. The steps to get to 2 sec nose-poke delay are shown in Figure 3.3 (error bars denote range of the

uniform distribution). It is important to note that the 2 seconds was not the limit the rats could wait in the nose-poke and the delay times could have been increased further. This was merely a time that we chose as to being enough for the purpose of our experiments.

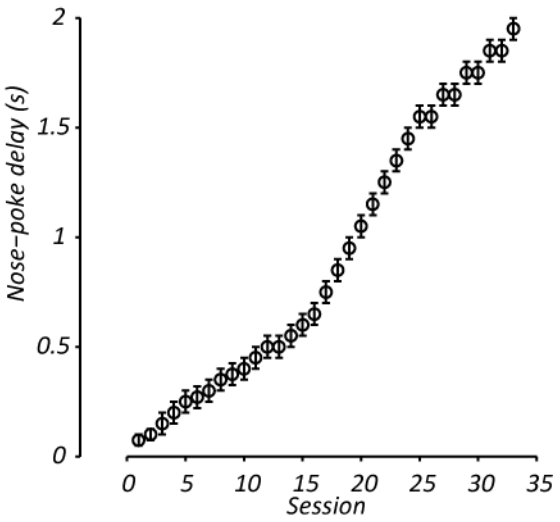

Figure 3.3: The steps to get to 2 sec nose-poke delay in the *Delay period shaping* of the passive task (error bars denote range of the uniform distribution).

Shaping in preparation for later recordings: animals are familiarized with a wider chamber and a delayed visual stimulus presentation for later electrophysiological measurements. For 12 sessions, the distance between the side walls of the chamber was increased (from 6.5 cm to 11 cm). The reason for this gradual change was to adapt the rats to perform in a wider chamber with the modified higher ceiling. During this stage the visual stimulus appeared 0.2 sec after the nose-poke initiation. The time before visual stimulus presentation (0.2 sec) was for later electrophysiological measurements. In any electrophysiological recording, it is essential to have a measure of the base-line activity of the neurons where the rat is stable in the nose-poke with all the other conditions the same

as the time during stimulus presentation. The auditory white noise signal was presented at a fixed delay of 2 sec. After 22 sessions at this stage of shaping, the rats were ready to be implanted for recording. Figure 3.4 summarizes the shaping of the animals for the passive task and its general structure.

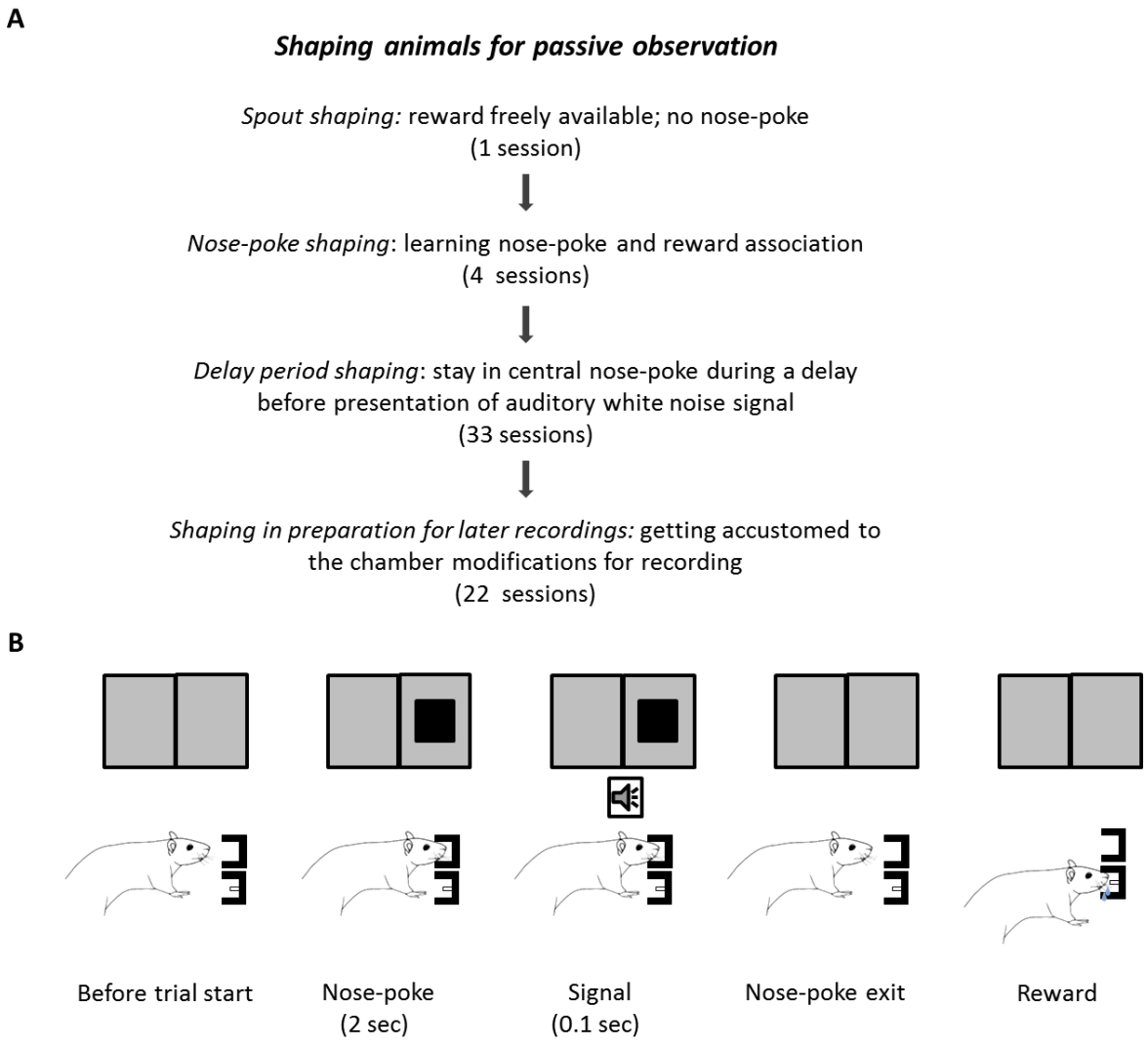

Figure 3.4: A. the steps for shaping of the animals in passive observation task. **B.** Schematic representation of the passive task. Rats approach a nose-poke aperture. Rats then initiate a trial by nose-poking into the aperture and a visual stimulus would appear with the nose-poke. After a delay of 2 sec during which nose-poke was continually maintained, rats receive an auditory signal (0.1 sec). Rats then make a behavioural decision by leaving the nose-poke and entering the reward spout after the presentation of the auditory signal and receive sucrose water.

3.2.8 Shaping animals for reaction time task (Active)

Spout shaping: animals learn that reward can be collected. Animals are placed in the experimental chamber for 30 mins to explore the chamber and collect reward from the reward spout. Upon approach to the reward spout sucrose reward was provided. One shaping session was provided. During this session the central nose-poke was removed from the post and the stimulus monitors were turned off.

Nose-poke shaping: animals learn association between central nose-poke and reward spout. The central nose-poke was attached and animals were required to enter it to initiate a trial. Sucrose reward was provided only if entrance to the central nose-poke was followed by entrance to the reward spout within 3 sec. In this stage of the shaping, a white circular aperture on a grey background was continually present on each monitor. The white apertures briefly turned black (0.15 sec) as soon as the central nose-poke was entered, signaling the availability of reward. Once rats learned to nose-poke (1 session), I gradually decreased the maximum execution latency to 1 sec (2 sessions).

Delay period shaping: animals learn to stay in central nose-poke during a delay before a visual signal (luminance change). The delay between entrance to the central nose-poke and visual change was gradually increased from 0 to 0.45 sec over 9 sessions (by increasing the fixed delay time 0.05 sec on each session). False-alarms led to an auditory beep played through speakers and 1 sec was added to the inter trial interval. The system was nonresponsive during this penalty time.

Countering timing-based performance: completion of the task may simply reflect accurate internal clock and prediction of the time required to obtain access to reward. To counter this potential cue the following two steps were applied. First, once animals had

learnt to wait for delay periods of 0.45 sec, the maximum execution latency was decreased to 0.5 sec (over 15 sessions). Second, over 27 additional sessions, variability was gradually added to the delay period, eventually reaching a delay range of 0.45-1.45 sec (uniform distribution). This increase in variability was achieved in steps of 0.05 sec. The criteria for moving to a session with longer variable delay were twofold: the percentage of 'hits' for that session was at least 75%, and the actual time spent at the central nose-poke was significantly longer in the later half of delay periods than the earlier half. The steps to get to 0.45-1.45 sec variable nose-poke delay are shown in Figure 3.5 (error bars denote range of the uniform distribution).

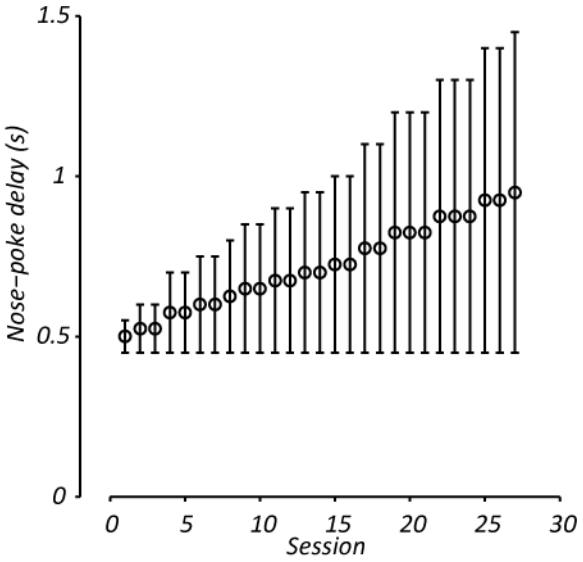

Figure 3.5: The steps to get to 0.45-1.45 sec variable nose-poke delay in the *Countering timing-based performance* of the active task (error bars denote range of the uniform distribution).

At the end of this stage of the shaping, the animals were moved to the testing phase to investigate whether selective visual attention can be demonstrated in rats. The manipulation of attention load and the testing phase forms Chapter 4 of the current thesis.

Figure 3.6 summarizes the shaping of the animals for the active task and its general structure.

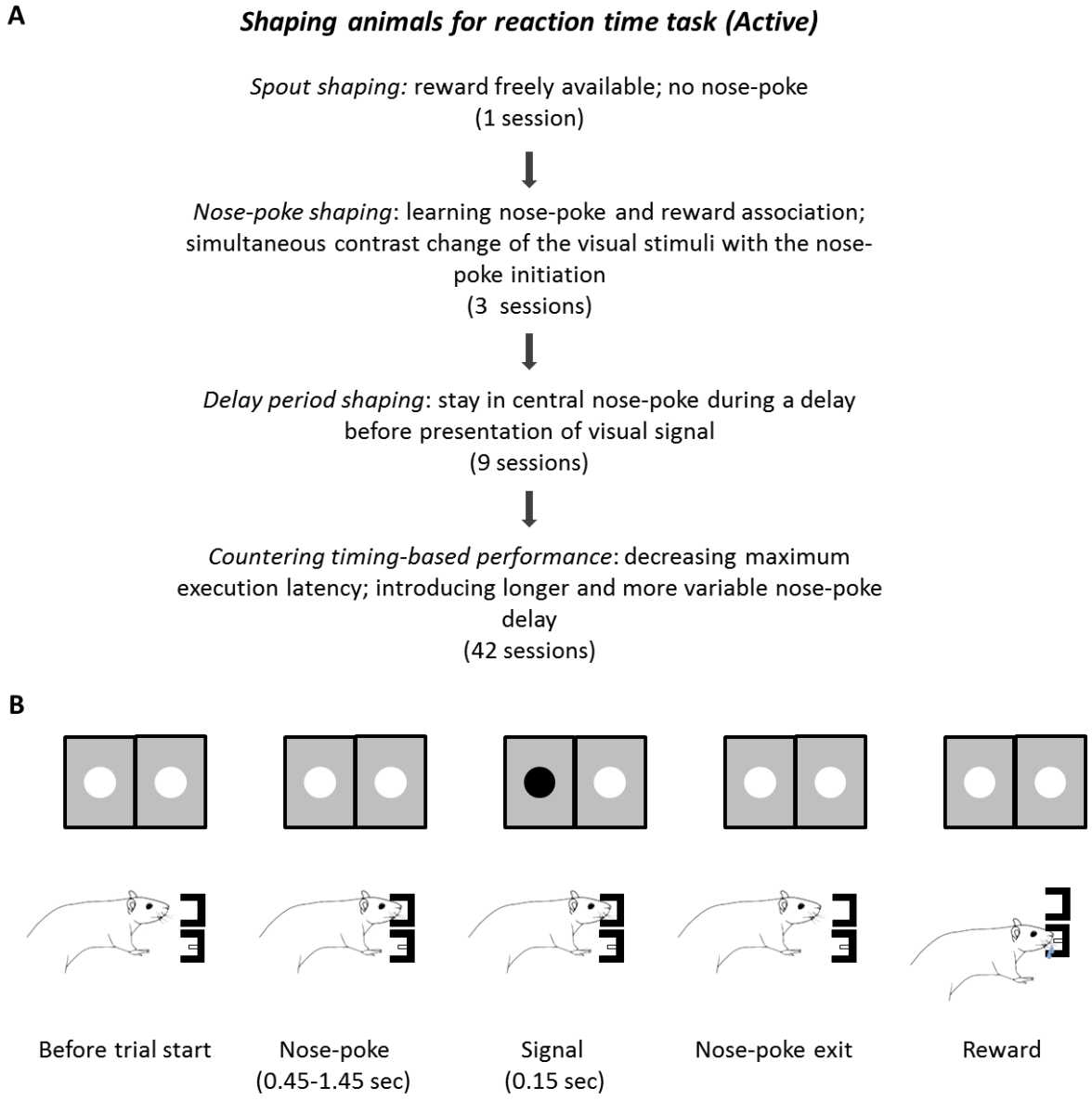

Figure 3.6: A. the steps for shaping of the animals in the reaction time active task. **B.** Schematic representation of the active detection task. Rats approach a nose-poke aperture and a white circular aperture on a grey background was continually present on each monitor. Rats then initiate a trial by nose-poking into the aperture. After a delay of between 0.45-1.45 sec during which nose-poke was continually maintained, rats receive a visual signal. The visual signal is one of the white apertures briefly turning black (0.15 sec) signaling the availability of reward. Rats then make a behavioural decision by leaving the

nose-poke and entering the reward spout if they identify the presences of the visual signal. Correct detection is rewarded by sucrose water.

3.2.9 Development of shaping procedures

The shaping procedures above were arrived at following earlier experiments (4 rats) in which animals did not learn to associate the presence of visual change (signal) and the availability of reward.

First, in earlier experiments the white apertures were not present continually: the monitors were grey and white apertures would appear only after entrance into central nose-poke. Animals then needed to wait for the contrast change to occur before leaving the nose-poke, whereupon the apertures would disappear and appear again at the next entrance to the central nose-poke. The problem with this arrangement was that the visual stimulus was changing more than once during each trial. The appearance and disappearance of the white apertures appears to have been confused by the rats with the actual signal change, which was also a contrast change in the visual stimulus. The rats therefore did not learn the visual signal change and made many false-alarms (around 40%). If rats left the nose-poke consequent to the visual signal detection, the time spent in the nose-poke would depend on the duration of the delay before signal presentation. However the actual time spent at the central nose-poke was not significantly longer in the later half of delay periods than the earlier half (Wilcoxon rank sum test; $p>0.05$). In the final experiments the white apertures were constantly present and the only luminance change was the signal.

Second, a common practice in training rats in visual tasks (for example Meier et al., 2011) is to present flickering screens after false-alarm or error trials, indicating the system is

nonresponsive during the resultant penalty time. Flickering screens following false-alarm trials, however, appeared to have reduced the capacity of animals to associate the visual signal with reward, likely for similar reasons to that discussed above. Our task was a luminance change detection, having a flickering screen seemed to have confused the rats and decreased the significance of the contrast change of the actual signal. The rats failed to learn about the visual change - made many false-alarms (around 40%) and the time spent at the central nose-poke was not significantly longer in the later half of delay periods than the earlier half (Wilcoxon rank sum test; $p>0.05$). In the final experiments an auditory beep (instead of flickering screens) was presented for the false-alarm trials indicating the system was nonresponsive.

Third, long maximum execution latency (time allowed between signal and arrival to the reward spout) seemed to encourage animals to adopt timing-based method for task success instead of visual signal. In these animals, performance was high when the maximum execution latency was long (1 sec) but the actual time spent at the central nose-poke was not significantly longer in the later half of delay periods than the earlier half (Wilcoxon rank sum test; $p>0.05$). When the maximum execution latency was reduced to 0.5 sec, performance dropped significantly (t-test; $p<0.01$). It is therefore important that the nose-poke delays come from a wide range and the maximum execution latency is short.

Fourth, in the earlier experiments, a clear auditory tone was provided as a secondary reinforcer with the visual change, to guide the shaping. The idea was that the auditory tone is a stronger signal and the simultaneous presentation of the tone and the visual change would help the rats to learn about the visual change. The volume of the auditory tone would then be gradually decreased until the tone was completely off. However, instead of helping with the learning, the tone appeared to block learning of the visual change. Performance

was high when the auditory tone was present, but when entirely extinguished performance dropped dramatically (t-test; $p<0.01$), indicating that the animals associated tone and reward but not visual change and reward. Subsequent attempts to train animals over 27 sessions without the tone did not lead to successful association. I then reintroduced the tone with a lower volume with the following structure: on 10% of the trials, tone was presented alone and was not rewarded; on 10% of trials visual signal was presented alone and was rewarded with a larger amount of sucrose; on other trials both tone and visual signal were presented together and rewarded. However even with this new arrangement the animals did not learn the association between reward and visual change. For the trials with tone, the actual time spent at the central nose-poke was significantly longer in the later half of delay periods than the earlier half (Wilcoxon rank sum test; $p<0.01$). However, this was not the case for the visual only trials (Wilcoxon rank sum test; $p>0.05$).

Fifth, a challenge in training animals is to alleviate frustration when not receiving reward. In initial experiments it became clear that it was important not to penalise non-valid trials, in which animals left the nose-poke before signal presentation but did not go to the reward spout. Originally I categorised these trials as false-alarms, a penalty time was added to inter trial interval, and a beep provided to indicate incorrect behaviour. Video observation, however, showed that in many of these trials the animals did not appear to intend to initiate a trial and had instead accidentally activated the sensor (e.g. whiskers breaking the sensor beam). Penalising the animals on these trials led to apparent frustration. Additionally, inter trial interval beyond 5 sec, and long false-alarm penalty time (more than 2 sec) appeared to increase frustration, and they continually checked the reward port during these periods.

3.2.10 Electrophysiology

Rats were implanted with either Axona Versa Drive Microdrives (Axona System, London) or Neuralynx VersaDrive-4 (Neuralynx, Inc.) that allowed independent movement of 4 tetrodes (4.0 mm travel distance and 0.25 mm pitch; Figure 3.1B). To make a tetrode, four Platinum 10% Iridium 7µm Microwires were twisted together and were plated with platinum black and gold solution. The Microdrive was then assembled using 4 tetrodes (16 recording channels). The spacing between the tetrodes was 0.6 mm. Electrodes were implanted in the superior colliculus (6.8 mm from Bregma, 1.5mm lateral from midline).

3.2.11 Analysis

All Analyses were performed in MATLAB (Mathworks). Spike sorting was performed using Plexon Offline Sorter (Plexon Systems, TX). The successful implantation served to demonstrate feasibility of recording neuronal activity during the behavioural paradigm. As the isolated units were not responsive to visual stimuli, neuronal data is not reported in the thesis.

3.2.12 High-Speed Videography and eye Tracking

Eye and head position were monitored non-invasively using a high-speed video camera, but we did not enforce fixation. High-speed video (76 frames/s) was acquired from above the nose-poke through a lens (M5018-MP2; f = 50mm F1.8) by a High-speed camera

(USB 2.0 Monochrome Industrial Camera; DMK 22BUC03) with a resolution of 744x480 pixels. Infrared Illumination was provided constantly. For each video sequence, we obtain 85 frames following nose-poke onset.

3.3 Results

3.3.1 Passive observation

The aim of the passive behavioural tasks was to provide a platform for electrophysiological measurements of visual responses in the brain in awake and unrestrained rats. As shown in Figure 3.7A, both rats successfully performed hundreds of trials per session (rat 1: 293 ± 12 trials; rat 2: 290 ± 11 trials). The rats learnt to stay in central nose-poke during the nose-poke delay before presentation of the auditory white noise signal (Figure 3.7B). This delay was gradually increased from 0 to 2 sec over 33 sessions (*Delay period shaping* described in Section 3.2.7; the dashed red line in Figure 3.7 represents day 33 where the nose-poke delay reached the goal of 2 sec). Day 33 onwards shows shaping where nose-poke delay was fixed at 2 sec and animals were familiarized with a wider chamber and the higher ceiling for electrophysiological measurements (*Shaping in preparation for later recordings* in Section 3.2.7). Therefore both rats showed a drop in the number of trials performed on some of the sessions with increased distance between the side-walls. Both rats showed high hit rate across sessions (Figure 3.7C; rat 1: 85 ± 1.4; rat 2: 81 ± 1.5). Figure 3.7 contains more sessions for rat 2 as rat 1 was implanted with the Micro-drive earlier.

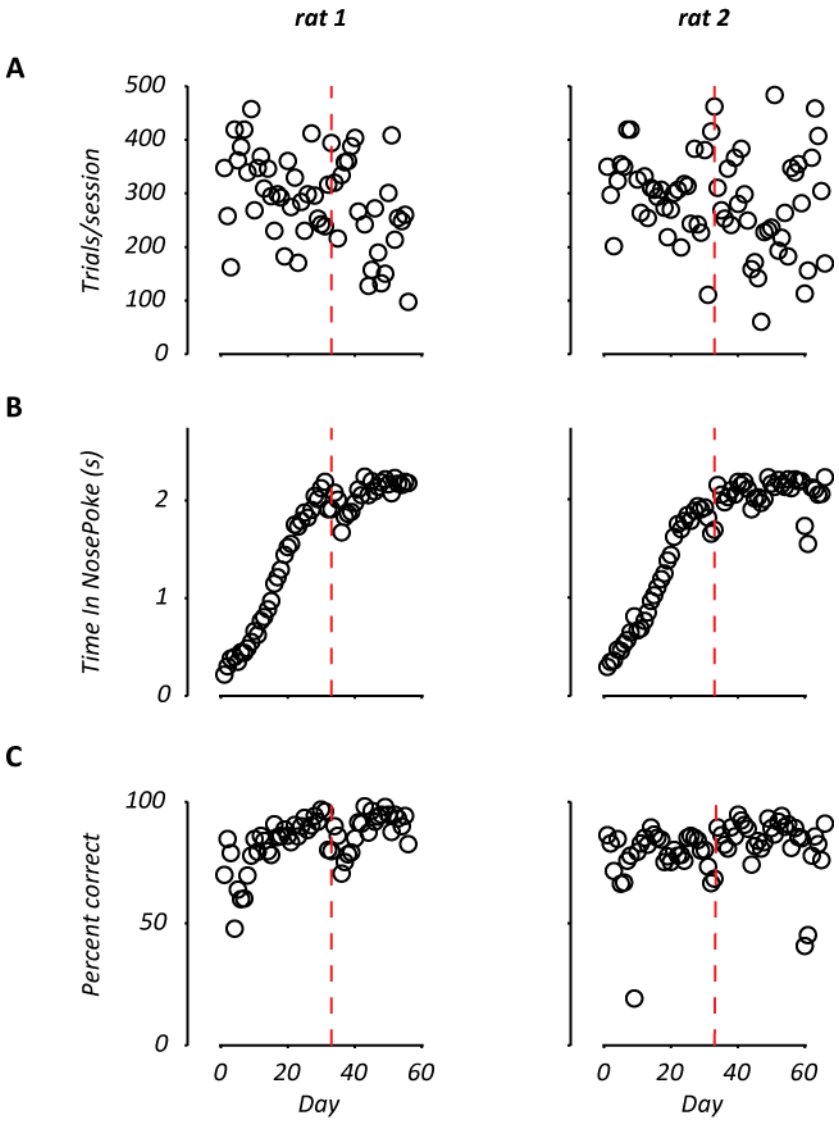

Figure 3.7: A. Both rats performed multiple trials per day. Day 0 indicates the time when the rats had learnt the association between central nose-poke and reward spout (end of *nose-poke shaping*, beginning of *Delay period shaping* described in the methods section). The dashed red line represents day 33 where the nose-poke delay reached the goal of 2 sec (end of *Delay period shaping,* beginning of *Shaping in preparation for later recordings*). **B.** The rats learnt to stay in central nose-poke during the nose-poke delay before presentation of the auditory white noise signal. This delay was gradually increased from 0 to 2 sec over 33 days. **C.** Both rats showed high performance (hits over all the trials) across days. The performance drop for Days 59 and 60 was due to a problem with the sucrose reward.

3.3.2 Reaction time task (active)

The details of the reaction time task and the selective attention manipulations will be explained in chapter 4. Here I only present results to indicate that our design was also successful in a reaction time active task. Similar to rats in the passive observation group, both rats in the reaction time task successfully performed hundreds of trials per session (Figure 3.8A; rat 1: 324 ± 14 trials; rat 2: 350 ± 14 trials). Note that on day 18, the rats were provided rat chow before the experiment by mistake and therefore performed fewer trials. The mean reaction time, the time between signal onset and the animal's exit from the nose-poke, was stable across sessions (Figure 3.8B; rat 1: 0.22 ± 0.003 sec; rat 2: 0.23 ± 0.003 sec). For the data shown in Figure 3.8, the nose-poke delay variability was 0.45-1.45 sec (uniform distribution). In Figure 3.8C, this variability is plotted against the actual time spent at the central nose-poke. If rats left the nose-poke consequent to signal detection, the time spent in the nose-poke would depend on the duration of the delay before signal presentation. Indeed, the rats learnt to stay in central nose-poke during the nose-poke delay before presentation of visual signal with the time in nose-poke significantly longer for later signals (Wilcoxon rank sum test; $p<0.05$). Thus the completion of the task did not simply reflect prediction of time required to obtain access to reward. Please note that for rat 1 it seems that the curve saturates at large delays before signal presentation. This reflects that fact that for long delays, the rat left the nose-poke too soon before the signal presentation (False Alarm). This has been discussed in the next chapter (Section 4.3.1) where the probability of leaving the nose poke when the stimulus was absent increases with time.

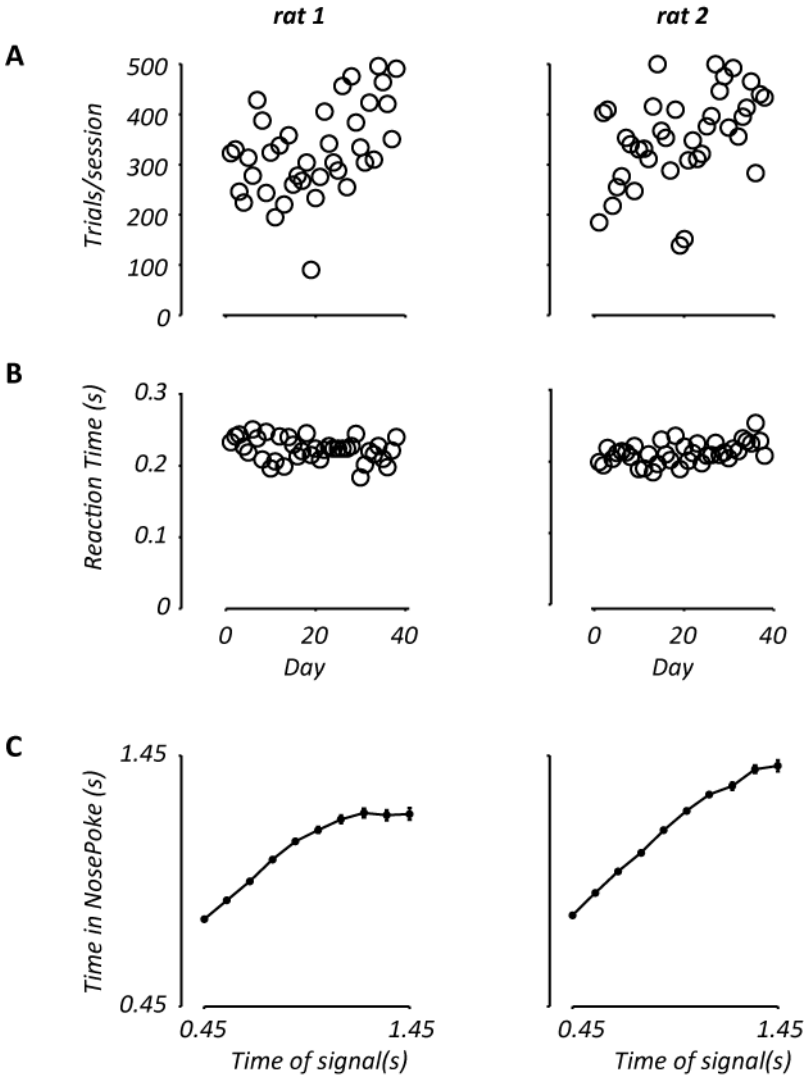

Figure 3.8: A. Both rats performed multiple trials per day. Day 0 indicates the first day when the nose-poke delay variability was 0.45-1.45 sec (uniform distribution). **B.** The mean reaction time, the time between signal onset and the animal's exit from the nose-poke, is plotted across days and was stable across sessions. **C.** Actual time spent at the central nose-poke is plotted against the time of signal occurrence (nose-poke delay). The rats stayed longer in central nose-poke for later signals. Error bars represent ± SEM.

3.3.3 Head and eye stability in the nose-poke

An ideal setup for pairing behaviour with electrophysiological measurements allows restricted range of head movements and the monitoring of eye position. We monitored eye and head position non-invasively using a high-speed video camera. We then analysed the recorded data for each trial by choosing the region of interest around the eye. A custom written Matlab code detected the pupil position at every frame. Figure 3.9 shows an example of chosen region of interest and the detected pupil for rat 1 in the passive task.

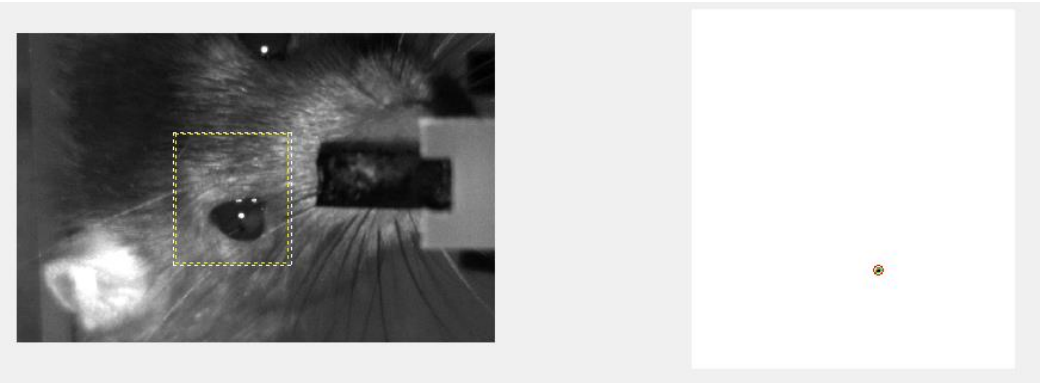

Figure 3.9: An example of the Matlab gui window where the region of interest (dotted lines) around the eye is selected. Please note that the detected pupil within the region of interest is shown on the right (the black dot with detected confidence circles around it).

Figure 3.10A plots the pupil x and y positions relative to the median position during the nose-poke poke duration in one trial. The example images on the top of the figure show the rat's position at times 0, 0.4, 0.8 and 1.2 sec respectively. In this example trial, the head seems to be stable in the nose-poke with small position changes in both x and y axes. The

red dots are the frames which the program detected the current frame to have low correlation (less than 0.2) with the average. Close investigation of these instances revealed that these are the occurrences where there is head movements to get to the central position of the nose-poke or the eye was closed. The positon changes observed in this panel can be due to head or eye movements. We therefore tried to isolate the eye movements by compensating for the head movements using a custom written Matlab code, using affine transformations (rotation and translation) to register the images. The circumference of the eye is the dominant feature, and is what guides the registration. These registered files are then analysed the same as above by finding the pupil x and y position for the same trial (Figure 3.10B). The positional change of the pupil was converted into an angular change in eye position. This was done by using the following formula based on the eye radius of rats (2.623 mm; Zoccolan *et al.*, 2010) and millimetre per camera pixel of our images (0.06):

$$\text{Position in Degrees} = \frac{180}{\pi} \sin^{-1} \frac{|\text{eye position} - \text{median(eye position)} \times \text{MmPerCameraPix}|}{\text{EyeRadius}}$$

Equation 3.1

The eye seems stable and is not moving during the nose-poke. Red dots here also indicate substantial head movements or the eye being closed and therefore the program cannot obtain an estimate of the pupil position. Thus these instances do not indicate eye movement. It is important to note that occasionally the animal's whiskers cover the pupil and distort the estimate of pupil position. As yet we haven't been able to identify an algorithm that can identify these frames generically. An example is at time 1.2 sec where the whisker occluded the pupil (the last image).

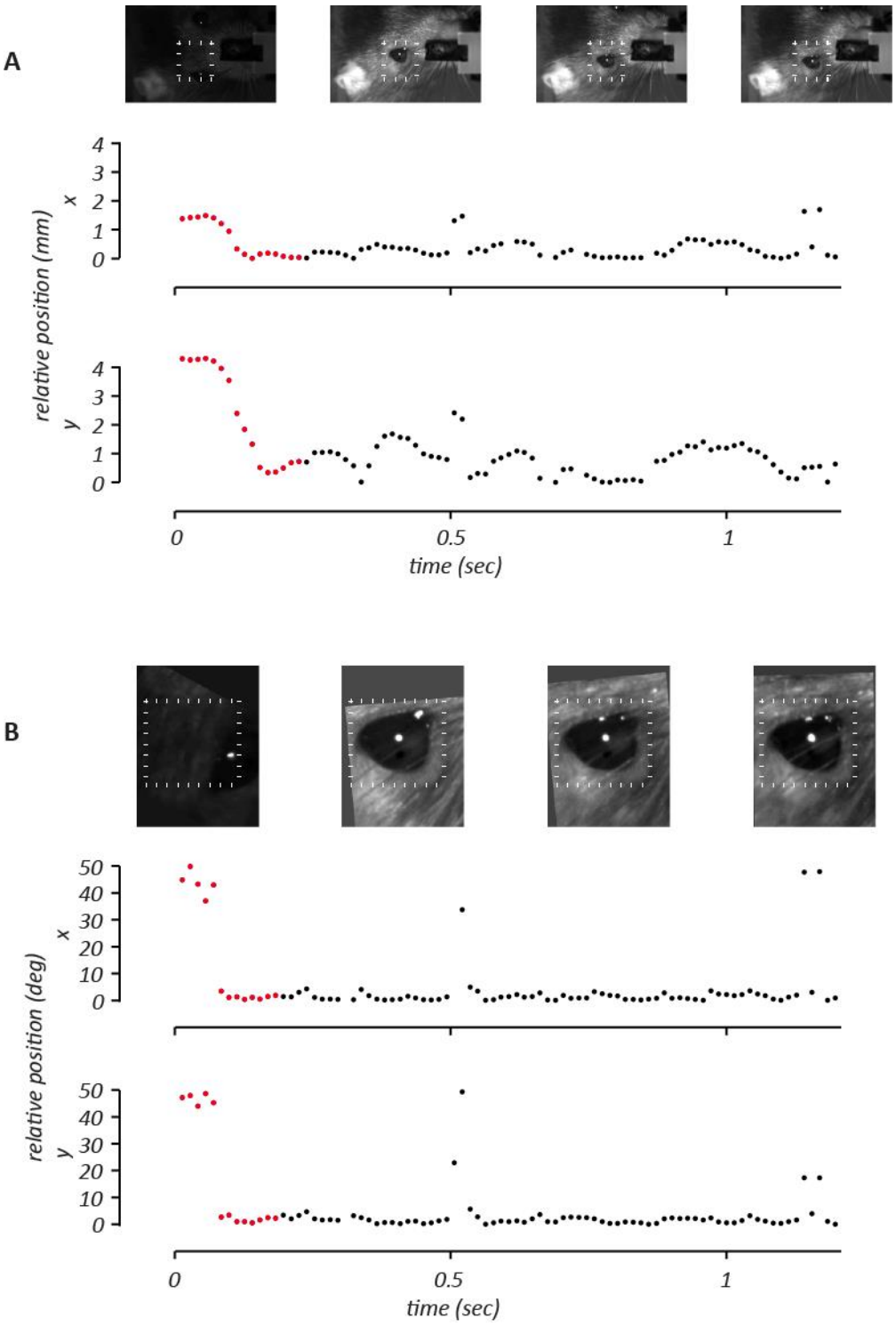

Figure 3.10: An example eye tracking during one trial. A. The pupil x and y relative positions during the nose-poke poke duration. **B.** The pupil x and y relative positions compensated for the head movements. The example images on the top represent 0, 0.4, 0.8 and 1.2 sec respectively. The region of interest is shown as white dotted lines. The red dots are the frames that the program detected the current frame to have low correlation (less than 0.2) with the average.

Across trials (n = 17 for each rat), both rats were stable in the nose-poke with minimal head/eye movements (Figures 3.11, 3.12 and 3.13). The median x and y positions for rat 1 are 0.28 and 0.57 mm respectively. For rat 2, median x and y positions are 0.48 and 1.04 mm respectively. The median eye movements acquired from the registered files compensating for the head movements are as follows for rat1: x position is 1.22 and y position 1.11 degrees. The corresponding values for rat 2 are 3.98 and 3.79 degrees respectively. In general, rat 2 was less stable in the nose-poke.

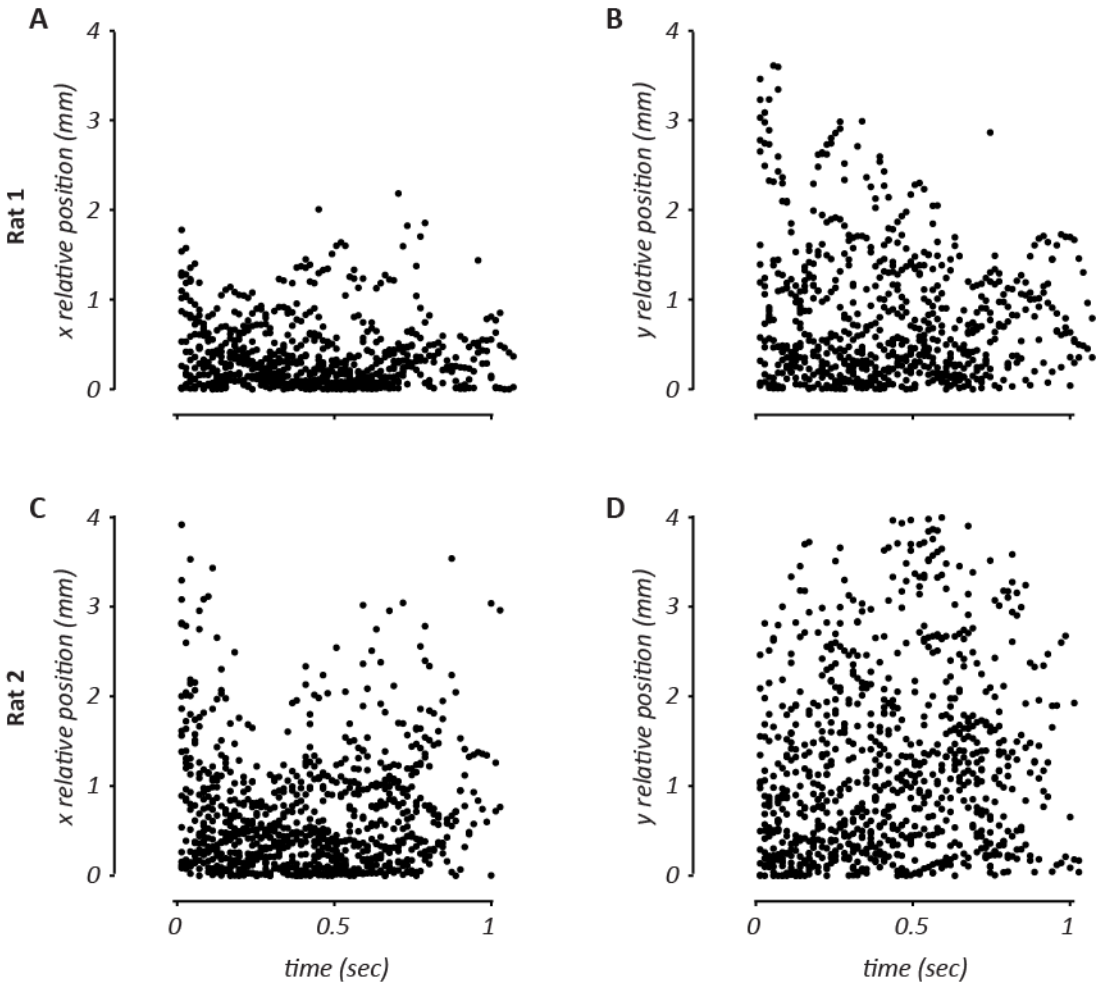

Figure 3.11: Relative pupil positions on every frame during the nose-poke across 17 trials (absolute values are calculated; hence all positive values). The relative positions are plotted

separately for rat 1 (**A.** x positions and **B.** y positions) and rat 2 (**C.** x positions and **D.** y positions).

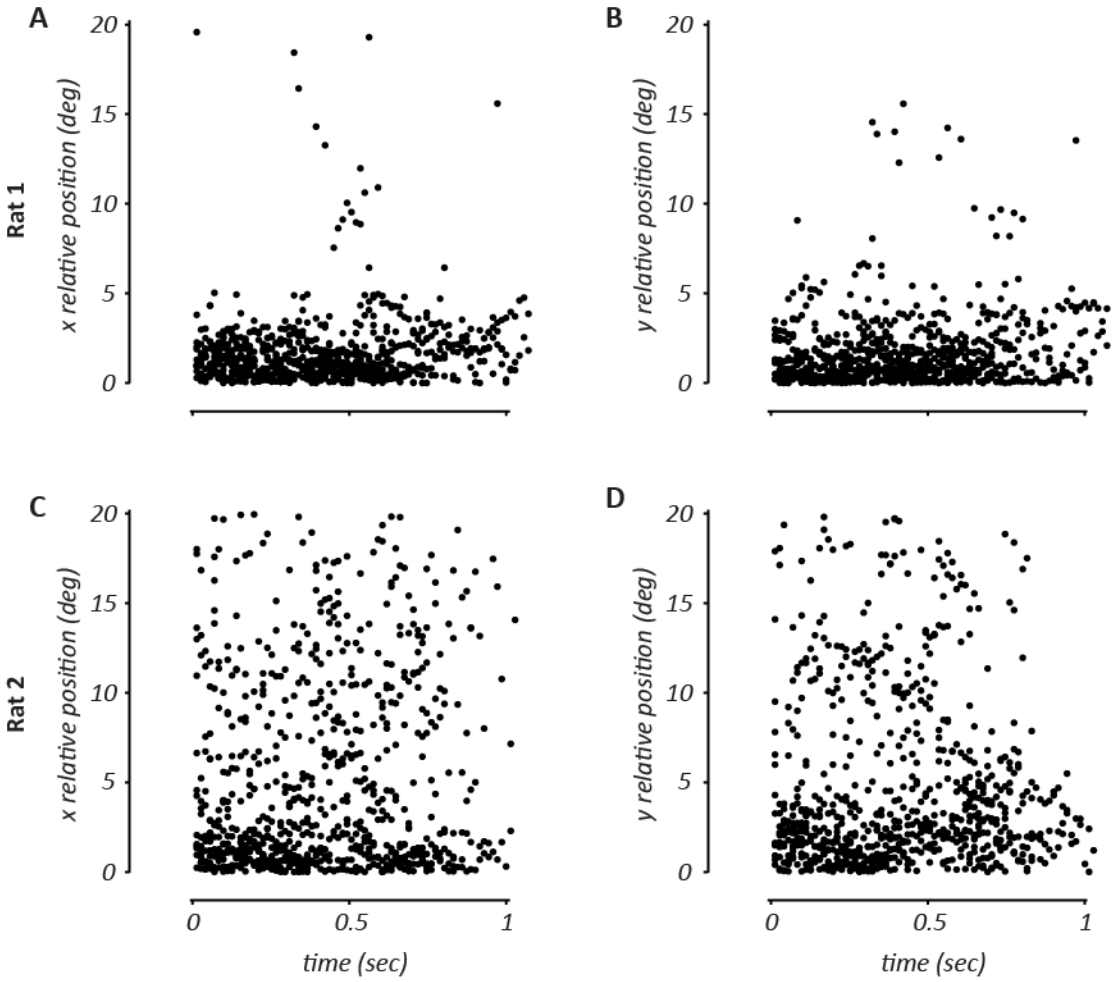

Figure 3.12: Relative pupil positions during the nose-poke across 17 trials compensated for the head movements. The relative positions are plotted separately for rat 1 (**A.** x positions and **B.** y positions) and rat 2 (**C.** x positions and **D.** y positions).

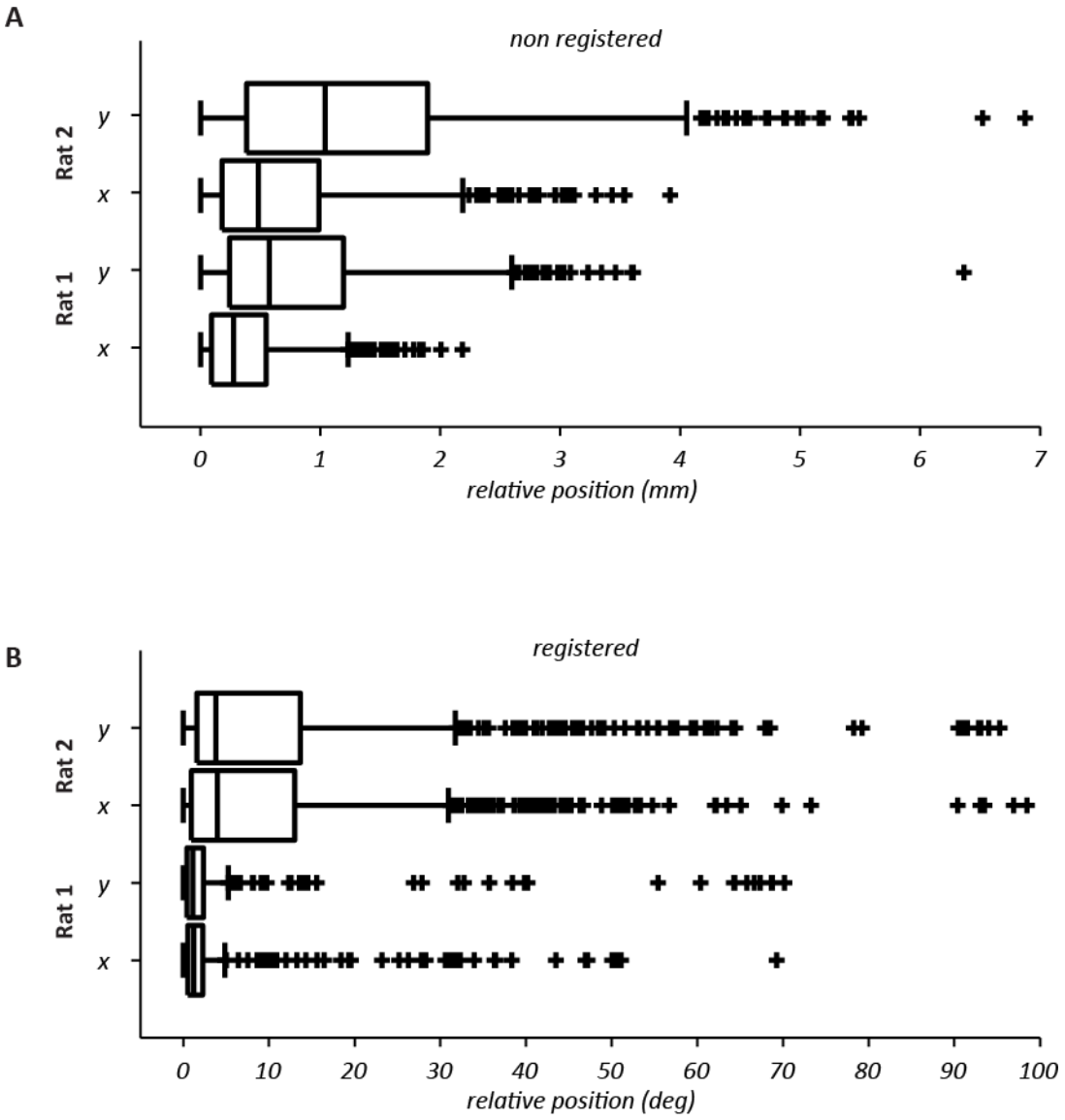

Figure 3.13: Relative pupil positions during the nose-poke across 17 trials. **A.** x and y relative positions for both rats. The median x and y positions for rat 1 are 0.28 and 0.57 mm respectively. For rat 2, median x and y positions are 0.48 and 1.04 mm respectively. **B.** x and y relative positions for both rats compensating for the head movements. The median x and y

positions are for rat1 are 1.22 and 1.11 degrees respectively. The corresponding values for rat 2 are 3.98 and 3.79 degrees respectively. It is important to note the outliers in the relative positions. These outliers indicate those instances that there was substantial head movements or the eye being closed and therefore the program could not obtain an estimate of the pupil position. Thus these instances do not indicate eye movement. It is also important to note that occasionally the animal's whiskers cover the pupil and distort the estimate of pupil position. As yet we have not been able to identify an algorithm that can identify these frames generically.

3.4 Discussion

I have developed a rodent behavioural setup that can easily be paired with electrophysiological measurements. The design is adaptable to a variety of detection and discrimination tasks. The rat's task is to initiate a trial by entering a central nose-poke, and to maintain the nose-poke until a relevant signal indicates availability of reward. Rats successfully performed hundreds of trials in a restricted period of time and learnt to stay in central nose-poke during the nose-poke delay before presentation of the signal. Head position was restricted in the central nose-poke without head-fixation and the eyes could be constantly monitored via video camera. Both rats were stable in the nose-poke with minimal head/eye movements.

3.4.1 Go/NoGo task

The basic task structure is a main step when designing any behavioural experiment probing perceptual decisions. The task structure includes the number of stimuli given to the animals in each trial and the number of responses the animal can produce. One of the simplest designs is a Go/NoGo task where the animal reports the presence of a single stimulus by performing or withholding a single response (for example lick a spout). We

employed a Go/NoGo task for our experiments as it is often used in rodent studies (Abraham *et al.*, 2004; Andermann *et al.*, 2010; O'Connor *et al.*, 2010; Smear *et al.*, 2011; Histed *et al.*, 2012).

Two key issues to consider with Go/NoGo detection tasks are impulsivity and motivation of the animals (Schwarz *et al.*, 2010; Carandini & Churchland, 2013). The motivation and impulsivity of the animal can be examined respectively by the following: does each and every signal lead to a response? And is a response where the signal was not present, due to internal non-sensory drive? It is therefore important to measure not only the rate of correct detections, but also the rate of false alarms. In our experiments, motivation of the animals was high as they performed hundreds of trials per session and the proportion of misses was low. The false alarm rate is a measure of impulsivity and was measured in the trials where signal was going to be presented late (1.35-1.45 sec after the nose poke onset) but the animals left the nose-poke even though the stimulus was not actually presented. Generally, in detection tasks, a false alarm rate of 10-20% is desirable as lower rate has the risk of overestimating detection threshold with conservative animals (Schwarz *et al.*, 2010).

In spite of its demonstrated practicality and efficiency, the Go/NoGo paradigm has three main limitations. These limitations are less applicable to my experiments as I used relatively easy signals for both the passive and active tasks. First, true signal misses can be confounded with lack of motivation such as frustration or satiation. This can be a particular issue in the detection experiments where stimuli of various intensities are used to measure psychometric functions (e.g. contrast psychometric curve). To overcome this problem, it is important to employ stimuli containing not only deflections close to threshold, but also strong supra-threshold stimuli (Schwarz *et al.*, 2010). These strong stimuli serve as constant

monitor for the motivation of the animal over the session as they should have near 100% GO responses if the motivation of the animal is high. Second, true detection of signal is confounded with internal timing predictions or random guessing responses. Sometimes rats lick randomly to increase their chance of receiving reward on hard signals. Using catch trials where no stimulus is actually presented is a good method to measure response due to random licking strategies. The third issue is lack of feedback to the animal in the case of misses and correct rejections. The animal is only rewarded for hits but not correct rejections and is punished (usually by a time-out penalty) for false alarms but not misses. Giving feedback on these trials (i.e. rewarding correct rejections and punishing misses) can however confuse the animal especially in the case of near threshold signals (Schwarz *et al.*, 2010). The reason for a possible confusion in these near threshold trials is that the animal sometimes gets punished (for misses) and sometimes gets rewarded (for correct rejections) while the internal state of the animal is the same (no signal detected).

The distribution of delays between the nose-poke onset and the stimulus that signal the availability of food can either be uniformly distributed or exponentially distributed. In the former case, the frequency of each signal occurrence within a specified range is uniform but the momentary probability of the signal (i.e. the hazard function) increases as time progresses. With the exponentially distributed signals, short delays are more frequent than longer delay, but the momentary probability of the signal is constant across time within the trial. Previous work has shown that rats' response rates remain stable as time progresses during the trial when stimuli are uniformly distributed, whereas their response rates declines when the stimuli are exponentially distributed (Harris *et al.*, 2011). Therefore, in our reaction time active experiments we chose uniformly distributed stimuli. Choosing exponentially distributed stimuli would have led to a flat hazard function however the rats'

response rate would have declined for the low probability late stimuli. This would have promoted a timing strategy and leaving the nose-poke early into the trial.

3.4.2 Adaptability of our design and its contrast with others

A major advantage of our design in studying visual behaviour is that the rats view the monitors directly not through a transparent screen as in some existing set-ups. Another advantage of our set-up is its simplicity by employing a Go/NoGo task. Nevertheless the experimental design is adaptable to two-alternative forced choice (2AFC) with minor modifications. In the 2AFC paradigms, two reward ports are placed on either sides of a central nose-poke and in a discrimination task, the animal has to go to the left or right reward port depending on the trial. The 2AFC paradigm has been successfully developed to study complex visual tasks in rats such as shape processing and objection recognition (Zoccolan *et al.*, 2009; Tafazoli *et al.*, 2012; Vermaercke & Op de Beeck, 2012; Alemi-Neissi *et al.*, 2013; Rosselli *et al.*, 2015). These studies have shown that rats are capable of efficiently processing complex information about a visual object. Extension of our paradigm to 2AFC visual detection and discrimination tasks can be achieved by putting two posts around the nose-poke post for having the reward spouts. The paradigm can also be extended to tasks employing different sensory modalities such as whisker stimulation. A vibrating mesh can be placed on a post next to nose-poke for applying whisker stimuli. Multisensory integration can also be investigated by for example presentation of both visual and whisker stimuli.

3.4.3 Head and eye movement

The design of the experimental apparatus restricted the range of head motions without head-fixation, allowing eye-position to be monitored via video feed. As we did not employ head-fixation, the rats were free to move. Nevertheless they generally kept their head stable at the central nose-poke during visual stimulation. Sriram and Reinagel (2012) monitored the eye position of head-fixed rats in a visual task, using an infrared tracker. They noted that when aroused rats perform very infrequent low-amplitude (<5 degrees) saccades. After saccades, the eye position typically decays back to the central fixation point. The rats maintain fixation within a 5 degrees circle around the mean eye position more than 65% of the time (Sriram & Reinagel, 2012). Similarly, Zoccolan and colleagues (2010) showed that awake head-fixed rats show low amplitude saccades with median amplitude of 3.6 degrees. The inter-saccadic interval had a mean of 137.9 sec however in some cases they observed short inter-saccadic intervals of 0.750 sec (Zoccolan *et al.*, 2010). The infrequent eye movements provide sufficient durations to record neuronal activity and to investigate the correlation between behaviour and neuronal responses. The low amplitude of eye movement further helps to maintain the position of the receptive field within a full-field stimulus.

In our experiments we achieved a measurement of head and eye displacement on the image plane. This is serves as a first-order understanding of whether the rat gaze was stable during a trial. However, unless a calibration procedure is developed, which is able to map the orientation of the head and gaze with respect to the monitor, then no precise information about what monitor location the rat is pointing to (within a trial or across trials) can be achieved (Wallace *et al.*, 2013). Knowledge of absolute head-induced slip could be

obtained by having some form of template, and or head tracking, and this may be a target of future experiments. The apparatus and the analysis here are designed to obtain a relatively stable eye and head position to restrict movements and maintain the position of receptive fields within a large stimulus. Experiments requiring small visual stimulus tailored to the receptive field of neurons should employ a head-fixation apparatus.

4.0 Are rats capable of selective, spatial attention?

4.1 Introduction

Selective attention is a process by which brain focuses on events that offer organisms survival advantages. Selective attention is apparently required because brain does not have the capacity to process all possible information from the outside world and must select those events that are likely to be relevant. Understanding selective attention requires research on animals: it is not possible to simulate attention *in vitro*, because attention is defined by its impact on behaviour; we cannot yet rely on non-invasive methods in humans because we do not yet know how attentional signals are communicated between nerve cells. Non-human primates are currently the primary animal models of selective attention. In this chapter we aim to establish the feasibility of studying selective attention in rodents and develop a behavioural model of selective visual attention in rats.

Humans and other animals often move their eyes, head or body to improve sensory perception, providing one form of selective attention, but the brain can also focus on aspects of the external world without orientation of the body. This covert orienting by the brain is also a form of selective attention. A seminal procedure in the study of human covert attention is the Posner cueing paradigm, where participants direct their gaze to a central fixation point and respond as quickly as possible to a peripheral target, which is preceded by a cue (Posner, 1980). The cue may either be presented close to the fixation point (an arbitrary symbol indicating to where the subject has to orient attention covertly), or close to the peripheral target location. In addition, the cue can correctly indicate the target location on some proportion of trials; on the remainder of trials the cue incorrectly predicts the

target location. This paradigm allows the comparison of performance and reaction time (RT) in conditions where attention is directed to a location (attended), or away from that location (unattended). Performance in detecting a target is typically better and RT is shorter in trials in which the target appears at the cued location (valid trials) than at uncued locations (invalid trials). This improvement in performance is evidence of spatial attention.

The shorter RT and better performance during the Posner cueing paradigm are revealed for certain combinations of variables, including Stimulus-Onset Asynchrony (SOA; the time from the onset of the cue to the onset of the target), cue predictability, and cue type (peripheral or central), suggesting that different processes underlie orienting of attention (Luck & Vecera, 2002; Marote & Xavier, 2011). In humans, RTs to validly cued targets are usually faster for SOAs of up to about 250 ms. This is termed facilitation. In contrast, for SOAs of greater than 300 ms, invalidly cued targets show shorter RTs, and this effect is termed inhibition of return (IOR; Klein, 2000). Therefore the pattern of RTs in the spatial cueing paradigm seems be biphasic, with facilitation at short SOAs followed by IOR (see Samuel and Kat, 2003, for a review).

In covert attention tasks involving humans, participants are asked not to move their eyes and look at a fixation point. Thus, during target presentation, the same sensory information is provided in valid and invalid trials. Likewise, the same motor response is required in valid and invalid trials. Therefore, the difference between RTs in invalid and valid trials reflects both the benefit achieved by the prior orienting of attention towards the expected target location and the costs of prior orienting of attention towards an incorrect target location. Thus in the invalid cue trials, inhibition of attentional focus and the re-orienting of attention is required to detect the target presented at another location (Posner, 1980; Posner & Cohen, 1984).

Variations on the Posner paradigm have been widely used in non-human primates where a monkey has to covertly detect a target on one side of the screen. The target location can be cued by grouping trials into blocks, or by providing a spatial cue shortly before each trial. For example, in block designs, one of the two stimuli will be the location of the change on 80% of trials within the block. If a spatial cue is used, it will be a valid cue on 80% of trials. If the response is made within the allowed time, the monkey receives a reward (e.g. fruit juice). If the monkey responds too early, the trial is aborted, no reward is provided, and the monkey is required to wait (time-out penalty) before the next trial is initiated. That the monkey was attending to one of the locations is established by greater accuracy and shorter RT for targets at the cued location, compared to the uncued location. Bowman and colleagues (1993) showed that macaques can endogenously attend to cued locations, such that faster RT for valid cues is observed for SOAs as short as 100 ms. This is shorter than what is observed in humans. The difference can reflect species differences or the extensive training to achieve the level of performance required in these kinds of behavioural tasks.

The Posner paradigm has not been widely deployed in work on rodent attention. Instead the standard 5-CSRTT paradigm (Carli *et al.*, 1983; Muir *et al.*, 1996; Broersen & Uylings, 1999; Inglis *et al.*, 2001; Milstein *et al.*, 2007; Harati *et al.*, 2008; Bushnell & Strupp, 2009) resembles the following. A rodent is placed in a chamber with five opening ports in a horizontal arrangement along front wall of the chamber and a food port with a transparent door located on the back wall. The animal can initiate a trial by opening door of the food port. A small and brief flash of light is then presented in one of the five ports after a short delay. That task requires the animal to indicate via a nose poke the location of the visual flash. If the animal chooses the correct port, a food pellet or liquid reward is delivered into

the food port. If the animal fails to respond on time or responds in the wrong port, a short period of time-out is presented (e.g. darkness of the chamber) and no reward is delivered. This task is well suited to measuring sustained attention as the animal must maintain attention to all of the ports to detect the flash and respond quickly and accurately, but it is not useful for studying selective spatial attention.

Limited attempts have employed 5-CSRTT or its 3 holes alternative and have explored whether rats can use cues to spatial location (Ward & Brown, 1996; Bushnell, 1998; Weese *et al.*, 1999; Phillips *et al.*, 2000; Bushnell & Strupp, 2009; Marote & Xavier, 2011; Wagner *et al.*, 2014). Marote and Xavier (2011) and Wagner and colleagues (2014) focused on covert orienting of attention itself, while the other studies investigated the effect of lesions or pharmacological interventions on covert attention. Figure 4.1 shows the procedure to test spatial attention in a 2-alternative forced choice (or 3-hole paradigm).

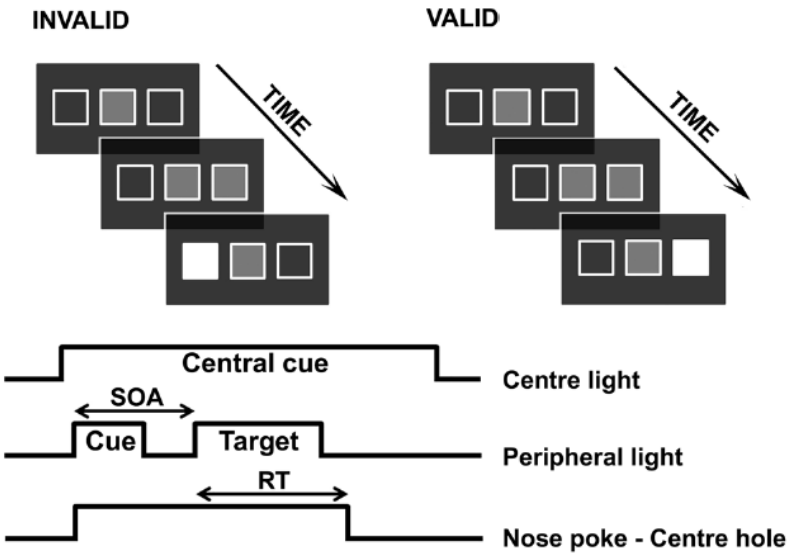

Figure 4.1: 3-hole nose-poke task in rats. Trial starts with a light at the centre port. When the animal nose pokes in the centre port, a cue appears in a peripheral port. The cue is a dim light which is followed by a bright target after a set SOA. RT is defined as the time between onset of the target and nose-poke offset. *Adapted from Wagner et al. (2014).*

Marote and Xavier (2011) used SOAs of 200, 400, 600, 800 and 1200 ms and showed reduced RT or greater accuracy at cued locations for some SOAs. IOR has not been robustly demonstrated in rats (Wagner *et al.*, 2014). These studies have not measured the position of the head or eyes during the task. These studies therefore do not tell us whether improved performance (where present) reflects changes in position of the body with respect to the stimuli, or whether it reflects the allocation of selective attention.

Here we train rats in a visual detection task, where they are required to respond to a change in the luminance or the orientation of a visual stimulus. Rats initiate a trial by nose-poke into a small aperture, after which a visual change (reduction in luminance, or rotation in orientation) occurs in either the left or right visual field, at a random time. Change on either left or right indicates to the animal to leave the aperture and seek sugar water reward from a small spout below it.

To attempt to manipulate spatial attention we utilise two methods: (1) we vary the probability with which the signal is presented on left or right: such that its location is either fully-predictable, random, or in blocks where it is more likely to be presented on one side; (2) we present a spatial cue indicating that the change is more likely to occur on that side than the other. Our aim is to develop a behavioural model of selective visual attention in rats. The work here will complement the more general models of sustained attention in rodents.

4.2 Methods

4.2.1 Subjects

Adult male hooded rats (Long Evans; n = 2; 6 weeks at the start of the training) were obtained from the Florey Neuroscience Institute located at Melbourne University. All procedures were approved by the Animal Care and Ethics Committee at the Australian National University. Rats were housed in an independently ventilated and air filtered transparent plastic box (two rats per box). The colony room was climate controlled and had a 12 hour light-dark cycle, with lights turned off at 7pm. In the 3 days prior to commencement of the study, each rat was handled for 15 minutes per day to accustom them to the experimenter and to ease any anxiety.

4.2.2 Food and water regulation

To provide motivation rats were provided regulated access to food and water, which they were gradually adapted to. Measured rat chow (5g per 100g of body weight) was provided after each daily experiment. Water was removed from the home cage 2-4 hours before the start of the experiment, but was provided ad libitum at all other times. Rats readily adapted to this scheduling of food and water access, showed normal growth trajectories, and no signs of distress. On weekends and days that behavioural experiments were not run, rats received measured rat chow (5g per 100g of body weight) and ad libitum access to water. Weight, social behaviour and grooming behaviour were monitored each week day. We estimated expected weight as 85% of the weight before implementation of food and water regulation, with additional cumulative 3g/wk up to a maximum of 400g. Body weight was always above 85% of the expected weight.

4.2.3 Task Structure

The experimental apparatus, the overall task structure, response categories and shaping procedure have been explained in details in Chapter 3 (Section 3.2.3, Section 3.2.6 and Section 3.2.8). Briefly, I trained rats in a visual detection task, where they were required to respond to a change (0.15 s) in the luminance of a visual stimulus. Rats initiated a trial by nose-poke into a small aperture, after which a visual change (reduction in luminance from white to black) occurred in either the left or right visual field, at a random time (0.45-1.45 sec, uniform distribution). Change on either left or right cued the animal to leave the aperture and seek sugar water reward from a small spout below it within 0.5 sec. On trials that the rats left the nose-poke before 0.15 sec is finished, the stimulus turned off as soon as they left the nose-poke. To promote faster responses, the volume of the sucrose reward was greater for responses within half of the maximum time allowed (Kaneko *et al.*, 2006). We did not set a minimum reaction time for delivering the reward. Licking before the change (false-alarm) caused the trial to be cancelled, presentation of an auditory beep, and a time-out period. After the rats learnt the task with a luminance change of white to black, the signal luminance was reduced - the change was from white to mean luminance grey. Figure 4.2 schematically illustrates the task structure. To test if the rats could transfer their knowledge of visual luminance change to another visual change feature, in additional experiments the signal was a change in the orientation of the visual stimulus. After the rats learnt the task with an orientation change of 90 degrees, the orientation change was reduced gradually to 20 degrees. I will explain these experiments from Section 4.3.2 onwards.

The rats were monitored visually through a closed-circuit video camera and were under constant infrared illumination. A high speed camera above the nose-poke monitored head and pupil positions.

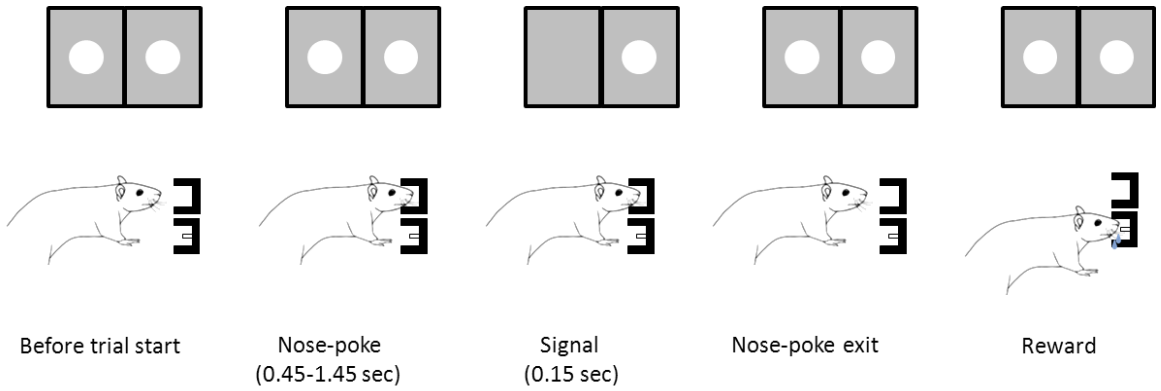

Figure 4.2. Schematic representation of luminance change task. Rats approach a nose-poke aperture and a white circular aperture on a grey background is continually present on each monitor. Rats then initiate a trial by nose-poking into the aperture. After a delay of between 0.45-1.45 sec during which nose-poke is continually maintained, rats receive a visual signal. The visual signal is one of the white apertures briefly turning grey (0.15 sec) signaling the availability of reward. Rats then make a behavioural decision by leaving the nose-poke and entering the reward spout if they identify the presences of the visual signal. Correct detection is rewarded by sucrose water.

4.2.4 Performance calculations

I utilise several methods to compare performance accuracy across different experimental conditions, and in the following I explain why I chose a particular method for the analyses. A conventional way to calculate performance is hits over all the trials as follows:

$$Performance = \frac{Hit}{Hit + Miss + False\ Alarm}$$

Equation 4.1

This is a powerful way to calculate the overall performance of an animal. However, it is important to note that the false-alarms occur before the rat is exposed to the signal and therefore, one cannot assign its occurrence to any within-trial conditions. Thus, the behavioural performance needs to be calculated without considering the false-alarms and then corrected for chance which is based on the occurrence of false-alarms. The performance (p) is corrected using the following formula (Tanner & Swets, 1954):

$$p = \frac{p' - c}{1 - c}$$

Equation 4.2

Where p' is the observed hit rate and c is the false alarm proportion as follows:

$$p' = \frac{Hit}{Hit + Miss}$$

Equation 4.3

$$c = \frac{False\ Alarm}{False\ Alarm + Correct\ Rejection}$$

Equation 4.4

Note that correct rejection is staying in the nose-poke and not leaving the nose-poke while waiting for the late signal to occur. As we didn't have any trials with no signal

appearing, the late stimuli (the last time bin of 100 ms) was used to investigate the false-alarm rate and the correct rejection.

Given that the false-alarm proportion changes with time, the chance performance at any point in time is different. Therefore chance performance needs to be computed separately as a function of time using the following formula:

$$Chance\ performance\ (t)\ =\ c\ (t)\ x\ Probability\ of\ Reward\ (t)\ x\ Bin\ width$$

Equation 4.5

where c is the false-alarm rate at any point in time. Probability of reward at any point in time depends on the maximum execution latency (MEL; maximum time between signal onset and arrival to the reward spout for the reward to be available) and on range of nose-poke delays (time between nose-poke initiation and signal onset). The probability of reward is calculated as follows:

$$0.45 < t < MEL + 0.45 \quad \rightarrow \quad Probability\ of\ Reward\ (t)\ =\ (t - 0.45)\ /\ (1.45 - 0.45)$$
$$MEL + 0.45 \leq t < 1.45 \quad \rightarrow \quad Probability\ of\ Reward\ (t)\ =\ MEL\ /\ (1.45 - 0.45)$$

Equation 4.6

where *MEL* is the maximum execution latency and is 0.5 sec in all the experiments.

4.2.5 Analysis

All Analyses were performed in MATLAB (Mathworks). Multiple factor analysis of variance (ANOVA) with 1 or 2 models was used to compare performance and RT for different experiments and across factors such as SOA and validity. When required, post-hoc analyses involved an analysis of variance of contrast variables (Tukey-Kramer: for multiple comparison of population marginal means).

4.3 Results

In the first set of experiments, I varied the probability with which the signal was presented on left or right: either fully-predictable (100% on one side), random (50% on each side), or in blocks where it was more likely (90%) to be presented on one side (Table 4.1). In experiment 1 the signal was randomly presented on left or right (8 sessions). In experiment 2 the signal was fully-predictable and was presented 100% on one side throughout a given session (16 sessions). In experiment 3 the signal was more likely (90%) to be presented on one side throughout a given session (32 sessions, with the high probability side chosen randomly each session).

Table 4.1: The probability with which the signal was presented on left or right on different experiments. The same colour coding used in this table (Left: Magenta; Right: Cyan) will be used throughout the chapter.

	Left Trials %	Right Trials %
Left high-probability	90 %	10%
Right high-probability	10 %	90 %
Random	50 %	50 %
Left fully-predictable	100 %	0 %
Right fully-predictable	0 %	100 %

4.3.1 Luminance change experiments

4.3.1.1 Rats learn the detection task and show a bias for the left side

In the luminance change detection task the signal was reduction in luminance from white to grey for 0.15 second. Both rats learned the task, completing hundreds of trials per session (rat 1: 324 ± 14; rat 2: 350 ± 14). To characterize overall performance for left and right stimuli, for each rat we first combine the trials of a given side across sessions in which

the signal was randomly presented on left or right (50% on each side). False alarm rates were generally low and consistent for both rats (Figure 4.3; rat 1: mean = 25.80 ± 0.86 %; rat2: mean = 19.66± 0.71 %; all reported error measures are standard errors). As in this experiment left and right signals were presented randomly within each session, false-alarm rates are the same for right and left sided signal (the signal is not presented to the animal when it leaves). While the side on which the signal was presented was chosen randomly, both rats showed a leftward bias in performance: hit rates were higher and misses were lower for left sided signals than the right sided signals (Figure 4.3).

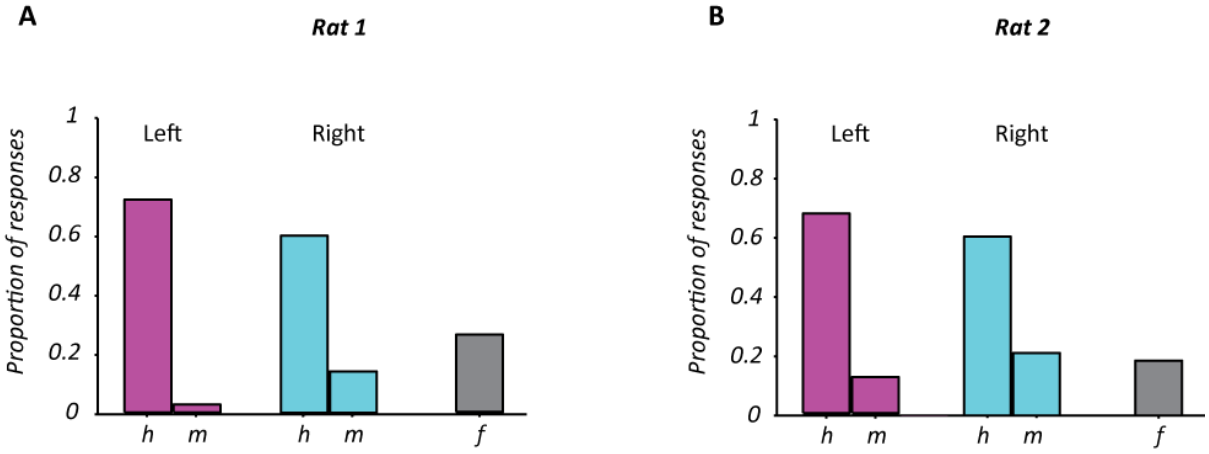

Figure 4.3: The proportion of hits (h), misses (m) and false-alarms (f) in the luminance detection task is plotted separately for **A.** Rat 1 and **B.** Rat2. False alarm rates are the same for right and left sided signal because in these trials the signal is not presented to the animal when it leaves.

To ensure that behaviour was based on signal detection and not non-specific strategies such as an internal clock, the signal was presented after a variable nose-poke delay time (uniformly distributed from 0.45 sec to 1.45 sec). Figure 4.4 A&B illustrate the performance (defined as hits over all the trials; Equation 4.1) as a function of the time after nose-poke that the stimulus was presented. Please note that each session is divided into 10 time bins. These time bins are formed based on the time the signal occurred and are 100 ms each. In both rats performance drops for later signals. In these analyses I use the conventional method, where false alarm rates are considered in the calculation for each time bin. The false alarms, however, occur irrespective of any experimental manipulation as by definition they happen before the rats are exposed to the signal. It is therefore important to consider the false alarm rates separately.

At any point in time, the probability of leaving the nose poke when the stimulus was absent is plotted in Figure 4.4 C&D (Equation 4.4). For both rats, this measure of false alarm rate increases with time. Performance measures can be recalculated to factor out this increase in false alarm rate (Section 4.2.4) and Figure 4.5 A&B show this corrected performance (black symbols; Equation 4.2). The corrected measures are very similar to performance calculated simply on the basis of hits and misses trials (grey symbols; Equation 4.3). As described in section 4.2.4, the chance performance at any point in time is calculated based on the false alarm rate for that time (red dashed line; Equations 4.5 and 4.6). In Figure 4.5C&D, the performance is plotted separately for left and right side. For both rats the performance was greater for the left sided than right sided targets and especially higher at early delay times (t-test p-value < 0.01).

Because the analyses produce such similar results, but the conventional measure is easier to comprehend and calculate, throughout the rest of the chapter I will use proportion

of hits over hits and misses as the measure of performance when comparing different conditions (Equation 4.3).

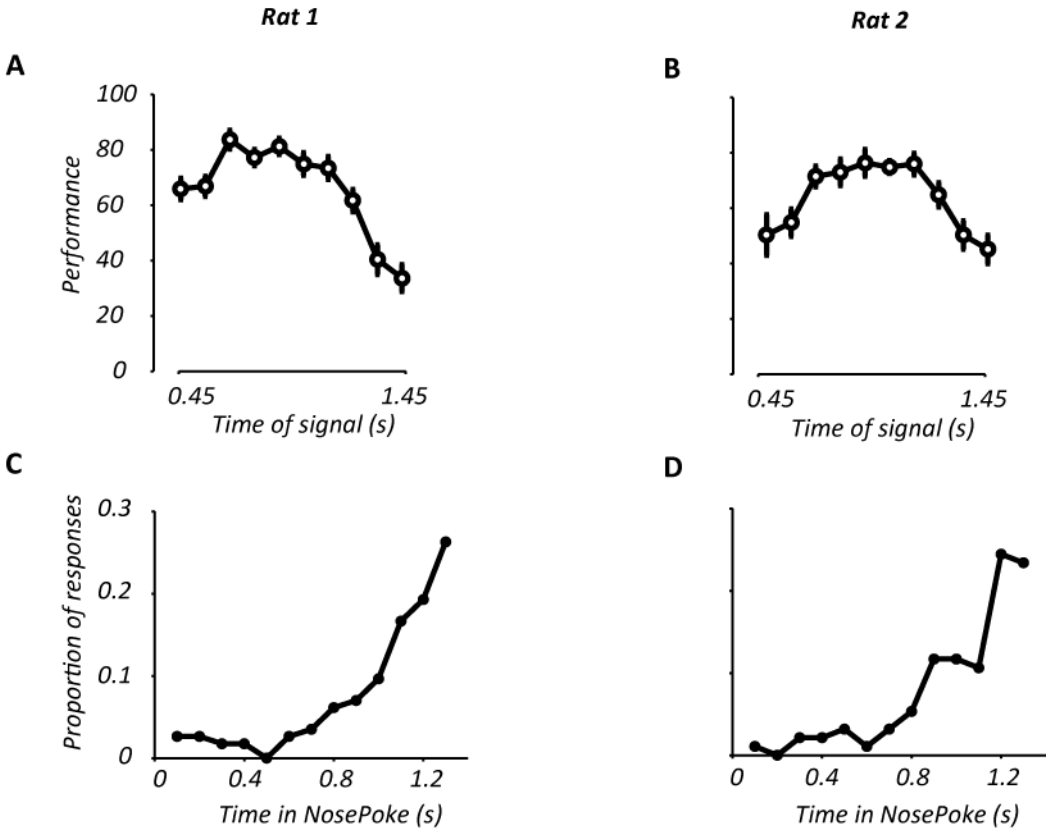

Figure 4.4: The performance defined as hits over all the trials is plotted as a function of the time signal after nose-poke initiation for **A.** Rat 1 and **B.** Rat2. In both rats performance drops for later signals. Error bars represent ± SEM. False-alarm rate at any point in time after nose-poke initiation is plotted for **C.** Rat 1 and **D.** Rat2. False-alarm rate is the probability of leaving the nose-poke when the stimulus was absent.

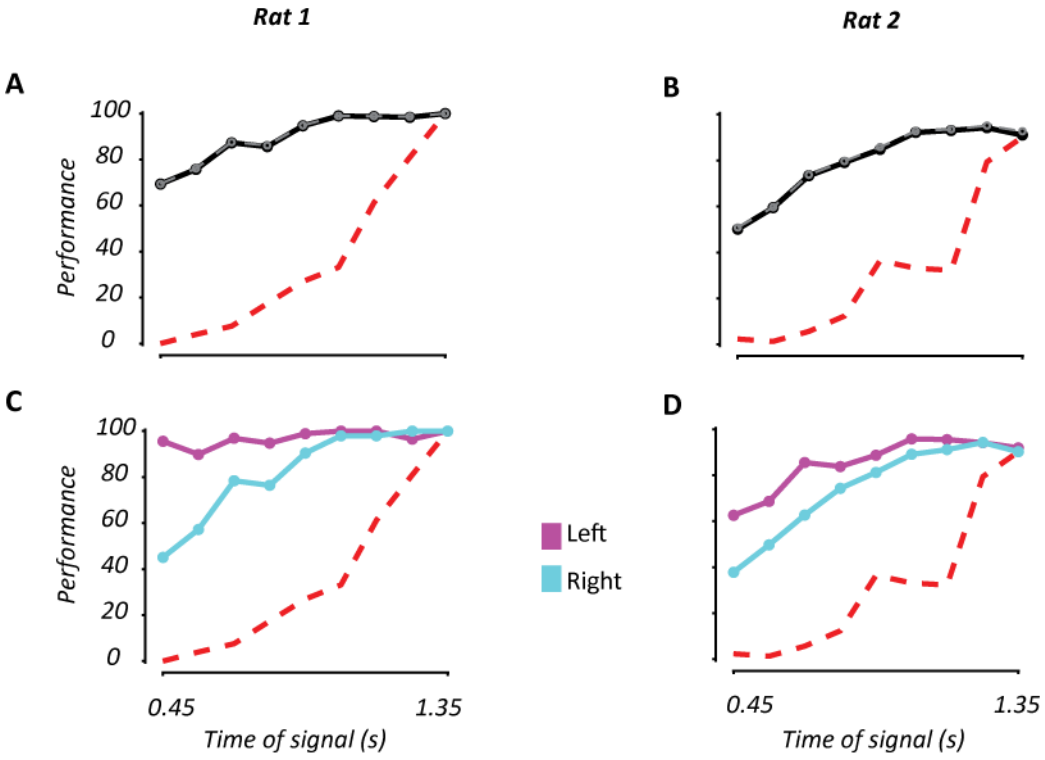

Figure 4.5: Performance measures corrected for the false-alarm rate increase overtime is plotted in black for **A.** Rat 1 and **B.** Rat2. The grey lines plot the performance measures defined as hits over hit and miss trials. The red dashed lines plot the chance performance at any point in time which is calculated based on the false alarm rate for that time. The corrected performance is plotted separately for left and right sided signals for **C.** Rat 1 and **D.** Rat2

4.3.1.2 Reaction time

We used several analysis techniques to explore the difference in RT (the time between signal onset and nose-poke exit) between different conditions. In this section I will

present these techniques for comparing RT for the signals that were randomly presented to left and right sides. In later sections I will return to the RT comparison between different predictability conditions.

Figure 4.6 shows RT comparisons for left and right sided signals (rat 1: panels A-E; rat 2: panels F-J). Consistent across all the analysis techniques, rat 1 had faster RT for the left side than right side (t-test pvalue < 0.01) whereas rat 2 showed similar RT for both sides (t-test pvalue > 0.05). For rat 1, the distribution of RT for left sided signals showed an earlier and sharper peak than those for right-sided signals (panel A). The overlap between the two RT distributions was quantified by applying multiple criterion levels, ranging from the minimum to the maximum observed RT. The cumulative response functions are then plotted for both left and right sides as a function of RT (panel B). The obtained cumulative response functions for left and right are then plotted against each other (panel C). The area under the curve was then calculated by sum of the trapezoids between two consecutive criteria (connected by straight lines). The area of the curve falls within the range of 0 to 1 where 0.5 reflects no difference between the distributions. Statistical significance was determined by rearranging the two RT distributions 1000 times (shuffling of the two distributions).

For rat1, the RT to left side was significantly faster than the right side (area under the curve = 0.6; $p<0.01$). The median RT was faster for left side than the right side (panel D; $p<0.01$) and this difference was preserved across different signal delay times (panel E). With the same format as panels A-I, panels F-J compare the RT for left and right sided target for rat 2. This rat's RT was similar for left and right signals despite the greater performance for the left sided targets. Both rats showed faster RT for later signal times (Figure 4.6 E&J). As

the experiment consisted of variable signal delays (0.45-1.45 sec), the animals' expectation of a signal increases with time. This is almost certainly the reason that the RT is faster for later signals.

The results from different RT comparison techniques are consistent with each other. Thus for simplicity purposes, to compare RT between different predictability conditions, I will only present the cumulative response analysis throughout the rest of the chapter.

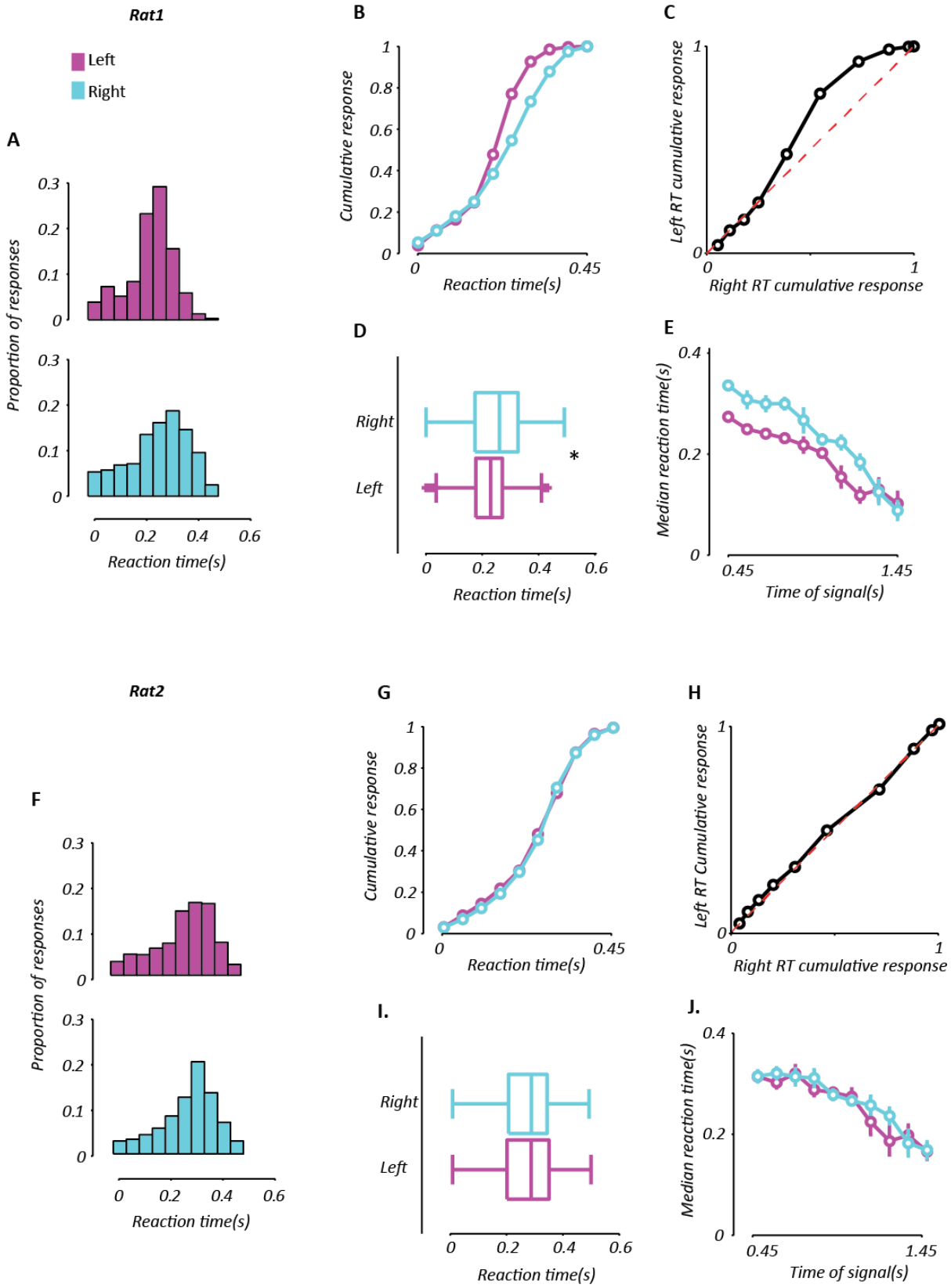

Figure 4.6: Reaction time comparisons for left and right sided signals. A. The RT distribution for left and right sided signals for rat 1. **B.** The cumulative response functions for

both left and right sides as a function of RT. **C.** The cumulative response functions for left and right plotted against each other. **D.** Box and whisker plot of right and left RT showing that the median RT was faster for left side than the right side. **E.** Left and right RT across different signal delay times. Error bars represent ± SEM. With the same format as panels **A-I**, panels **F-J** compare the RT for left and right sided target for rat 2.

4.3.1.3 Effects of predictability on performance luminance change experiments

Does being able to predict the likely side of the stimulus modulate the speed and accuracy of stimulus detection in rats? To address this question, we varied the probability with which the signal was presented on left or right: either fully-predictable (100% on one side; 16 sessions), random (50% on each side; 8 sessions), or in blocks where it was more likely (90%) to be presented on one side (32 sessions, with the high probability side chosen randomly each session).

Consistent with the above results where the signal was randomly presented on left or right (section 4.3.1.1), hit rates were higher and misses were lower for left sided signals than the right sided signal in other experiments (Figure 4.7). The overall false alarm rate was high for the experiments where the signal was always or most of the time presented on the right side.

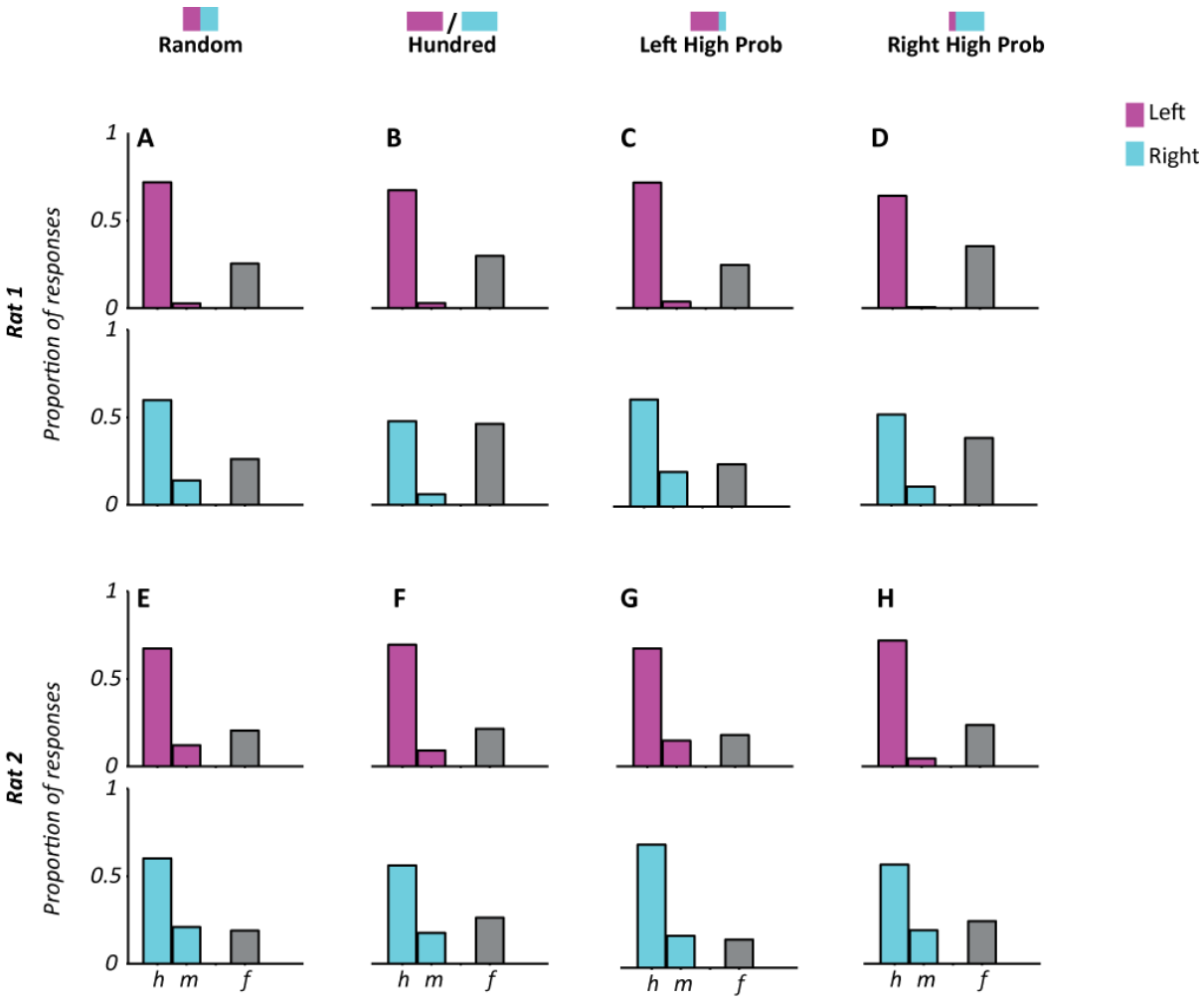

Figure 4.7: The proportion of hits (h), misses (m) and false-alarms (f) in the luminance detection task for different predictability modulation experiments. Panels **A-D** show the proportion of responses for rat 1. **A.** The sessions where the signal was presented randomly on left or right (50% on each side). **B.** The sessions where the signal was fully-predictable (100% on one side). **C.** The sessions where the signal was presented on the left side on 90% of the trials and 10% on the right. **D.** The sessions where the signal was presented on the right side on 90% of the trials and 10% on the left. Panels **E-H** show proportion of responses for rat 2.

Figure 4.8 shows performance in different predictability manipulations. Please note that each session is divided into 10 time bins. These time bins are formed based on the time the signal occurred and are 100 ms each. Therefore for each predictability condition and each stimulus side, the data from all the sessions of the same time bin have been pooled together. For rat 1, the performance for the left side was high on all the experiments (panel A). Multiple factor ANOVA with 2 models, revealed significant effect of time of signal and predictability group ($F_{9,544} = 8.35$; $F_{3,544} = 5.36$; $p<0.01$). There was a significant performance difference (post-hoc contrast test using Tukey-Kramer) between high probability and low probability trials such that the performance on the low probability trials was 2.5% higher. Multiple factor ANOVA also revealed significant time x group interaction effect ($F_{27,544} = 3.26$; $p<0.01$), indicating that the magnitude of the difference between groups depended on signal time. For the right side (panel B), there were significant effects of time of signal and group ($F_{9,544} = 42.38$; $F_{3,544} = 7.68$; $p<0.01$) but the interaction was not significant ($F_{27,554} = 0.91$; $p>0.05$). The rat's performance was significantly higher for the sessions when the signal was fully presented on the right compared to the other predictability modulation conditions.

Similar to rat 1, rat 2 had significant performance effect for the left side on the time of signal and group as well as interaction between the two (panel C; $F_{9,569} = 49.05$; $F_{3, 569} = 49.26$; $F_{27, 569} = 4.21$; $p<0.01$). The performance was significantly higher for the low probability trials compared to all the other conditions. Performance was significantly lower for high probability trials compared to the fully predictable trials. For the right sided signals

(panel D), the performance was significantly different across groups and across time ($F_{3,578} = 5.63$; $F_{9, 578} = 46.38$; $p<0.01$). The time x group interaction effect was not significant ($F_{27, 578} = 0.82$; $p>0.05$). The rat's performance was significantly higher for the low probability trials compared to the high probability and fully predictable trials.

Together, these results indicate that performance was modulated by predictability, but there was substantial variability between rats and the spatial arrangement of the stimuli. Indeed performance seems to be slightly higher for the low probability trials compared to the other conditions (except for the right sided signals in rat 1 where performance was highest in the fully predictable condition).

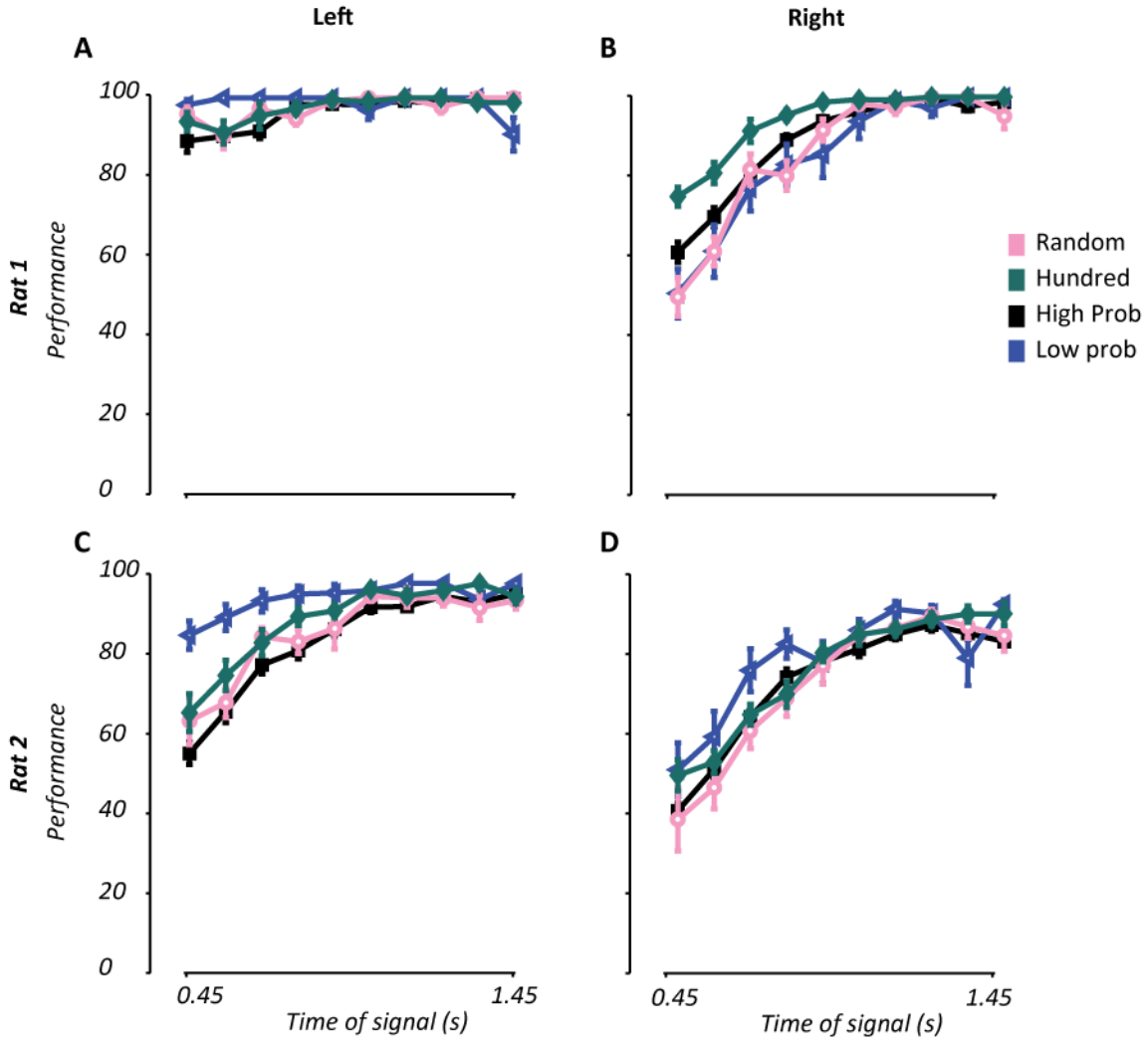

Figure 4.8: Performance comparison across different predictability modulation experiments in the luminance **change tasks. A.** Performance comparisons for left sided targets in rat 1, **B.** for right sided targets in rat 1, **C.** for left sided targets in rat 2 and **D.** for right sided targets in rat 2. Performance is calculated as hits over hits and misses (Equation 4.3). Error bars represent ± SEM.

4.3.1.4 Effects of predictability on reaction time in luminance change experiments

RT was systematically modulated by predictability: across both rats and spatial arrangement, RT was fastest for the fully-predictable and slowest for the random signals. When intermixed, RT was faster on low-probability than high-probability trials.

For rat 1, the RT for the left sided targets was significantly different between different predictability conditions (Figure 4.9 panel A; One-way ANOVA; $F_{3,6628} = 23.68$; $p<0.01$). We performed a multiple comparison (Tukey-Kramer) of reaction times using one-way ANOVA. This method determines which means are significantly different using confidence level of 95 %. Small graphs on Figure 4.9 show the mean reaction time for each condition and the magnitude of the differences. These panels display a graph of the means comparisons with the confidence intervals around them. Non-overlapping confidence intervals show a significant difference (p-value <0.05). RT was significantly slower for the random signals compared to the other three conditions, and was significantly faster for fully-predictable than other conditions. In addition RT was significantly faster on low-probability than high-probability trials (post-hoc contrast test using Tukey-Kramer). RT for right sided targets was also significantly different between experiments (panel B; $F_{3,6136} = 26.28$; $p<0.01$).

For rat 2, RT for the left sided targets was significantly different between experiments (panel C; One-way ANOVA; $F_{3,6875} = 30.77$; $p<0.01$). Similar to rat 1, RT was significantly slower for the random signals compared to the other three conditions (post-hoc contrast test using Tukey-Kramer). It was significantly faster for fully-predictable than other conditions. RT for the right sided targets was also significantly different between experiments (panel D; $F_{3,6136} = 35.42$; $p<0.01$).

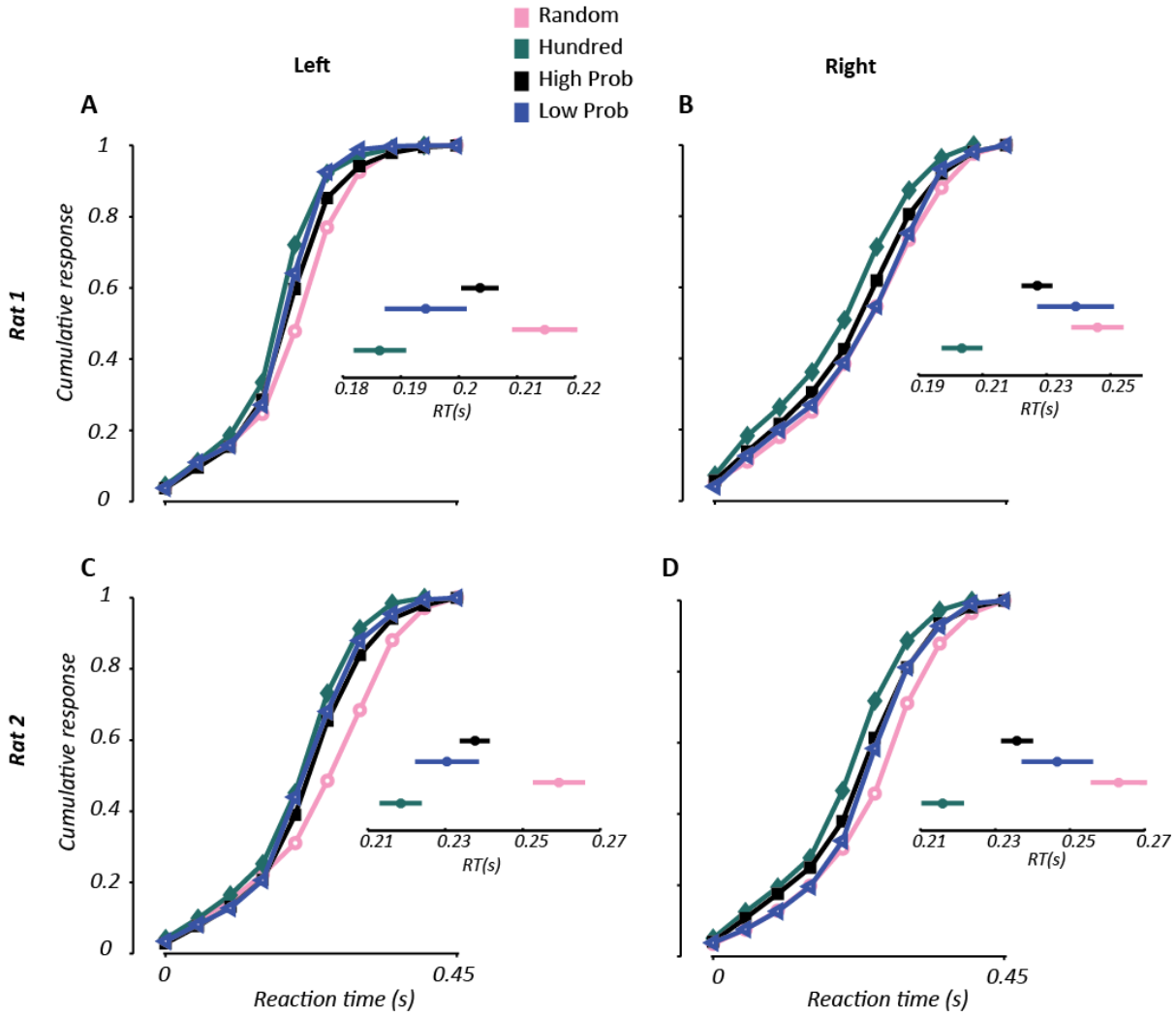

Figure 4.9: Reaction time comparison across different predictability modulation experiments in the luminance change tasks. A. Cumulative for left sided targets in rat 1, **B.** for right sided targets in rat 1, **C.** for left sided targets in rat 2 and **D.** for right sided targets in rat 2. Small graphs on the figure show the mean reaction time for each condition and the magnitude of the differences. These panels display a graph of the means comparisons with the confidence intervals around them. Non-overlapping confidence intervals show a significant difference (p-value <0.05).

4.3.2 Orientation change experiments

The orientation change experiments were similar to the luminance change tasks except the rats were required to respond to a change of orientation of one of the gratings (0.15 sec) instead of the luminance change. As schematically illustrated in Figure 4.10, rats initiated a trial by nose-poke into a small aperture, after which a rotation in orientation occurred in either the left or right visual field, at a random time (0.45-1.45 sec, uniform distribution). Change on either left or right cued the animal to leave the aperture and seek sugar water reward from a small spout below it within 0.5 sec.

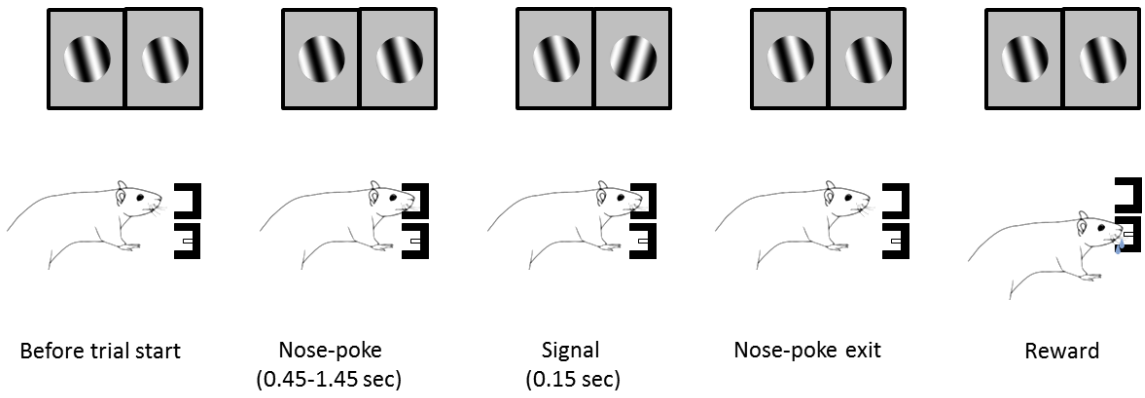

Figure 4.10: Schematic representation of orientation change task. Rats approach a nose-poke aperture and a circular grating on a grey background is continually present on each monitor. Rats then initiate a trial by nose-poking into the aperture. After a delay of between 0.45-1.45 sec during which nose-poke is continually maintained, rats receive a visual signal. The visual signal is one of the gratings briefly changes orientation (0.15 sec) signaling the availability of reward. Rats then make a behavioural decision by leaving the nose-poke and entering the reward spout if they identify the presences of the visual signal. Correct detection is rewarded by sucrose water.

4.3.2.1 Effects of predictability on performance in orientation change experiments

Similar to the luminance change task, both rats learned the orientation change task and showed a leftward bias in performance. When the side on which the orientation change occurred was chosen randomly, for both rats, hit rates were higher and misses were lower for left sided signals than the right sided signals (Figure 4.11A&B). For both rats, the misses and false alarm rates were very similar to the luminance change experiment (refer to Figure 4.3) suggesting that rats' overall motivation and impulsivity remained the same over months of training. Figure 4.11C&D plots the performance at any point in time separately for left and right side. For both rats the performance was greater for the left sided than right sided targets and especially higher at early delay times.

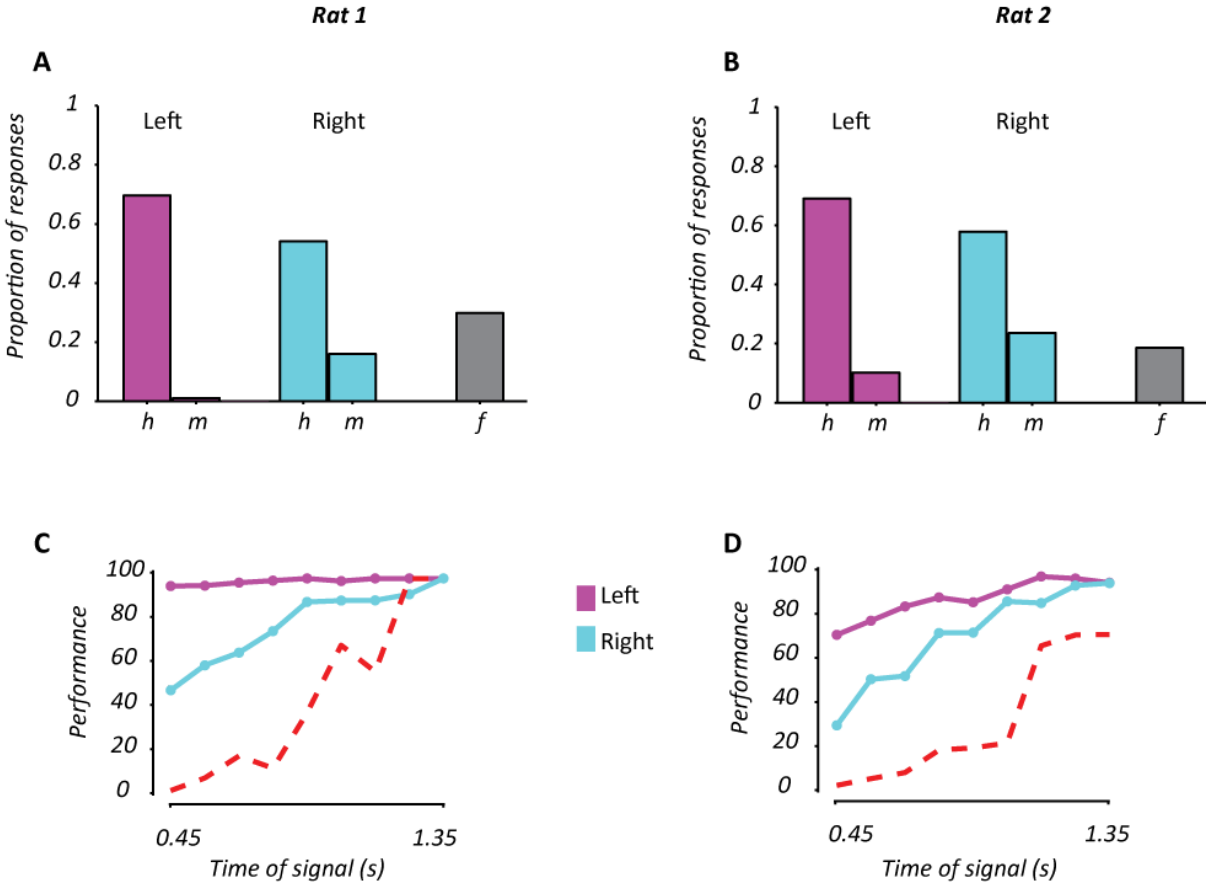

Figure 4.11: The proportion of hits (h), misses (m) and false-alarms (f) in the orientation change task is plotted separately for **A.** Rat 1 and **B.** Rat2. False-alarm rates are the same for right and left sided signal because in these trials the signal is not presented to the animal when it leaves. Performance measures corrected for the false-alarm rate increase overtime and are plotted separately for left and right sided signals for **C.** Rat 1 and **D.** Rat2. The red dashed lines plot the chance performance at any point in time which is calculated based on the false-alarm rate for that time.

Figure 4.12 shows performance in different predictability manipulations. For rat 1, the performance for the left side was high on all the experiments (panel A). Multiple factor ANOVA revealed significant effect of time of signal and predictability group ($F_{9,271} = 6.08$;

$F_{3,271} = 9.2$; $p<0.01$). The performance was significantly lower for the condition where the signal was fully-predictable than the other three conditions (Tukey-Kramer: for multiple comparison of population marginal means; $p<0.05$). ANOVA also revealed significant time x group interaction effect ($F_{27,271} = 1.97$; $p<0.01$), indicating that the magnitude of the difference between groups depended on signal time. For the right side (panel B), there were significant effects of time of signal and group ($F_{9,273} = 50.60$; $F_{3,544} = 25.95$; $p<0.01$) and their interaction was also significant ($F_{27,273} = 1.87$; $p<0.01$). The rat's performance was significantly lower for the low-probability trials compared to all the other predictability conditions.

Rat 2 had significant performance effect for the left side on the time of signal and group as well as interaction between the two (panel C; Multiple factor ANOVA; $F_{9,273} = 20.96$; $F_{3,273} = 27.73$; $F_{27,273} = 2.85$; $p<0.01$). The performance was significantly lower for the fully-predictable condition compared to all the other conditions (Tukey-Kramer: for multiple comparison of population marginal means; $p<0.05$). Performance was significantly lower for high-probability trials compared to low-probability trials. For the right sided signals (panel D), the performance was significantly different across groups, time as well as their interaction ($F_{3,274} = 44.31$; $F_{9,274} = 20.24$; $F_{27,274} = 2.25$; $p<0.01$). The rat's performance was significantly higher for the low-probability trials compared to all the other predictability modulation conditions. Performance was significantly lower for the fully-predictable trials than the high-probability trials.

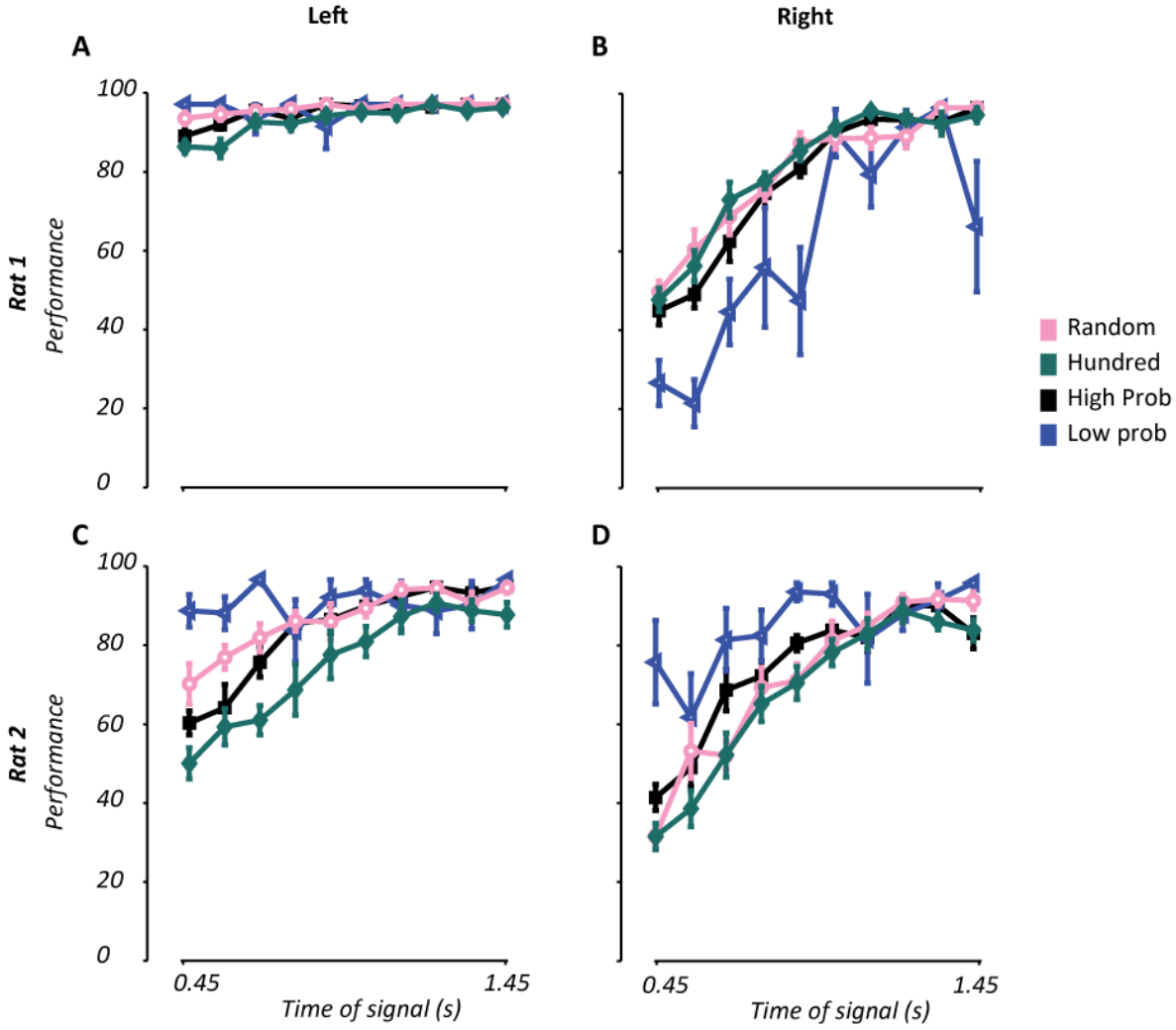

Figure 4.12: Performance comparison across different predictability modulation experiments in the orientation change tasks. A. Performance comparisons for left sided targets in rat 1, **B.** for right sided targets in rat 1, **C.** for left sided targets in rat 2 and **D.** for right sided targets in rat 2. Performance is calculated as hits over hits and misses (Equation 4.3). Error bars represent ± SEM.

4.3.2.2 Effects of predictability on reaction time in orientation change experiments

RT was systematically modulated by predictability. For rat 1, the RT for the left sided targets was significantly different between different predictability conditions (Figure 4.13 panel A; one-way ANOVA; $F_{3,4307}= 8.59$; $p<0.01$). RT was significantly slower for the fully-predictable signals compared to random and low-probability signals. RT was significantly faster on low-probability than random trials. The RT for the right sided targets was also significantly different between experiments (panel B; $F_{3,3779} = 8.87$; $p<0.01$). RT was significantly faster for fully-predictable compared to all three other conditions.

For rat 2, the RT for the left sided targets was significantly different between experiments (panel C; $F_{3,4465} = 6.94$; $p<0.01$). RT was significantly faster for the fully-predictable signals compared to random and high-probability signals. RT for the right sided targets was also significantly different between experiments (panel D; $F_{3,3924} = 5.02$; $p<0.01$). RT was significantly slower for the random signals compared to fully-predictable and high-probability conditions.

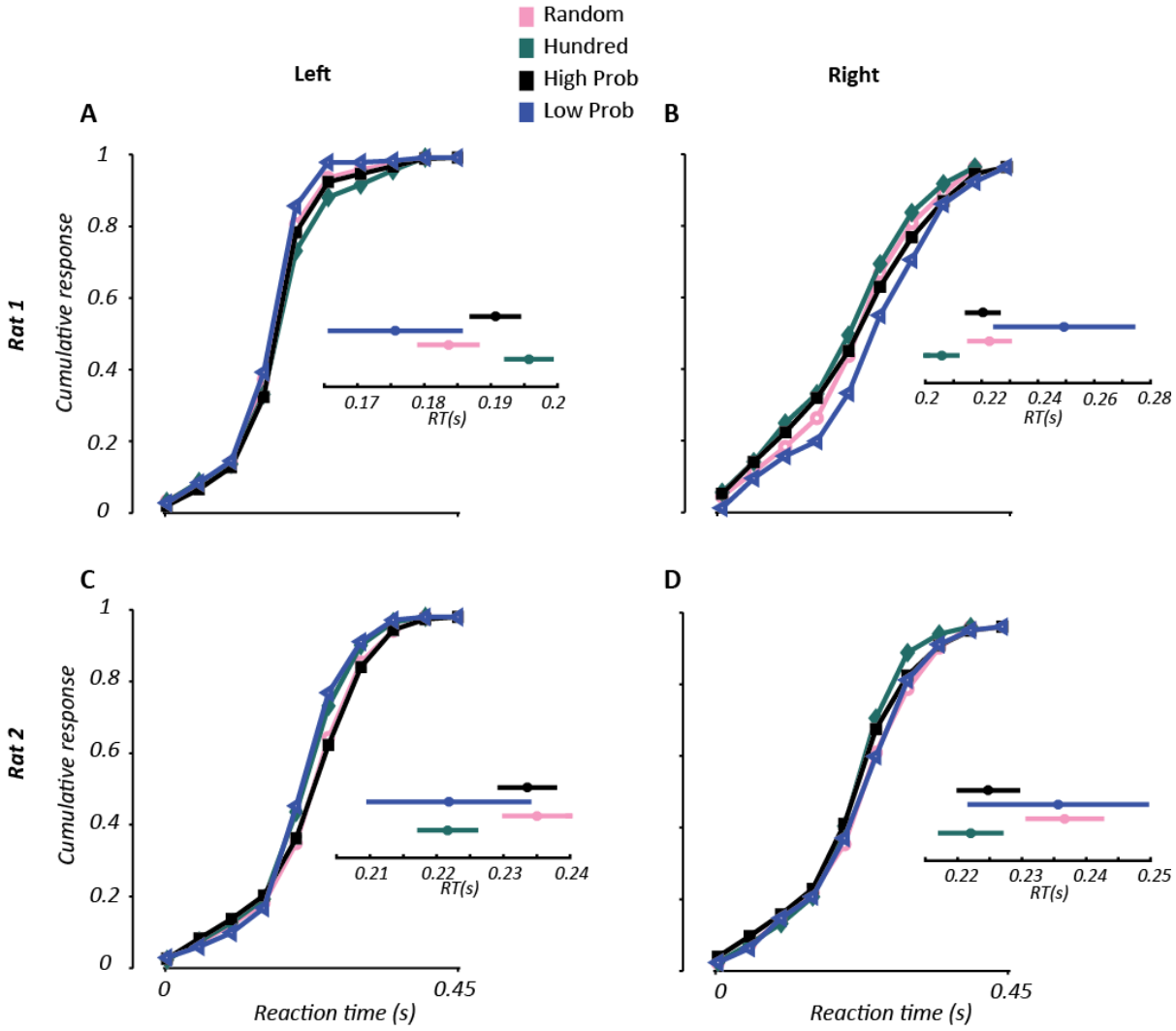

Figure 4.13: Reaction time comparison across different predictability modulation experiments in the orientation change tasks. A. Cumulative RT for left sided targets in rat 1 **B.** for right sided targets in rat 1 **C.** for left sided targets in rat 2 **D.** for right sided targets in rat 2. Small graphs on the figure show the mean reaction time for each condition and the magnitude of the differences. These panels display a graph of the means comparisons with the confidence intervals around them. Non-overlapping confidence intervals show a significant difference (p-value <0.05).

In summary, RT was systematically modulated by predictability in both luminance and orientation change experiments. Together, across both rats and both sides, it was fastest for the fully-predictable (204ms) and slowest for the random signals (235ms). The RT was on average 6ms faster on low-probability than high-probability trials.

4.3.3 Spatial cueing experiments

In the next stage, the same rats were trained in a cued version of the previous paradigm to signal the rats as to the location of the target. In this set of experiments, we presented the spatial cue (0.2 sec) as soon as the rats entered the nose-poke. The spatial cue was black screen around the grating (Figure 4.14). The rats were required to respond to the orientation change of either left or right grating at a random SOA time (time between the onset of the cue and the signal presentation; 0.45-1.45 sec, uniform distribution).

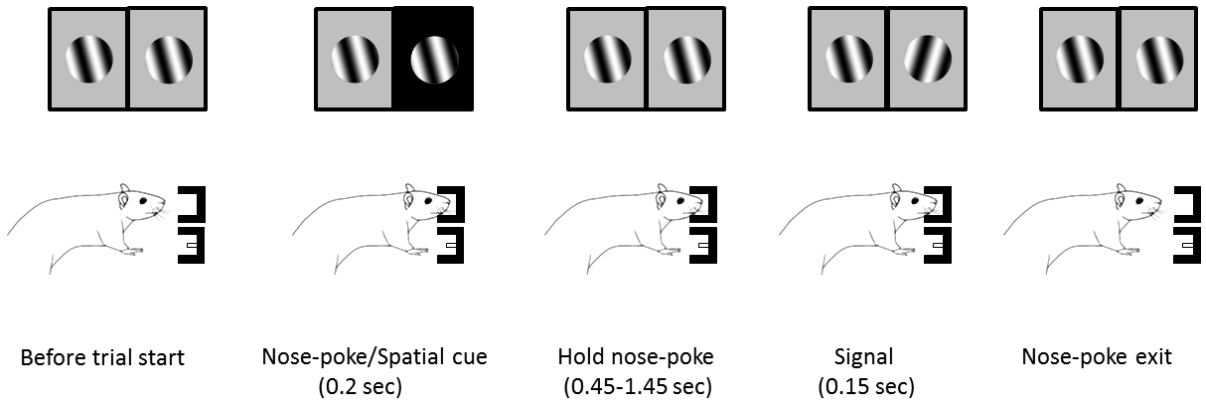

Figure 4.14: Schematic representation of spatial cueing orientation change task. Rats approach a nose-poke aperture and a circular grating on a grey background is continually present on each monitor. Rats then initiate a trial by nose-poking into the aperture when a spatial cue of black screen around the grating (0.2 sec) appeared. The example in this figure is a valid cue where the cue side is on the same side as the orientation change. After a delay of between 0.45-1.45 sec during which nose-poke is continually maintained, rats receive the orientation change signal. The visual signal is one of the gratings briefly changed orientation (0.15 sec) signaling the availability of reward.

4.3.3.1 Valid and neutral cues

In this experiment (16 sessions) the signal was presented randomly on each side. On 80% of the trials a spatial cue was presented on the same side that would undergo orientation change (valid cue). The rest of the trials (20%) contained a neutral cue where the cue was presented on both screens but only one of the screens would undergo the orientation change (Table 4.2).

Table 4.2: The probability with which the signal and the spatial cues were presented.

	Left Trials %		Right Trials %	
	Valid	Neutral	Valid	Neutral
Random	50 %		50 %	
	80 %	20 %	80 %	20 %

Figures 4.15 and 4.16 compare the performance and RT for the trials where the signal was validly cued (valid cue; green) and trials where the spatial cue was presented on both screens (neutral cue; yellow) and therefore did not indicate the position of the signal. For both rats, the performance and RT did not differ between the valid and neutral cue trials (ANOVA; $p>0.05$). Note that SOA is the time between the onset of the cue and the signal presentation and as the onset of the cue is the same as the nose-poke onset, SOA is the same as time of signal in previous experiments.

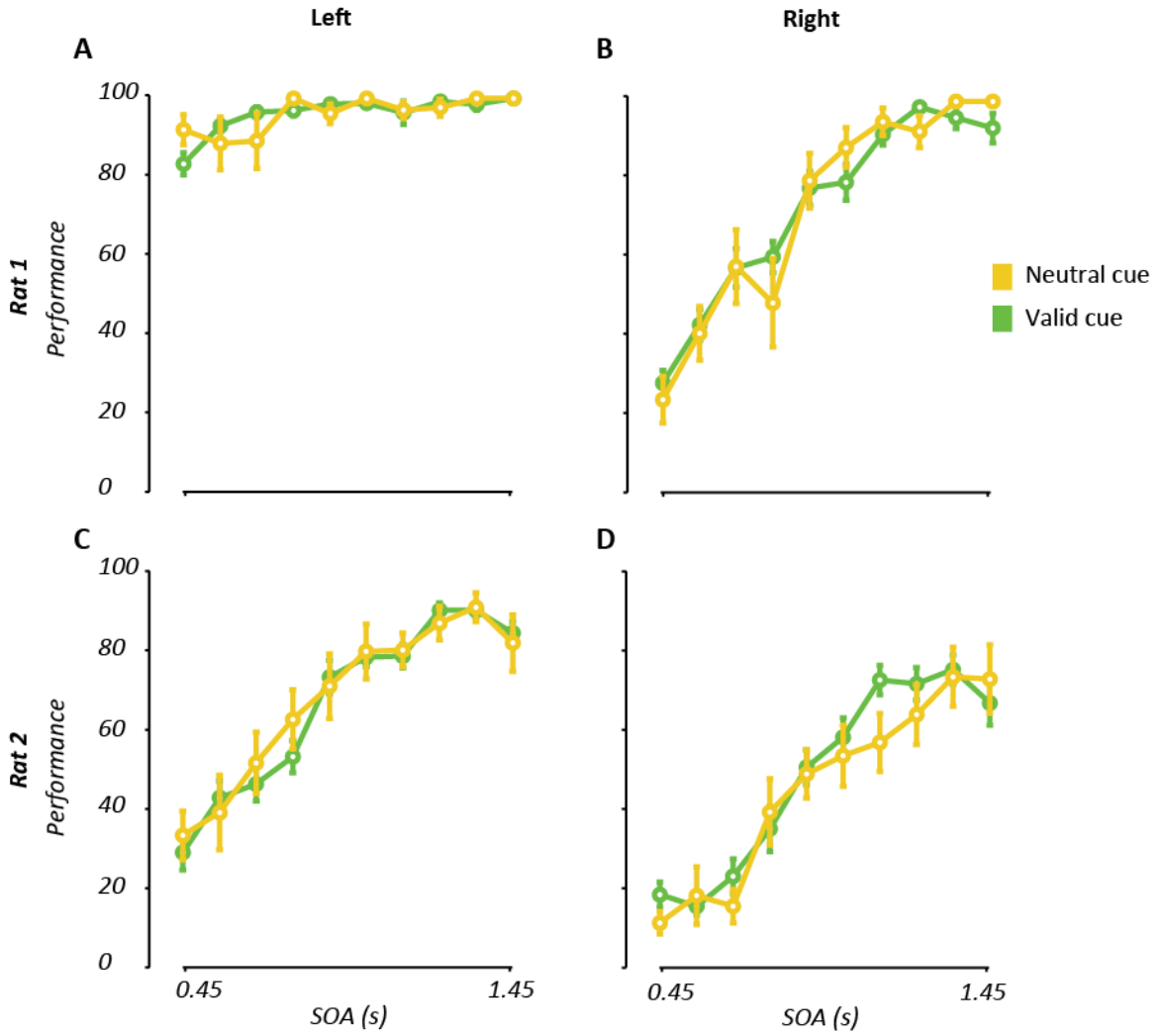

Figure 4.15: Performance comparison for the neutral and valid trials in the spatial cueing task. A. Performance comparisons for left sided targets in rat 1, **B.** for right sided targets in rat 1, **C.** for left sided targets in rat 2 and **D.** for right sided targets in rat 2. Performance is calculated as hits over hits and misses (Equation 4.3). Error bars represent ± SEM.

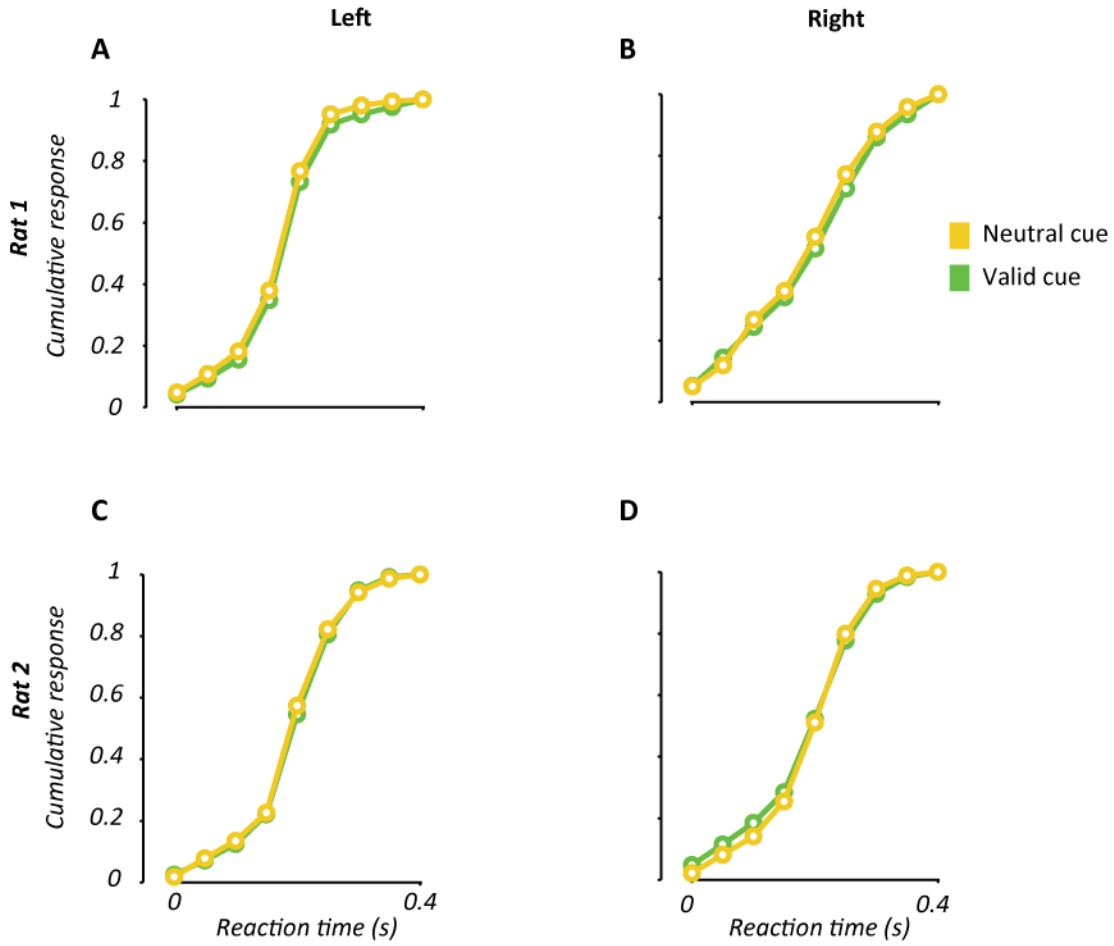

Figure 4.16: Reaction time comparison for the neutral and cue trials in the spatial cueing task. A. Cumulative RT for left sided targets in rat 1, **B.** for right sided targets in rat 1, **C.** for left sided targets in rat 2 and **D.** for right sided targets in rat 2.

4.3.3.2 Valid and invalid cues

In these experiments, the percentage of the valid cues was the same as the previous experiment (80%) but for the rest of the trials, instead of having a neutral cue presented on both screens, an invalid cue was presented on the side that the signal was not going to appear. For 16 sessions, the signal was presented randomly on each side (Table 4.3A). Next,

for 46 sessions, the signal was more likely (80%) to be presented on the right side (Table 4.3B).

Table 4.3: The probability with which the signal and the spatial cues were presented.

A	Left Trials %		Right Trials %	
	Valid	Invalid	Valid	Invalid
Random	50 %		50 %	
	80 %	20 %	80 %	20 %

B	Left Trials %		Right Trials %	
	Valid	Invalid	Valid	Invalid
Right high-probability	20 %		80 %	
	80 %	20 %	80 %	20 %

Similar to the previous experiment with neutral cues, there was no significant performance or RT differences on the trials with valid and invalid cues (ANOVA; $p>0.05$). This was the case for both random and right high-probability experiments. For simplicity, I am not presenting the corresponding figures.

4.3.3.3 Increasing the reliability of the cue

Given that using SOAs of 0.45-1.45 sec we did not observe any accuracy or RT difference between valid and invalid cues, in the last two experiments we decreased the SOA further. In these experiments the SOA varied between 0.1 and 1.1 sec and the cue

duration was 0.1 sec (instead of 0.2 sec in the previous experiments). In one experiment (20 sessions), the percentage of the valid and invalid cues was the same as the previous experiments (80% valid; 20% invalid; Table 4.4A). In the other experiment (10 sessions), all the cues were valid (Table 4.4B). Therefore the cue was fully predictive of the signal side. It is important to note that in both of these experiments the probability of signal presentation was random and the difference was in the predictability of the cues.

Table 4.4: The probability with which the signal and the spatial cues were presented.

A

	Left Trials %		Right Trials %	
	Valid	Invalid	Valid	Invalid
Random	50 %		50 %	
Mostly-predictive	80 %	20 %	80 %	20 %

B

	Left Trials %		Right Trials %	
	Valid	Invalid	Valid	Invalid
Random	50 %		50 %	
Fully-predictive	100 %	0 %	100 %	0 %

Similar to the previous experiments, there was no significant performance or RT difference for the trials with valid and invalid cues (ANOVA; $p>0.05$). We then compared the performance and RT across experiments: for the experiment where the cue was fully-predictive of the signal side (purple on Figures 4.17 and 4.18) and when it was predictive on 80% of the trials (maroon on Figures 4.17 and 4.18). As fully-predictive experiment only

contained valid cues, to compare between the two experiments only valid cue trials were considered. Interestingly, for both rats the performance was slightly higher and the RT was faster for the fully-predictive compared to mostly-predictive experiment.

Figure 4.17 shows performance in the two manipulations. For rat 1, the performance for the left side was high on both experiments (panel A). ANOVA revealed significant effect of time of signal ($F_{9,279} = 25.43$; $F_{3,271} = 9.2$; $p<0.01$). However in this rat, for the left sided signals, there was no effect of group and the interaction between time and group was not significant ($F_{1,279} = 1.27$; $F_{9,279} = 1.62$; $p>0.05$). For the right side (panel B), there were significant effects of time of signal and group ($F_{9,280} = 131.25$; $F_{1,280} = 4.06$; $p<0.05$) but their interaction was not significant ($F_{9,280} = 1.32$; $p>0.05$). The rat's performance was significantly higher for the fully-predictive than mostly-predictive experiment.

Rat 2 showed significant performance effect between the two experiments for both left and right sided signals. Performance difference for the left sided signals was significant for the time of signal, group as well as interaction between the two (panel C; $F_{9,275} = 11.21$; $F_{1,275} = 17.29$; $P<0.01$; $F_{9,275} = 3.08$; $p<0.01$). The rat's performance was significantly higher for the fully-predictive than mostly-predictive experiment. For the right sided signals (panel D), the performance was significantly different across groups and time ($F_{9,276} = 44.59$; $F_{1,276} = 5.06$; $p<0.01$) but their interaction was not significant ($F_{9,276} = 0.33$; $p>0.05$). Performance was significantly higher for the fully-predictive than mostly-predictive experiment.

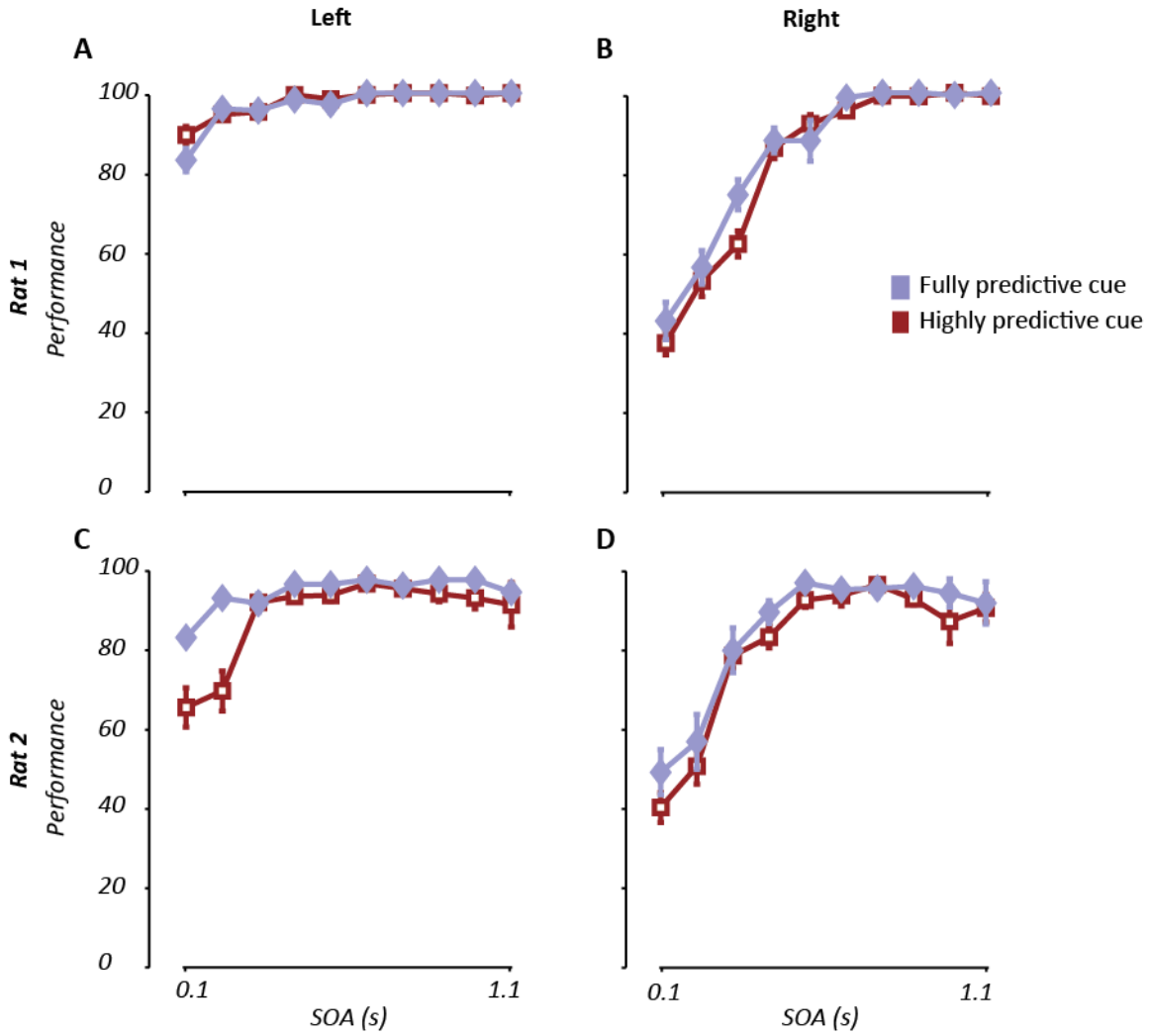

Figure 4.17: Performance comparison for the fully predictive cue experiment and the experiment where the cue predicted the position of the target on 80% of the trials. **A.** Performance comparisons for left sided targets in rat 1, **B.** for right sided targets in rat 1, **C.** for left sided targets in rat 2 and **D.** for right sided targets in rat 2. Performance is calculated as hits over hits and misses (Equation 4.3). Error bars represent ± SEM.

Next we compare the RT between the two signal predictability modulation experiments. For rat 1, the RT for the left sided targets was significantly faster for the fully-predictive cue compared to the mostly-predictive experiment (Figure 4.18 panel A; $F_{1,3705} = 8.59$; $p<0.01$). For this rat, the RT for the right sided targets was not significantly different between the two experiments (panel B; $F_{1,3124} = 0.01$; $p>0.05$).

For rat 2, the RT for both left (panel C) and right sided targets (panel D) was significantly faster for the fully-predictive cue compared to the mostly-predictive experiment ($F_{1,3305} = 24.08$; $F_{1,2943} = 6.22$; $p<0.05$).

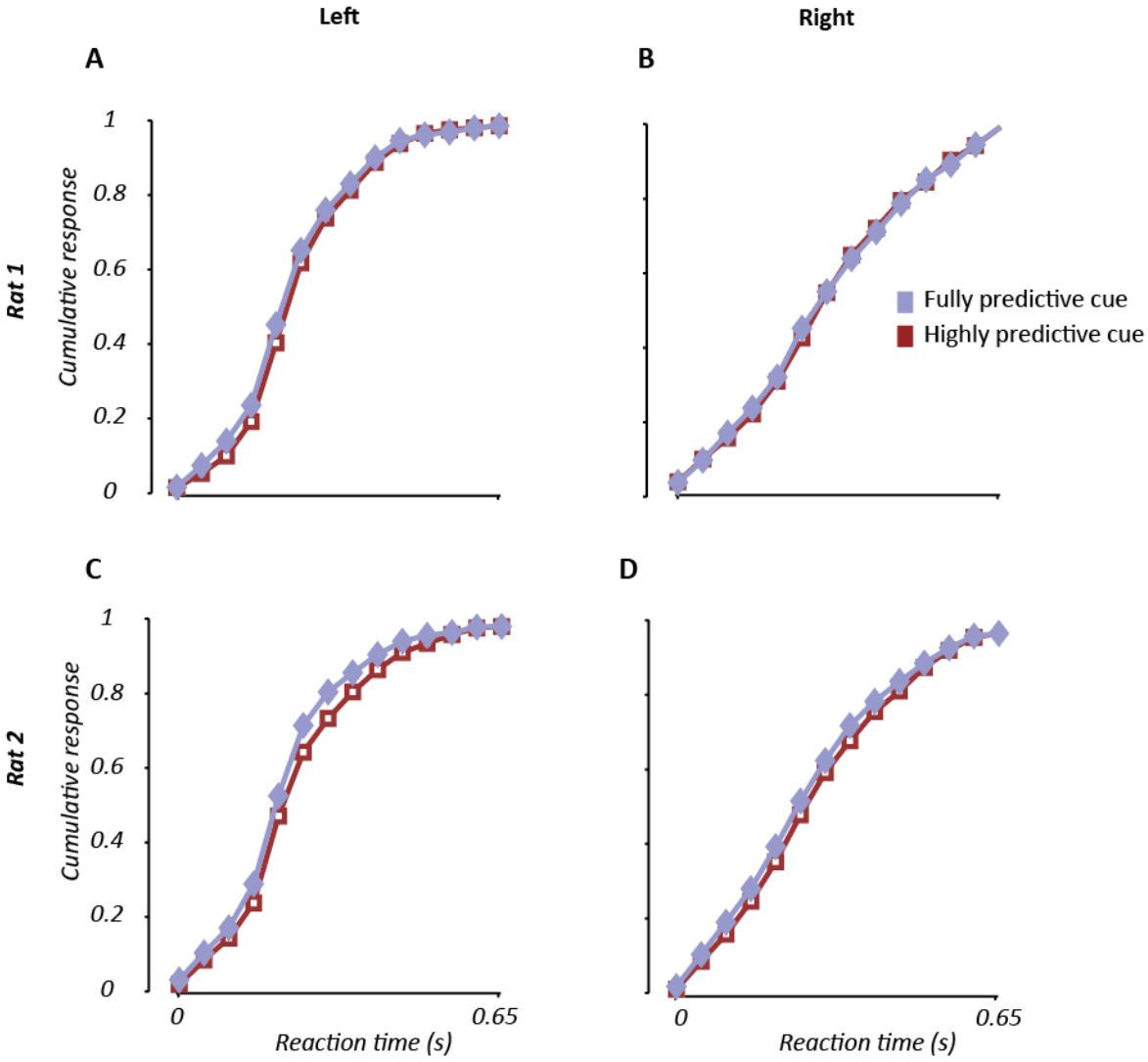

Figure 4.18: Reaction time comparison for the fully predictive cue experiment and the experiment where the cue predicted the position of the target on 80% of the trials. **A.** Cumulative RT for left sided targets in rat 1, **B.** for right sided targets in rat 1, **C.** for left sided targets in rat 2 and **D.** for right sided targets in rat 2.

4.4 Discussion

Selective attention is the process through which brain directs its processing capacity to events that are likely to be behaviourally relevant. Non-human primates are currently the primary animal models of selective attention. In this chapter I established the feasibility of studying selective attention in rodents and described a behavioural model of selective visual attention in rats. Rats responded to a change in the luminance or the orientation of a visual stimulus and performed >300 trials per session at a high level of performance on both tasks. I employed two key experimental manipulations: (1) I varied the probability with which the signal was presented on left or right: such that its location was either fully-predictable, random, or in blocks where it was more likely to be presented on one side; (2) I presented a spatial cue indicating the side where the signal was more likely to occur. The reaction time was systematically modulated by signal predictability: it was fastest for the fully-predictable and slowest for the random signals. Additionally, rats reacted faster to low-probability than high-probability trials. In the spatial cueing experiments, I did not observe performance or RT difference between trials with valid and invalid cues. Nevertheless, the performance was higher and the RT was faster when the cue was fully predictive of the signal side compared to when the cue was predictive on 80% of trials. In the following sections I assess the results above and previous work in the context of three models of attention allocation: no spatial covert attention, top-down attention, and combinations of top-down and bottom-up effects. I also briefly consider the side bias observed in both rats.

4.4.1 No covert spatial attention in rats?

In the spatial cueing experiments I did not observe performance or RT difference between trials that involved valid or invalid cues. This may indicate that unlike primates, rats

are not capable of covert spatial attention in the context of spatial cueing experiments. In this context it is important to note that in covert attention tasks involving humans and other primates, subjects fixate on a fixation point during signal presentation. In this way, the same sensory information is provided in valid and invalid trials. The difference between RTs in invalid and valid trials is thus taken to reflect both the benefit achieved by the prior orienting of attention towards the expected signal location and the costs of prior orienting of attention towards an incorrect target location (Posner and Cohen, 1984).

Unlike the work in primates, previous studies in rats have not measured the position of the head or eyes during the task (Weese et al., 1999; Marote and Xavier, 2011; Wagner et al., 2014). These studies therefore do not tell us whether the improved performance, which they observed in some of the SOAs, reflects the allocation of covert selective attention or whether the improved performance simply reflects changes in position of the body with respect to the stimuli. For example, in a trial that the cue is presented to the right side, the rat may pre-orient its body towards the right side before onset of the target. If the target is then presented to the right side (valid trial), the rat is expected to be faster and more accurate because of its prior body orientation. If however the target is presented to the left side (invalid trial), the rat is expected to miss the target or react slower to it because of its body orientation. Thus what appears to be a covert validity effect (Weese *et al.*, 1999; Marote & Xavier, 2011; Wagner *et al.*, 2014) may instead be the result of an overt orientation to the cued side. Even subtle prior orienting may induce measureable effects.

As shown in Chapter 3, in the paradigm developed in my thesis the arrangement of the nose-poke sensor, the reward spout and the monitors was such that the head and the eyes were relatively stable in the nose-poke. In the absence of overt body/eye orientation, the rats did not exhibit the validity effect. My results indicate that the observed validity

effects in previous rat experiments could have been due to overt body/head movements. It therefore remains an open question whether rats are capable of covert spatial attention in spatial cueing experiments.

In many primate studies, attention is manipulated on a single trial basis. In our rat experiments to attempt to manipulate spatial attention we utilised two methods: (1) we varied the probability with which the signal was presented on left or right: such that its location was either fully-predictable, random, or in blocks where it was more likely to be presented on one side; (2) we presented a spatial cue indicating that the change was more likely to occur on that side than the other. The question of whether attention is manipulated on a single trial basis cannot be answered based on the first method (varying the probability with which the signal is presented on left or right) as these probabilities are changed on a session by basis. The spatial cueing experiments can answer this question by for example examining the RT and performance in the experiment that the spatial cue was always present but the signal could randomly occur in left or right side. However we did not observe performance or RT improvements in our spatial cueing experiment. The failure to observe an effect of the spatial cue cannot be attributed to lack of motivation as the rats performed hundreds of trials per session.

4.4.2 Top-down modulation of attention?

I observed faster reaction times for fully-predictable signals compared to random signals. These results support idea that a mechanism of spatial attention is engaged by top-down mechanisms that have access to the predictability of signal location. A similar predictability effect was present for the RT and performance differences between fully

predictive spatial cue and the cues that predicted the side of the signal on 80% of trials. These results show that although the validity effect was not observed for the cued trials, the predictability still exerted a significant effect on behaviour. These results provide support for the top-down, endogenous, modulation of attention.

Endogenous modes of allocation are usually voluntary and provided through top-down mechanisms that are specifically tuned to immediate behavioural goals (Jonides & Irwin, 1981; Müller & Rabbitt, 1989; Folk *et al.*, 1992; Corbetta & Shulman, 2002; Berger *et al.*, 2005; Jack *et al.*, 2006). Exogenous modes of allocation are, on the hand, reflexive, relatively involuntary and driven by bottom-up stimulation (Prinzmetal *et al.*, 2005; Posner, 2012). We found a significant modulation by predictability through (putative) top-down mechanisms but did not observe any difference between valid and invalid cues (putatively bottom-up). The bottom-up capture of attention may depend on the stimulus properties such as the size or contrast of the cue or the signal. For example a study in humans showed that the physical characteristics of the cues and signals (such as luminance) affected the pattern of RTs at the shorter SOAs but not at the longer SOAs (Pratt *et al.*, 2001). The lack of bottom-up capture in our experiments may thus be due to the specific choice of stimulus parameters. On the other hand, it is possible that our findings point to fundamental differences between rats and humans in the way they sample the environment.

The performance was higher and the RT was faster when the cue was fully predictive of the signal side compared to when the cue was predictive on 80% of trials. One way to interpret these results is that the predictability exerted a significant effect on behaviour and supports the top-down, endogenous, modulation of attention. In these experiments, the onset of the cue is close in time to the onset of the signal on early trials (SOA varied

between 0.1 and 1.1 sec). Another way to interpret these results is that the cue is acting as a second signal, upon which the animal can make the decision. Therefore, given the time proximity of the cue and the signal on early SOAs, it is possible that the rats are responding to the cue itself. However, it is important to note that in these experiments the SOAs are all intermix within a session, therefore the fact that the rats actually waited for the longer signals is indicative that they are not just leaving the nose-poke based on the cue. If the response of the rats was based on the cue itself, then we would have expected a larger proportion of trials as early False Alarms. This is not what we observed.

4.4.3 Combinations of top-down and bottom-up effects

Slower reaction time for high-probability than low-probability signals may be related to more bottom-up mechanisms, repetition suppression and surprise. Repetition suppression is a robust phenomenon of reduction in neural responses to stimulus repetition (Summerfield *et al.*, 2008; Kaliukhovich & Vogels, 2012; Hsu *et al.*, 2014). Repetition suppression is thought to comprise of both top-down prediction and bottom-up adaptation effects (Hsu *et al.*, 2014). The associated reduction of neural response possibly allows the system to save resources and provide a more efficient representation (Pariyadath & Eagleman, 2007). Reduction of neural responses to high-probability stimuli may therefore allow low-probability stimuli to obtain attentional resources more easily (Desimone & Duncan, 1995). This in turn may be related to a well-known phenomenon called the oddball effect observed in humans. When a low-probability stimulus (oddball) appears in between a repeated presentation of high-probability stimuli, the judged duration of the oddball is overestimated (Tse *et al.*, 2004; Pariyadath & Eagleman, 2007; Schindel *et al.*, 2011).

Attention is complex and can be exerted through a combination of top-down and bottom-up mechanisms. In our experiments, the faster reaction time for fully-predictable signals compared to random signals supports the presence of a top-down mechanism. On the other hand, the slower reaction time for the high-probability than low-probability signals suggests that the bottom-up mechanisms are also involved. The extent to which the bottom-up mechanisms influence rodent behaviour remains an open question.

4.4.4 Side bias

While human data in attention experiments is often analysed for both sides combined (but see Berger, 2006), our analyses were done separately for each side. Both rats showed a leftward bias where the performance was higher for the left sided signals than the right. RTs for left-sided signals were also faster in Rat 1. Side bias in rats has been previously reported (Mittleman *et al.*, 1988; Rodriguez *et al.*, 1992; Ward & Brown, 1996; Cowell *et al.*, 1997; Weliky *et al.*, 2003; Wagner *et al.*, 2014). Consistent to our leftward bias, a previous experiment in rats studying the effects of spatial attention observed faster RTs to left-sided targets (Wagner *et al.*, 2014). Another study reported that rats have asymmetry in RT when trained to orient towards a visual signal presented to either eye (Mittleman *et al.*, 1988). When the visual signal is presented to the "dominant" eye, RTs are faster than to the "non-dominant" eye (Mittleman *et al.*, 1988). In this experiment, the right eye was the dominant eye in 65 % of the rats. Lateralised behaviour in rats has also been stated in other behavioural tasks such as in Morris water maze (Cowell *et al.*, 1997) and T-maze test (Rodriguez *et al.*, 1992). It would be interesting to investigate if these side biases are reflected anatomically.

5.0 Conclusion

The work in this thesis investigated multisensory integration and selective spatial attention in rats. We developed a simple behavioural paradigm to study rodents' visual behaviour. Rodents are gaining popularity as a viable animal model in visual neuroscience because of the access to molecular and sophisticated genetic tools and in vivo optical imaging techniques. These tools allow cell-type-specific neurophysiology and exquisite control of neuronal activity (Sohya *et al.*, 2007; Huber *et al.*, 2008; Cardin *et al.*, 2009; Kerlin *et al.*, 2010; Runyan *et al.*, 2010; Bock *et al.*, 2011). Other advantages of using rodents for behavioural experiments are that they are cheaper and depending on the task can be trained more rapidly than monkeys. For research involving sophisticated genetics, the mouse is currently the preparation of choice, however it remains to be determined whether mice can perform all the behavioural tasks that are now established in rats (Reinagel, 2014). Transgenic rats are starting to emerge and rats are the more generally used species in translational research as disease models. We consider rat model in vision research a valuable preparation which is complementary to other established models.

In Chapter 2, I showed that in rat SC, spiking activity was elevated by whisker or visual stimuli, but rarely both, when those stimuli were presented in isolation. Visually responsive sites were mainly found in superficial layers whereas whisker responsive sites were in intermediate layers. There were robust suppressive interactions between these two modalities, even though under uni-sensory conditions the non-preferred stimulus elicits

very weak or no response from those neurons. In order to maximise the chance for interactions between the two modalities, we used full-field visual flashes and multi-whisker vibrations (Wallace *et al.*, 2004; Lippert *et al.*, 2013). We therefore did not tailor the visual and whisker stimuli to the receptive field of individual neurons. It is possible that fine level of integration can only be observed when the stimuli are tailored to the receptive field. Future experiments can tackle on multisensory integration of visual and whisker inputs using single whisker stimulation and small visual flashes.

It is likely that integration is more prominent in behaving animals. Anaesthesia can reduce the sensitivity of the neurons and therefore supress the response to the non-preferred stimulus. Experiments involving multisensory stimulations are also more susceptible to the effects of changing brain states (Lippert *et al.*, 2013). Furthermore, in awake preparations the influence of neuronal oscillations on multisensory integration can be investigated (Lakatos *et al.*, 2007). Future research can investigate the effect of multisensory integration on SC of awake behaving rats in a preparation similar to the one I explained in Chapter 3.

In Chapter 3, I developed a rodent behavioural setup that can easily be paired with electrophysiological measurements. Our design is adaptable to a variety of detection and discrimination tasks. The paradigm can also be extended to tasks employing different sensory modalities such whisker stimulation. A vibrating mesh can be placed on a post next to nose-poke for applying whisker stimuli. Multisensory integration can also be investigated by for example presentation of both visual and whisker stimuli.

In Chapter 4, I investigated selective spatial attention in rats utilising the behavioural setup that I developed in Chapter 3. The reaction time was systematically modulated by attention: it was fastest for the fully-predictable and slowest for the random signals. The RT was faster on low-probability than high-probability trials. In the spatial cueing experiments the performance was higher and the RT was faster for the experiment where the cues were fully predictive of the signal side compared to mostly predictive experiment where the cue was predictive on 80% of the trials. Nevertheless, we did not observe performance or RT difference between trials with valid and invalid cues. Future experiments can explore the effect of the physical characteristics of cues and signals on RT and performance. For example a study in humans showed that the physical characteristics of the cues and signals (such as luminance) affected the pattern of RTs at the shorter SOAs but not at the longer SOAs (Pratt *et al.*, 2001).

A further approach to study the effect of selective spatial attention would be to use a different sensory modality as a cue (such as whisker vibrations or auditory cues). The signal can remain a visual change in these experiments. Before a rat can see a predator approaching, it might use the auditory cues or the vibrations induced by the predator's movement. These whisker or auditory cues might thus present a more ecological capture of attention.

References

Abraham NM, Spors H, Carleton A, Margrie TW, Kuner T & Schaefer AT (2004). Maintaining accuracy at the expense of speed: stimulus similarity defines odor discrimination time in mice. *Neuron* **44,** 865–876.

Ahmadlou M & Heimel JA (2015). Preference for concentric orientations in the mouse superior colliculus. *Nat Commun* **6,** 6773.

Akaike H (1973). Information theory and an extension of the maximum likelihood principle. In *International Symposium on Information Theory*, pp. 267–281.

Alemi-Neissi A, Rosselli FB & Zoccolan D (2013). Multifeatural shape processing in rats engaged in invariant visual object recognition. *J Neurosci* **33,** 5939–5956.

Alvarado JC, Vaughan JW, Stanford TR & Stein BE (2007). Multisensory versus unisensory integration: contrasting modes in the superior colliculus. *J Neurophysiol* **97,** 3193–3205.

Andermann ML, Kerlin a M & Reid RC (2010). Chronic cellular imaging of mouse visual cortex during operant behavior and passive viewing. *Front Cell Neurosci* **4,** 3.

Angelaki DE, Gu Y & DeAngelis GC (2009). Multisensory integration: psychophysics, neurophysiology, and computation. *Curr Opin Neurobiol* **19,** 452–458.

Anton-Erxleben K, Henrich C & Treue S (2007). Attention changes perceived size of moving visual patterns. *J Vis* **7,** 5 1–9.

Bari A, Dalley JW & Robbins TW (2008). The application of the 5-choice serial reaction time task for the assessment of visual attentional processes and impulse control in rats. *Nat Protoc* **3,** 759–767.

Bartolomeo P & Chokron S (2002). Orienting of attention in left unilateral neglect. *Neurosci Biobehav Rev* **26,** 217–234.

Bayliss AP & Tipper SP (2006). Predictive gaze cues and personality judgments: Should eye trust you? *Psychol Sci* **17,** 514–520.

Beauchamp MS, Argall BD, Bodurka J, Duyn JH & Martin A (2004). Unraveling multisensory integration: patchy organization within human STS multisensory cortex. *Nat Neurosci* **7,** 1190–1192.

Beck DM & Kastner S (2009). Top-down and bottom-up mechanisms in biasing competition in the human brain. *Vision Res* **49,** 1154–1165.

Bell AH, Meredith MA, Van Opstal AJ & Munoz DP (2005). Crossmodal integration in the primate superior colliculus underlying the preparation and initiation of saccadic eye movements. *J Neurophysiol* **93,** 3659–3673.

Bender DB & Youakim M (2001). Effect of Attentive Fixation in Macaque Thalamus and Cortex. *J Neurophysiol* **85,** 219–234.

Berger A (2006). Individual performance based on cognitive experimental measurements?

The case of inhibition of return. *Exp Psychol* **53,** 209–217.

Berger A, Henik A & Rafal R (2005). Competition Between Endogenous and Exogenous Orienting of Visual Attention.

Bezdudnaya T & Castro-Alamancos M a (2011). Superior colliculus cells sensitive to active touch and texture during whisking. *J Neurophysiol* **106,** 332–346.

Bezdudnaya T & Castro-Alamancos MA (2014). Neuromodulation of whisking related neural activity in superior colliculus. *J Neurosci* **34,** 7683–7695.

Bichot NP, Rossi AF & Desimone R (2005). Parallel and serial neural mechanisms for visual search in macaque area V4. *Science* **308,** 529–534.

Billington J, Wilkie RM, Field DT & Wann JP (2011). Neural processing of imminent collision in humans. *Proc Biol Sci* **278,** 1476–1481.

Binns K. (1999). The synaptic pharmacology underlying sensory processing in the superior colliculus. *Prog Neurobiol* **59,** 129–159.

Birch D & Jacobs GH (1979). Spatial contrast sensitivity in albino and pigmented rats. *Vision Res* **19,** 933–937.

Bizley JK & King AJ (2009). Visual influences on ferret auditory cortex. *Hear Res* **258,** 55–63.

Blasdel GG & Salama G (1986). Voltage-sensitive dyes reveal a modular organization in monkey striate cortex. *Nature* **321,** 579–585.

Blough D & Blough P (1977). *Handbook of operant behavior*. Prentice-Hall. Available at: https://books.google.com.au/books/about/Handbook_of_operant_behavior.html?id=LV9qAAAAMAAJ&pgis=1 [Accessed July 22, 2015].

Bock DD, Lee W-CA, Kerlin AM, Andermann ML, Hood G, Wetzel AW, Yurgenson S, Soucy ER, Kim HS & Reid RC (2011). Network anatomy and in vivo physiology of visual cortical neurons. *Nature* **471,** 177–182.

Bowman EM, Brown VJ, Kertzman C, Schwarz U & Robinson DL (1993). Covert orienting of attention in macaques. I. Effects of behavioral context. *J Neurophysiol* **70,** 431–443.

Brandão ML, Troncoso AC, de Souza Silva MA & Huston JP (2003). The relevance of neuronal substrates of defense in the midbrain tectum to anxiety and stress: empirical and conceptual considerations. *Eur J Pharmacol* **463,** 225–233.

Brett-Green B, Fifková E, Larue DT, Winer J a. & Barth DS (2003). A multisensory zone in rat parietotemporal cortex: Intra- and extracellular physiology and thalamocortical connections. *J Comp Neurol* **460,** 223–237.

Brett-Green B, Paulsen M, Staba RJ, Fifková E & Barth DS (2004). Two distinct regions of secondary somatosensory cortex in the rat: topographical organization and multisensory responses. *J Neurophysiol* **91,** 1327–1336.

Britten KH, Shadlen MN, Newsome WT & Movshon JA (1992). The analysis of visual motion: a comparison of neuronal and psychophysical performance. *J Neurosci* **12,** 4745–4765.

Brodeur DA & Pond M (1997). The Development of Selective Attention in Children With Attention Deficit Hyperactivity Disorder. *J Abnorm Child Psychol* **29,** 229–239.

Broersen L. & Uylings HB. (1999). Visual attention task performance in Wistar and Lister Hooded rats: response inhibition deficits after medial prefrontal cortex lesions. *Neuroscience* **94,** 47–57.

Brosch M, Selezneva E & Scheich H (2005). Nonauditory events of a behavioral procedure activate auditory cortex of highly trained monkeys. *J Neurosci* **25,** 6797–6806.

Buffalo EA, Fries P, Landman R, Liang H & Desimone R (2010). A backward progression of attentional effects in the ventral stream. *Proc Natl Acad Sci U S A* **107,** 361–365.

Bunsey MD & Strupp BJ (1995). Specific effects of idazoxan in a distraction task: Evidence that endogenous norepinephrine plays a role in selective attention in rats.

Burnett LR, Stein BE, Chaponis D & Wallace MT (2004). Superior colliculus lesions preferentially disrupt multisensory orientation. *Neuroscience* **124,** 535–547.

Buschman TJ & Miller EK (2007). Top-down versus bottom-up control of attention in the prefrontal and posterior parietal cortices. *Science* **315,** 1860–1862.

Bushnell PJ (1998). Behavioral approaches to the assessment of attention in animals. *Psychopharmacology (Berl)* **138,** 231–259.

Bushnell PJ & Strupp BJ (2009). Assessing Attention in Rodents. In *Methods of Behavior Analysis in Neuroscience*, 2nd edn., ed. Buccafusco J, p. Chapter 7. CRC Press, Boca Raton (FL). Available at: http://europepmc.org/abstract/med/21204340 [Accessed February 4, 2015].

Busse L, Ayaz A, Dhruv NT, Katzner S, Saleem AB, Schölvinck ML, Zaharia AD & Carandini M (2011). The detection of visual contrast in the behaving mouse. *J Neurosci* **31,** 11351–11361.

Busse L, Katzner S & Treue S (2008). Temporal dynamics of neuronal modulation during exogenous and endogenous shifts of visual attention in macaque area MT. *Proc Natl Acad Sci U S A* **105,** 16380–16385.

Cahill L, Ohl F & Scheich H (1996). Alteration of auditory cortex activity with a visual stimulus through conditioning: a 2-deoxyglucose analysis. *Neurobiol Learn Mem* **65,** 213–222.

Calvert G, Spence C & Stein BE (2004). *The Handbook of Multisensory Processes*. MIT Press. Available at: http://books.google.com/books?hl=en&lr=&id=CZS_yDoFV7AC&pgis=1 [Accessed January 20, 2015].

Calvert GA (2001). Crossmodal Processing in the Human Brain: Insights from Functional Neuroimaging Studies. *Cereb Cortex* **11,** 1110–1123.

Calvert GA & Thesen T (2004). Multisensory integration: methodological approaches and emerging principles in the human brain. *J Physiol Paris* **98,** 191–205.

Carandini M & Churchland AK (2013). Probing perceptual decisions in rodents. *Nat Neurosci* **16,** 824–831.

Carandini M & Heeger DJ (2012). Normalization as a canonical neural computation. *Nat Rev Neurosci* **13,** 51–62.

Cardin JA, Carlén M, Meletis K, Knoblich U, Zhang F, Deisseroth K, Tsai L-H & Moore CI

(2009). Driving fast-spiking cells induces gamma rhythm and controls sensory responses. *Nature* **459,** 663–667.

Carello CD & Krauzlis RJ (2004). Manipulating intent: evidence for a causal role of the superior colliculus in target selection. *Neuron* **43,** 575–583.

Carli M, Robbins TW, Evenden JL & Everitt BJ (1983). Effects of lesions to ascending noradrenergic neurones on performance of a 5-choice serial reaction task in rats; implications for theories of dorsal noradrenergic bundle function based on selective attention and arousal. *Behav Brain Res* **9,** 361–380.

Carrasco M (2011). Visual attention: the past 25 years. *Vision Res* **51,** 1484–1525.

Castro-Alamancos M & Keller A (2011). Vibrissal midbrain loops. *Scholarpedia* **6,** 7274.

Chalupa LM & Williams RW (2008). *Eye, retina, and visual system of the mouse*ed. Chalupa LM & Williams RW. MIT Press, Cambridge. Available at: http://agris.fao.org/agris-search/search.do?recordID=US201300128744 [Accessed July 10, 2015].

Chudler EH, Sugiyama K & Dong WK (1995). Multisensory convergence and integration in the neostriatum and globus pallidus of the rat. *Brain Res* **674,** 33–45.

Churchland MM et al. (2010). Stimulus onset quenches neural variability: a widespread cortical phenomenon. *Nat Neurosci* **13,** 369–378.

Clark RE, Reinagel P, Broadbent NJ, Flister ED & Squire LR (2011). Intact performance on feature-ambiguous discriminations in rats with lesions of the perirhinal cortex. *Neuron* **70,** 132–140.

Clery J, Guipponi O, Odouard S, Wardak C & Ben Hamed S (2015). Impact Prediction by Looming Visual Stimuli Enhances Tactile Detection. *J Neurosci* **35,** 4179–4189.

Cohen JD & Castro-Alamancos M a (2010*a*). Neural correlates of active avoidance behavior in superior colliculus. *J Neurosci* **30,** 8502–8511.

Cohen JD & Castro-Alamancos M a (2010*b*). Behavioral state dependency of neural activity and sensory (whisker) responses in superior colliculus. *J Neurophysiol* **104,** 1661–1672.

Cohen JD & Castro-Alamancos MA (2007). Early sensory pathways for detection of fearful conditioned stimuli: tectal and thalamic relays. *J Neurosci* **27,** 7762–7776.

Cohen JD & Castro-Alamancos MA (2010*c*). Detection of low salience whisker stimuli requires synergy of tectal and thalamic sensory relays. *J Neurosci* **30,** 2245–2256.

Cohen JD, Hirata A & Castro-Alamancos M a (2008). Vibrissa sensation in superior colliculus: wide-field sensitivity and state-dependent cortical feedback. *J Neurosci* **28,** 11205–11220.

Cohen MR & Maunsell JHR (2009). Attention improves performance primarily by reducing interneuronal correlations. *Nat Neurosci* **12,** 1594–1600.

Comoli E, Das Neves Favaro PP, Vautrelle N, Leriche M, Overton PG & Redgrave P (2012). Segregated anatomical input to sub-regions of the rodent superior colliculus associated with approach and defense. *Front Neuroanat* **6,** 9.

Condé F, Maire-Lepoivre E, Audinat E & Crépel F (1995). Afferent connections of the medial

frontal cortex of the rat. II. Cortical and subcortical afferents. *J Comp Neurol* **352,** 567–593.

Corbetta M & Shulman GL (2002). Control of goal-directed and stimulus-driven attention in the brain. *Nat Rev Neurosci* **3,** 201–215.

Corneil BD & Munoz DP (1996). The influence of auditory and visual distractors on human orienting gaze shifts. *J Neurosci* **16,** 8193–8207.

Cowell PE, Waters NS & Denenberg VH (1997). The Effects of Early Environment on the Development of Functional Laterality in Morris Maze Performance. *Laterality Asymmetries Body, Brain Cogn* **2,** 221–232.

Dahl CD, Logothetis NK & Kayser C (2009). Spatial organization of multisensory responses in temporal association cortex. *J Neurosci* **29,** 11924–11932.

Dean AF (1981). The variability of discharge of simple cells in the cat striate cortex. *Exp Brain Res* **44,** 437–440.

Dean P, Redgrave P, Sahibzada N & Tsuji K (1986). Head and body movements produced by electrical stimulation of superior colliculus in rats: Effects of interruption of crossed tectoreticulospinal pathway. *Neuroscience* **19,** 367–380.

Dean P, Redgrave P & Westby GW (1989). Event or emergency? Two response systems in the mammalian superior colliculus. *Trends Neurosci* **12,** 137–147.

Dehner L, Keniston L, Clemo H & Meredith M (2004). Cross-modal Circuitry Between Auditory and Somatosensory Areas of the Cat Anterior Ectosylvian Sulcal Cortex: A "New" Inhibitory Form of Multisensory Convergence. *Cereb Cortex* **14,** 387–403.

Desimone R & Duncan J (1995). Neural mechanisms of selective visual attention. *Annu Rev Neurosci* **18,** 193–222.

Dhande OS & Huberman AD (2014). Retinal ganglion cell maps in the brain: implications for visual processing. *Curr Opin Neurobiol* **24,** 133–142.

Dosher BA & Lu Z-L (2000). Noise Exclusion in Spatial Attention. *Psychol Sci* **11,** 139–146.

Douglas RM, Neve a, Quittenbaum JP, Alam NM & Prusky GT (2006). Perception of visual motion coherence by rats and mice. *Vision Res* **46,** 2842–2847.

Dräger U & Hubel D (1975*a*). Physiology of visual cells in mouse superior colliculus and correlation with somatosensory and auditory input. *Nature* **253,** 203–204.

Dräger UC & Hubel DH (1975*b*). Responses to visual stimulation and relationship between visual , auditory , and somatosensory inputs in mouse superior colliculus Inputs in Mouse Superior Colliculus. *J Neurophysiol* **38,** 690–713.

Dräger UC & Hubel DH (1976). Topography of visual and somatosensory projections to mouse superior colliculus. *J Neurophysiol* **39,** 91–101.

Driver J & Noesselt T (2008). Multisensory interplay reveals crossmodal influences on "sensory-specific" brain regions, neural responses, and judgments. *Neuron* **57,** 11–23.

Edwards SB, Ginsburgh CL, Henkel CK & Stein BE (1979). Sources of subcortical projections to the superior colliculus in the cat. *J Comp Neurol* **184,** 309–329.

Endo T & Isa T (2001). Functionally different AMPA-type glutamate receptors in morphologically identified neurons in rat superficial superior colliculus. *Neuroscience* **108,** 129–141.

Erlich JCC, Bialek M & Brody CDD (2011). A cortical substrate for memory-guided orienting in the rat. *Neuron* **72,** 330–343.

Ernst ZR, Boynton GM & Jazayeri M (2010). The spread of attention across features of a surface. *J Vis* **10,** 189–189.

Fagiolini M, Pizzorusso T, Berardi N, Domenici L & Maffei L (1994). Functional postnatal development of the rat primary visual cortex and the role of visual experience: dark rearing and monocular deprivation. *Vision Res* **34,** 709–720.

Favaro PDN, Gouvêa TS, de Oliveira SR, Vautrelle N, Redgrave P & Comoli E (2011). The influence of vibrissal somatosensory processing in rat superior colliculus on prey capture. *Neuroscience* **176,** 318–327.

Feinberg EH & Meister M (2014). Orientation columns in the mouse superior colliculus. *Nature* **519,** 229–232.

Feldon S, Feldon P & Kruger L (1970). Topography of the retinal projection upon the superior colliculus of the cat. *Vision Res* **10,** 135–143.

Felsen G & Mainen ZF (2008). Neural substrates of sensory-guided locomotor decisions in the rat superior colliculus. *Neuron* **60,** 137–148.

Fetsch CR, DeAngelis GC & Angelaki DE (2010). Visual-vestibular cue integration for heading perception: applications of optimal cue integration theory. *Eur J Neurosci* **31,** 1721–1729.

Fetsch CR, Pouget A, DeAngelis GC & Angelaki DE (2012). Neural correlates of reliability-based cue weighting during multisensory integration. *Nat Neurosci* **15,** 146–154.

Folk CL, Remington RW & Johnston JC (1992). Involuntary covert orienting is contingent on attentional control settings.

Foxe JJ, Simpson G V. & Ahlfors SP (1998). Parieto-occipital ~10 Hz activity reflects anticipatory state of visual attention mechanisms. *Neuroreport* **9,** 3929–3933.

Frens MA & Van Opstal AJ (1995). A quantitative study of auditory-evoked saccadic eye movements in two dimensions. *Exp Brain Res* **107,** 103–117.

Frens MA & Van Opstal AJ (1998). Visual-auditory interactions modulate saccade-related activity in monkey superior colliculus. *Brain Res Bull* **46,** 211–224.

Fries P, Schroder JH, Roelfsema PR, Singer W & Engel AK (2002). Oscillatory neuronal synchronization in primary visual cortex as a correlate of stimulus selection. *J Neurosci* **22,** 3739–3754.

Fries P, Womelsdorf T, Oostenveld R & Desimone R (2008). The effects of visual stimulation and selective visual attention on rhythmic neuronal synchronization in macaque area V4. *J Neurosci* **28,** 4823–4835.

Fu KMG, Johnston TA, Shah AS, Arnold L, Smiley J, Hackett TA, Garraghty PE & Schroeder CE

(2003). Auditory cortical neurons respond to somatosensory stimulation. *J Neurosci* **23,** 7510–7515.

Fukuda Y & Iwama K (1978). Visual receptive-field properties of single cells in the rat superior colliculus. *Jpn J Physiol* **28,** 385–400.

Furigo IC, de Oliveira WF, de Oliveira AR, Comoli E, Baldo MVC, Mota-Ortiz SR & Canteras NS (2010). The role of the superior colliculus in predatory hunting. *Neuroscience* **165,** 1–15.

Gaese BH & Johnen A (2000). Coding for auditory space in the superior colliculus of the rat. *Eur J Neurosci* **12,** 1739–1752.

Gaither N & Stein B (1979). Reptiles and mammals use similar sensory organizations in the midbrain. *Science (80-)* **205,** 595–597.

Gale SD & Murphy GJ (2014). Distinct Representation and Distribution of Visual Information by Specific Cell Types in Mouse Superficial Superior Colliculus. *J Neurosci* **34,** 13458–13471.

Gandhi NJ & Katnani HA (2011). Motor functions of the superior colliculus. *Annu Rev Neurosci* **34,** 205–231.

Gattass R & Desimone R (2014). Effect of microstimulation of the superior colliculus on visual space attention. *J Cogn Neurosci* **26,** 1208–1219.

Gendle MH, White TL, Strawderman M, Mactutus CF, Booze RM, Levitsky DA & Strupp BJ (2004). Enduring Effects of Prenatal Cocaine Exposure on Selective Attention and Reactivity to Errors: Evidence From an Animal Model. *Behav Neurosci* **118,** 290–297.

Ghazanfar AA & Chandrasekaran CF (2007). Paving the way forward: integrating the senses through phase-resetting of cortical oscillations. *Neuron* **53,** 162–164.

Ghazanfar AA, Maier JX, Hoffman KL & Logothetis NK (2005). Multisensory integration of dynamic faces and voices in rhesus monkey auditory cortex. *J Neurosci* **25,** 5004–5012.

Ghazanfar AA & Schroeder CE (2006). Is neocortex essentially multisensory? *Trends Cogn Sci* **10,** 278–285.

Ghose D, Barnett ZP & Wallace MT (2012). Impact of response duration on multisensory integration. *J Neurophysiol* **108,** 2534–2544.

Ghose D, Maier A, Nidiffer A & Wallace MT (2014). Multisensory response modulation in the superficial layers of the superior colliculus. *J Neurosci* **34,** 4332–4344.

Girman S V & Lund RD (2007). Most superficial sublamina of rat superior colliculus: neuronal response properties and correlates with perceptual figure-ground segregation. *J Neurophysiol* **98,** 161.

Girman S V, Sauvé Y & Lund RD (1999). Receptive field properties of single neurons in rat primary visual cortex. *J Neurophysiol* **82,** 301–311.

Gleiss S & Kayser C (2012). Audio-visual detection benefits in the rat. *PLoS One* **7,** e45677.

Goldberg ME & Wurtz RH (1972). Activity of superior colliculus in behaving monkey. I. Visual receptive fields of single neurons. *J Neurophysiol* **35,** 542–559.

Gordon B (1973). Receptive fields in deep layers of cat superior colliculus. *J Neurophysiol* **36,** 157–178.

Grant AC, Thiagarajah MC & Sathian K (2000). Tactile perception in blind braille readers: A psychophysical study of acuity and hyperacuity using gratings and dot patterns. *Percept Psychophys* **62,** 301–312.

Graybiel AM (1978). A satellite system of the superior colliculus: the parabigeminal nucleus and its projections to the superficial collicular layers. *Brain Res* **145,** 365–374.

Green DM & Swets JA (1966). Signal detection theory and psychophysics. *Wiley New York*. Available at: http://trove.nla.gov.au/work/7432279?selectedversion=NBD13637051 [Accessed July 31, 2015].

Gregoriou GG, Gotts SJ, Zhou H & Desimone R (2009). Long-range neural coupling through synchronization with attention. *Prog Brain Res* **176,** 35–45.

Groh JM & Sparks DL (1996*a*). Saccades to somatosensory targets. II. motor convergence in primate superior colliculus. *J Neurophysiol* **75,** 428–438.

Groh JM & Sparks DL (1996*b*). Saccades to somatosensory targets. III. eye-position-dependent somatosensory activity in primate superior colliculus. *J Neurophysiol* **75,** 439–453.

Gu Y, Angelaki DE & Deangelis GC (2008). Neural correlates of multisensory cue integration in macaque MSTd. *Nat Neurosci* **11,** 1201–1210.

Guitton D & Munoz DP (1991). Control of orienting gaze shifts by the tectoreticulospinal system in the head-free cat. I. Identification, localization, and effects of behavior on sensory responses. *J Neurophysiol* **66,** 1605–1623.

Hall WC, Fitzpatrick D, Klatt LL & Raczkowski D (1989). Cholinergic innervation of the superior colliculus in the cat. *J Comp Neurol* **287,** 495–514.

Harati H, Barbelivien A, Cosquer B, Majchrzak M & Cassel J-C (2008). Selective cholinergic lesions in the rat nucleus basalis magnocellularis with limited damage in the medial septum specifically alter attention performance in the five-choice serial reaction time task. *Neuroscience* **153,** 72–83.

Harris JA, Gharaei S & Pincham HL (2011). Response rates track the history of reinforcement times. *J Exp Psychol Anim Behav Process* **37,** 277–286. Available at: http://lib.bioinfo.pl/pmid:21500934 [Accessed November 13, 2012].

Harting JK, Hall WC, Diamond IT & Martin GF (1973). Anterograde degeneration study of the superior colliculus in Tupaia glis: evidence for a subdivision between superficial and deep layers. *J Comp Neurol* **148,** 361–386.

Harting JK, Updyke B V & Lieshout DPVAN (1992). Corticotectal Projections in the Cat : Anterograde Transport Studies of Twenty-Five Cortical Areas.

Hayward DA & Ristic J (2013). Measuring attention using the Posner cuing paradigm: the role of across and within trial target probabilities. *Front Hum Neurosci* **7,** 205.

Heesy CP (2009). Seeing in stereo: The ecology and evolution of primate binocular vision and stereopsis. *Evol Anthropol Issues, News, Rev* **18,** 21–35.

Hegdé J & Van Essen DC (2003). Strategies of shape representation in macaque visual area V2. *Vis Neurosci* **20,** 313–328.

Hemelt ME & Keller A (2007). Superior sensation: superior colliculus participation in rat vibrissa system. *BMC Neurosci* **8,** 12.

Hemelt ME & Keller A (2008). Superior colliculus control of vibrissa movements. *J Neurophysiol* **100,** 1245–1254.

Herbert H, Klepper A & Ostwald J (1997). Afferent and efferent connections of the ventrolateral tegmental area in the rat. *Anat Embryol (Berl)* **196,** 235–259.

Herrero JL, Roberts MJ, Delicato LS, Gieselmann MA, Dayan P & Thiele A (2008). Acetylcholine contributes through muscarinic receptors to attentional modulation in V1. *Nature* **454,** 1110–1114.

Herrmann K, Montaser-Kouhsari L, Carrasco M & Heeger DJ (2010). When size matters: attention affects performance by contrast or response gain. *Nat Neurosci* **13,** 1554–1559.

Hilbig H, Bidmon H-J, Ettrich P & Müller A (2000). Projection neurons in the superficial layers of the superior colliculus in the rat: a topographic and quantitative morphometric analysis. *Neuroscience* **96,** 109–119.

Hillyard SA & Anllo-Vento L (1998). Event-related brain potentials in the study of visual selective attention. *Proc Natl Acad Sci* **95,** 781–787.

Hirokawa J, Sadakane O, Sakata S, Bosch M, Sakurai Y & Yamamori T (2011). Multisensory information facilitates reaction speed by enlarging activity difference between superior colliculus hemispheres in rats. *PLoS One* **6,** e25283.

Histed MH, Carvalho L a. & Maunsell JHR (2012). Psychophysical measurement of contrast sensitivity in the behaving mouse. *J Neurophysiol* **107,** 758–765.

Van Hooser SD, Heimel JAF, Chung S, Nelson SB & Toth LJ (2005). Orientation selectivity without orientation maps in visual cortex of a highly visual mammal. *J Neurosci* **25,** 19–28.

Horwitz GD, Batista AP & Newsome WT (2004). Direction-selective visual responses in macaque superior colliculus induced by behavioral training. *Neurosci Lett* **366,** 315–319.

Hsu Y-F, Hämäläinen JA & Waszak F (2014). Repetition suppression comprises both attention-independent and attention-dependent processes. *Neuroimage* **98,** 168–175.

Hubel DH & Wiesel TN (1968). Receptive fields and functional architecture of monkey striate cortex. *J Physiol* **195,** 215–243.

Huber D, Petreanu L, Ghitani N, Ranade S, Hromádka T, Mainen Z & Svoboda K (2008). Sparse optical microstimulation in barrel cortex drives learned behaviour in freely moving mice. *Nature* **451,** 61–64.

Huber GC & Crosby EC (1943). A Comparison of the mammalian and reptilian tecta. *J Comp Neurol* **78,** 133–168.

Huerta MF & Harting JK (1984). Connectional organization of the superior colliculus. *Trends Neurosci* **7,** 286–289.

Hughes A (1971). Topographical relationships between the anatomy and physiology of the rabbit visual system. *Doc Ophthalmol* **30,** 33–159.

Hughes HC, Reuter-Lorenz PA, Nozawa G & Fendrich R (1994). Visual-Auditory Interactions in Sensorimotor Processing: Saccades Versus Manual Responses. *J Exp Psychol Hum Percept Perform* **20,** 131–153.

Humby T, Laird FM, Davies W & Wilkinson LS (1999). Visuospatial attentional functioning in mice: interactions between cholinergic manipulations and genotype. *Eur J Neurosci* **11,** 2813–2823.

Hurvich CM & Tsai C-L (1989). Regression and time series model selection in small samples. *Biometrika* **76,** 297–307.

Ibrahim LA, Mesik L, Ji X-Y, Fang Q, Li H-F, Li Y-T, Zingg B, Zhang LI & Tao HW (2016). Cross-Modality Sharpening of Visual Cortical Processing through Layer-1-Mediated Inhibition and Disinhibition. *Neuron* **89,** 1031–1045.

Ignashchenkova A, Dicke PW, Haarmeier T & Thier P (2004). Neuron-specific contribution of the superior colliculus to overt and covert shifts of attention. *Nat Neurosci* **7,** 56–64.

Illing R-B & Graybiel AM (1986). Complementary and non-matching afferent compartments in the cat's superior colliculus: Innervation of the acetylcholinesterase-poor domain of the intermediate gray layer. *Neuroscience* **18,** 373–394.

Illing R-B, Vogt DM & Spatz WB (1990). Parvalbumin in rat superior colliculus. *Neurosci Lett* **120,** 197–200.

Inayat S, Barchini J, Chen H, Feng L, Liu X & Cang J (2015). Neurons in the Most Superficial Lamina of the Mouse Superior Colliculus Are Highly Selective for Stimulus Direction. *J Neurosci* **35,** 7992–8003.

Inglis WL, Olmstead MC & Robbins TW (2001). Selective deficits in attentional performance on the 5-choice serial reaction time task following pedunculopontine tegmental nucleus lesions. *Behav Brain Res* **123,** 117–131.

Isa T, Endo T & Saito Y (1998). The visuo-motor pathway in the local circuit of the rat superior colliculus. *J Neurosci* **18,** 8496–8504.

Isa T & Hall WC (2009). Exploring the superior colliculus in vitro. *J Neurophysiol* **102,** 2581–2593.

Jack AI, Shulman GL, Snyder AZ, McAvoy M & Corbetta M (2006). Separate modulations of human V1 associated with spatial attention and task structure. *Neuron* **51,** 135–147.

Jaramillo S & Zador AM (2011). The auditory cortex mediates the perceptual effects of acoustic temporal expectation. *Nat Neurosci* **14,** 246–251.

Jay MF & Sparks DL (1987*a*). Sensorimotor integration in the primate superior colliculus. I. Motor convergence. *J Neurophysiol* **57,** 22–34.

Jay MF & Sparks DL (1987*b*). Sensorimotor integration in the primate superior colliculus. II.

Coordinates of auditory signals. *J Neurophysiol* **57,** 35–55.

Jiang W, Jiang H & Stein BE (2002). Two corticotectal areas facilitate multisensory orientation behavior. *J Cogn Neurosci* **14,** 1240–1255.

Jiang W, Wallace MT, Jiang H, Vaughan JW & Stein BE (2001). Two cortical areas mediate multisensory integration in superior colliculus neurons. *J Neurophysiol* **85,** 506–522.

Jonides J & Irwin DE (1981). Capturing attention. *Cognition* **10,** 145–150.

Kadunce DC, Vaughan JW, Wallace MT, Benedek G & Stein BE (1997). Mechanisms of within- and cross-modality suppression in the superior colliculus. *J Neurophysiol* **78,** 2834–2847.

Kaliukhovich D a. & Vogels R (2012). Stimulus repetition affects both strength and synchrony of macaque inferior temporal cortical activity. *J Neurophysiol* **107,** 3509–3527.

Kaneko H, Tamura H, Kawashima T & Suzuki SS (2006). A choice reaction-time task in the rat: a new model using air-puff stimuli and lever-release responses. *Behav Brain Res* **174,** 151–159.

Katyal S & Ress D (2014). Endogenous attention signals evoked by threshold contrast detection in human superior colliculus. *J Neurosci* **34,** 892–900.

Katzner S, Nauhaus I, Benucci A, Bonin V, Ringach DL & Carandini M (2009). Local origin of field potentials in visual cortex. *Neuron* **61,** 35–41.

Kawamura S, Hattori S, Higo S & Matsuyama T (1982). The cerebellar projections to the superior colliculus and pretectum in the cat: An autoradiographic and horseradish peroxidase study. *Neuroscience* **7,** 1673–1689.

Kayser C & Logothetis NK (2007). Do early sensory cortices integrate cross-modal information? *Brain Struct Funct* **212,** 121–132.

Kayser C, Logothetis NK & Panzeri S (2010). Visual enhancement of the information representation in auditory cortex. *Curr Biol* **20,** 19–24.

Kayser C, Petkov CI & Logothetis NK (2008). Visual modulation of neurons in auditory cortex. *Cereb Cortex* **18,** 1560–1574.

Keay K a, Redgrave P & Dean P (1988). Cardiovascular and respiratory changes elicited by stimulation of rat superior colliculus. *Brain Res Bull* **20,** 13–26.

Kerlin AM, Andermann ML, Berezovskii VK & Reid RC (2010). Broadly tuned response properties of diverse inhibitory neuron subtypes in mouse visual cortex. *Neuron* **67,** 858–871.

King AJ & Palmer AR (1985). Integration of visual and auditory information in bimodal neurones in the guinea-pig superior colliculus. *Exp brain Res* **60,** 492–500.

King AJ, Schnupp JW & Thompson ID (1998). Signals from the superficial layers of the superior colliculus enable the development of the auditory space map in the deeper layers. *J Neurosci* **18,** 9394–9408.

King AJ, Schnupp JWH, Carlile S, Smith AL & Thompson ID (1996). *Extrageniculostriate Mechanisms Underlying Visually-Guided Orientation Behavior*. Elsevier. Available at:

http://www.sciencedirect.com/science/article/pii/S0079612308633403 [Accessed July 9, 2015].

Klein RM (2000). Inhibition of return. *Trends Cogn Sci* **4,** 138–147.

Kleiner M, Brainard D & Pelli D (2007). What's new in Psychtoolbox-3? *Percept ECVP Abstr*; DOI: 10.1068/v070821.

Krauzlis RJ & Dill N (2002). Neural Correlates of Target Choice for Pursuit and Saccades in the Primate Superior Colliculus. *Neuron* **35,** 355–363.

Krauzlis RJ, Lovejoy LP & Zénon A (2013). Superior colliculus and visual spatial attention. *Annu Rev Neurosci* **36,** 165–182.

Krubitzer L (2007). The magnificent compromise: cortical field evolution in mammals. *Neuron* **56,** 201–208.

Lakatos P, Chen C-M, O'Connell MN, Mills A & Schroeder CE (2007). Neuronal oscillations and multisensory interaction in primary auditory cortex. *Neuron* **53,** 279–292.

Lane RH, Allman JM, Kaas JH & Miezin FM (1973). The visuotopic organization of the superior colliculus of the owl monkey (Aotus trivirgatus) and the bush baby (Galago senegalensis). *Brain Res* **60,** 335–349.

Lashley KS (1938). The Mechanism of Vision: XV. Preliminary Studies of the Rat's Capacity for Detail Vision. *J Gen Psychol* **18,** 123–193.

Lee PH, Helms MC, Augustine GJ & Hall WC (1997). Role of intrinsic synaptic circuitry in collicular sensorimotor integration. *Proc Natl Acad Sci* **94,** 13299–13304.

Lee S-H, Govindaiah G & Cox CL (2007). Heterogeneity of firing properties among rat thalamic reticular nucleus neurons. *J Physiol* **582,** 195–208.

Lee TS & Nguyen M (2001). Dynamics of subjective contour formation in the early visual cortex. *Proc Natl Acad Sci USA* **98,** 1907–1911.

Lemke G & Reber M (2005). Retinotectal mapping: new insights from molecular genetics. *Annu Rev Cell Dev Biol* **21,** 551–580.

Lemus L, Hernández A, Luna R, Zainos A & Romo R (2010). Do sensory cortices process more than one sensory modality during perceptual judgments? *Neuron* **67,** 335–348.

Lennie P (2003). The cost of cortical computation. *Curr Biol* **13,** 493–497.

Leonard CM (1969). The prefrontal cortex of the rat. I. Cortical projection of the mediodorsal nucleus. II. Efferent connections. *Brain Res* **12,** 321–343.

Lewis R & Noppeney U (2010). Audiovisual synchrony improves motion discrimination via enhanced connectivity between early visual and auditory areas. *J Neurosci* **30,** 12329–12339.

Liang F, Xiong XR, Zingg B, Ji X, Zhang LI & Tao HW (2015). Sensory Cortical Control of a Visually Induced Arrest Behavior via Corticotectal Projections. *Neuron* **86,** 755–767.

Lippert MT, Takagaki K, Kayser C & Ohl FW (2013). Asymmetric multisensory interactions of visual and somatosensory responses in a region of the rat parietal cortex. *PLoS One* **8,**

e63631.

Liu Y-J, Wang Q & Li B (2011). Neuronal responses to looming objects in the superior colliculus of the cat. *Brain Behav Evol* **77,** 193–205.

Lovejoy LP & Krauzlis RJ (2010). Inactivation of primate superior colliculus impairs covert selection of signals for perceptual judgments. *Nat Neurosci* **13,** 261–266.

Luck SJ & Vecera SP (2002). Attention. In *Handbook of Experimental Psychology: Vol. 1: Sensation and Perception*, 3rd edn., ed. Yantis S, pp. 235–286. New York: Wiley. — Center for Mind and Brain. Available at: http://mindbrain.ucdavis.edu/people/sjluck/pdfs/Luck 2002 Stevens Handbook.pdf/view [Accessed July 23, 2015].

Lund RD & Lund JS (1972). Development of synaptic patterns in the superior colliculus of the rat. *Brain Res* **42,** 1–20.

Ma WJ & Pouget A (2008). Linking neurons to behavior in multisensory perception: a computational review. *Brain Res* **1242,** 4–12.

Mackay-Sim a, Sefton AJ & Martin PR (1983). Subcortical projections to lateral geniculate and thalamic reticular nuclei in the hooded rat. *J Comp Neurol* **213,** 24–35.

MacKinnon LM, Troje NF & Dringenberg HC (2010). Do rats (Rattus norvegicus) perceive biological motion? *Exp Brain Res* **205,** 571–576.

Malpeli JG & Schiller PH (1978). Lack of blue OFF-center cells in the visual system of the monkey. *Brain Res* **141,** 385–389.

Marote CFO & Xavier GF (2011). Endogenous-like orienting of visual attention in rats. *Anim Cogn* **14,** 535–544.

Massaro DW (2004). From Multisensory Integration to Talking Heads and Language Learning. In *The Handbook of Multisensory Processes*, pp. 153–176. MIT Press. Available at: http://citeseerx.ist.psu.edu/viewdoc/summary?doi=10.1.1.4.4668 [Accessed July 8, 2015].

Mathis C, Savier E, Bott J-B, Clesse D, Bevins N, Sage-Ciocca D, Geiger K, Gillet A, Laux-Biehlmann A, Goumon Y, Lacaud A, Lelièvre V, Kelche C, Cassel J-C, Pfrieger FW & Reber M (2015). Defective response inhibition and collicular noradrenaline enrichment in mice with duplicated retinotopic map in the superior colliculus. *Brain Struct Funct* **220,** 1573–1584.

May PJ (2006). The mammalian superior colliculus: laminar structure and connections. *Prog Brain Res* **151,** 321–378.

McAdams CJ & Maunsell JHR (1999). Effects of attention on orientation tuning functions of single neurons in macaque cortical area V4. *J Neurosci* **19,** 431–441.

McAlonan K, Cavanaugh J & Wurtz RH (2008). Guarding the gateway to cortex with attention in visual thalamus. *Nature* **456,** 391–394.

McHaffie JG, Kao CQ & Stein BE (1989). Nociceptive neurons in rat superior colliculus: response properties, topography, and functional implications. *J Neurophysiol* **62,** 510–525.

McHaffie JG, Kruger L, Clemo HR & Stein BE (1988). Corticothalamic and corticotectal somatosensory projections from the anterior ectosylvian sulcus (SIV cortex) in neonatal cats: an anatomical demonstration with HRP and 3H-leucine. *J Comp Neurol* **274,** 115–126.

McHaffie JG & Stein BE (1982). Eye movements evoked by electrical stimulation in the superior colliculus of rats and hamsters. *Brain Res* **247,** 243–253.

McPeek RM & Keller EL (2002). Saccade Target Selection in the Superior Colliculus During a Visual Search Task. *J Neurophysiol* **88,** 2019–2034.

Meier P, Flister E & Reinagel P (2011). Collinear features impair visual detection by rats. *J Vis* **11,** 1–16.

Meier P & Reinagel P (2011). Rat performance on visual detection task modeled with divisive normalization and adaptive decision thresholds. *J Vis* **11,** 1–17.

Meredith M a & Stein BE (1986). Visual, auditory, and somatosensory convergence on cells in superior colliculus results in multisensory integration. *J Neurophysiol* **56,** 640–662.

Meredith MA (2002). On the neuronal basis for multisensory convergence: a brief overview. *Cogn Brain Res* **14,** 31–40.

Meredith MA, Keniston LR, Dehner LR & Clemo HR (2006). Crossmodal projections from somatosensory area SIV to the auditory field of the anterior ectosylvian sulcus (FAES) in Cat: further evidence for subthreshold forms of multisensory processing. *Exp brain Res* **172,** 472–484.

Meredith MA, Nemitz JW & Stein BE (1987). Determinants of multisensory integration in superior colliculus neurons. I. Temporal factors. *J Neurosci* **7,** 3215–3229.

Meredith MA & Stein BE (1990). The visuotopic component of the multisensory map in the deep laminae of the cat superior colliculus. *J Neurosci* **10,** 3727–3742.

Meredith MA & Stein BE (1996). Spatial determinants of multisensory integration in cat superior colliculus neurons. *J Neurophysiol* **75,** 1843–1857.

Mesulam M-M (2010). Attentional and confusional States. *Continuum (Minneap Minn)* **16,** 128–139.

Middlebrooks JC & Knudsen EI (1984). A neural code for auditory space in the cat's superior colliculus. *J Neurosci* **4,** 2621–2634.

Milliken B, Lupiáñez J, Roberts M & Stevanovski B (2003). Orienting in space and time: Joint contributions to exogenous spatial cuing effects. *Psychon Bull Rev* **10,** 877–883.

Milstein JA, Lehmann O, Theobald DEH, Dalley JW & Robbins TW (2007). Selective depletion of cortical noradrenaline by anti-dopamine beta-hydroxylase-saporin impairs attentional function and enhances the effects of guanfacine in the rat. *Psychopharmacology (Berl)* **190,** 51–63.

Mirabella G, Bertini G, Samengo I, Kilavik BE, Frilli D, Della Libera C & Chelazzi L (2007). Neurons in area V4 of the macaque translate attended visual features into behaviorally relevant categories. *Neuron* **54,** 303–318.

Mitchell JF, Sundberg K a & Reynolds JH (2009). Spatial attention decorrelates intrinsic activity fluctuations in macaque area V4. *Neuron* **63,** 879–888.

Mittleman G, Whishaw IQ & Robbins TW (1988). Cortical lateralization of function in rats in a visual reaction time task. *Behav Brain Res* **31,** 29–36.

Mize RR (1992). The organization of GABAergic neurons in the mammalian superior colliculus. *Prog Brain Res* **90,** 219–248. Available at: http://www.scopus.com/inward/record.url?eid=2-s2.0-0026572642&partnerID=tZOtx3y1.

Moran J & Desimone R (1985). Selective attention gates visual processing in the extrastriate cortex. *Science (80-)* **229,** 782–784.

Morgan RE, Garavan H, Smith EG, Driscoll LL, Levitsky DA & Strupp BJ (2001). Early lead exposure produces lasting changes in sustained attention, response initiation, and reactivity to errors. *Neurotoxicol Teratol* **23,** 519–531.

Mufson EJ, Martin TL, Mash DC, Wainer BH & Mesulam M-M (1986). Cholinergic projections from the parabigeminal nucleus (Ch8) to the superior colliculus in the mouse: a combined analysis of horseradish peroxidase transport and choline acetyltransferase immunohistochemistry. *Brain Res* **370,** 144–148.

Muir JL, Everitt BJ & Robbins TW (1996). The Cerebral Cortex of the Rat and Visual Attentional Function: Dissociable Effects of Mediofrontal, Cingulate, Anterior Dorsolateral, and Parietal Cortex Lesions on a Five-Choice Serial Reaction Time Task. *Cereb Cortex* **6,** 470–481.

Müller HJ & Rabbitt PM (1989). Reflexive and voluntary orienting of visual attention: Time course of activation and resistance to interruption.

Mysore SP, Asadollahi A & Knudsen EI (2010). Global inhibition and stimulus competition in the owl optic tectum. *J Neurosci* **30,** 1727–1738.

Mysore SP, Asadollahi A & Knudsen EI (2011). Signaling of the strongest stimulus in the owl optic tectum. *J Neurosci* **31,** 5186–5196.

Nagy A, Kruse W, Rottmann S, Dannenberg S & Hoffmann K-P (2006). Somatosensory-motor neuronal activity in the superior colliculus of the primate. *Neuron* **52,** 525–534.

Naka K-I & Rushton WH (1966). S-potentials from colour units in the retina of fish (Cyprinidae). *J Physiol* **185,** 536–555.

Nandy A, Sharpee T, Reynolds J & Mitchell J (2013). The Fine Structure of Shape Tuning in Area V4. *Neuron* **78,** 1102–1115.

Neisser U (1967). *Cognitive psychology*. Appleton-Century-Crofts, New York.

Netser S, Ohayon S & Gutfreund Y (2010). Multiple manifestations of microstimulation in the optic tectum: eye movements, pupil dilations, and sensory priming. *J Neurophysiol* **104,** 108–118.

Newsome WT, Britten KH & Movshon JA (1989). Neuronal correlates of a perceptual decision. *Nature* **341,** 52–54.

Ngan NH, Matsumoto J, Takamura Y, Tran AH, Ono T & Nishijo H (2015). Neuronal correlates of attention and its disengagement in the superior colliculus of rat. *Front Integr Neurosci* **9,** 9.

Niebergall R, Khayat PS, Treue S & Martinez-Trujillo JC (2011). Expansion of MT neurons excitatory receptive fields during covert attentive tracking. *J Neurosci* **31,** 15499–15510.

Nienborg H & Cumming B (2010). Correlations between the activity of sensory neurons and behavior: How much do they tell us about a neuron's causality? *Curr Opin Neurobiol* **20,** 376–381.

Noudoost B, Chang MH, Steinmetz N a & Moore T (2010). Top-down control of visual attention. *Curr Opin Neurobiol* **20,** 183–190.

Nummela SU & Krauzlis RJ (2010). Inactivation of primate superior colliculus biases target choice for smooth pursuit, saccades, and button press responses. *J Neurophysiol* **104,** 1538–1548.

O'Connor DH, Clack NG, Huber D, Komiyama T, Myers EW & Svoboda K (2010). Vibrissa-based object localization in head-fixed mice. *J Neurosci* **30,** 1947–1967.

O'Connor DH, Fukui MM, Pinsk MA & Kastner S (2002). Attention modulates responses in the human lateral geniculate nucleus. *Nat Neurosci* **5,** 1203–1209.

Ohki K, Chung S, Ch'ng YH, Kara P & Reid RC (2005). Functional imaging with cellular resolution reveals precise micro-architecture in visual cortex. *Nature* **433,** 597–603.

Ohshiro T, Angelaki DE & DeAngelis GC (2011). A normalization model of multisensory integration. *Nat Neurosci* **14,** 775–782.

Ozen G, Augustine GJ & Hall WC (2000). Contribution of Superficial Layer Neurons to Premotor Bursts in the Superior Colliculus. *J Neurophysiol* **84,** 460–471.

Palmer LA & Rosenquist AC (1974). Visual receptive fields of single striate cortical units projecting to the superior colliculus in the cat. *Brain Res* **67,** 27–42.

Pariyadath V & Eagleman D (2007). The effect of predictability on subjective duration. *PLoS One* **2,** e1264.

Paxinos G & Watson C (1986). The rat brain in stereotaxic coordinates. Available at: https://scholar.google.com/scholar?q=the+rat+brain+in+stereotaxic+coordinates+paxinos++watson+1986&btnG=&hl=en&as_sdt=0%2C5#2 [Accessed June 16, 2015].

Perrault TJ, Vaughan JW, Stein BE & Wallace MT (2003). Neuron-specific response characteristics predict the magnitude of multisensory integration. *J Neurophysiol* **90,** 4022–4026.

Perrault TJ, Vaughan JW, Stein BE & Wallace MT (2005). Superior colliculus neurons use distinct operational modes in the integration of multisensory stimuli. *J Neurophysiol* **93,** 2575–2586.

Petersen SE & Posner MI (2012). The attention system of the human brain: 20 years after. *Annu Rev Neurosci* **35,** 73–89.

Phillips JM, McAlonan K, Robb WGK & Brown VJ (2000). Cholinergic neurotransmission influences covert orientation of visuospatial attention in the rat. *Psychopharmacology (Berl)* **150,** 112–116.

Pinto-Hamuy T, Montero VM & Torrealba F (2004). Neurotoxic lesion of anteromedial/posterior parietal cortex disrupts spatial maze memory in blind rats. *Behav Brain Res* **153,** 465–470.

Populin LC & Yin TCT (2002). Bimodal interactions in the superior colliculus of the behaving cat. *J Neurosci* **22,** 2826–2834.

Posner MI (1980). Orienting of attention. *Q J Exp Psychol* **32,** 3–25.

Posner MI (1988). Asymmetries in Hemispheric Control of Attention in Schizophrenia. *Arch Gen Psychiatry* **45,** 814.

Posner MI (2012). *Cognitive Neuroscience of Attention*. Guilford Press. Available at: https://books.google.com.au/books/about/Cognitive_Neuroscience_of_Attention.html?id=8yjEjoS7EQsC&pgis=1 [Accessed June 8, 2015].

Posner MI & Cohen Y (1984). Components of visual orienting. Attention and Performance X: Control of Language Processes. In, ed. Bouma H & Bonwhuis. D, pp. 551–556. Hillsdale, N. J., Erlbaum. Available at: http://www.psych.utoronto.ca/users/ferber/teaching/visualattention/readings/Sept22/1984_Posner_Cohen_Attention&PerformanceX.pdf [Accessed July 23, 2015].

Pratt J, Hillis J & Gold JM (2001). The effect of the physical characteristics of cues and targets on facilitation and inhibition. *Psychon Bull Rev* **8,** 489–495.

Prinzmetal W, McCool C & Park S (2005). Attention: Reaction Time and Accuracy Reveal Different Mechanisms. *J Exp Psychol Gen* **134,** 73–92.

Prusky GT & Douglas RM (2004). Characterisation of mouse cortical spatial vision. *Vision Res* **44,** 3411–3418.

Prusky GT, West PW. & Douglas RM (2000). Behavioral assessment of visual acuity in mice and rats. *Vision Res* **40,** 2201–2209.

Rafal RD, Posner MI, Friedman JH, Inhoff AW & Berstein E (1988). ORIENTING OF VISUAL ATTENTION IN PROGRESSIVE SUPRANUCLEAR PALSY. *Brain* **111,** 267–280.

Raposo D, Sheppard JP, Schrater PR & Churchland AK (2012). Multisensory decision-making in rats and humans. *J Neurosci* **32,** 3726–3735.

Read JC a & Cumming BG (2003). Measuring V1 receptive fields despite eye movements in awake monkeys. *J Neurophysiol* **90,** 946–960.

Redgrave P, Simkins M, McHaffie JG & Stein BE (1996). Nociceptive neurones in rat superior colliculus. *Exp Brain Res* **109,** 197–208.

Reep RL, Corwin J V, Hashimoto a & Watson RT (1987). Efferent connections of the rostral portion of medial agranular cortex in rats. *Brain Res Bull* **19,** 203–221.

Reinagel P (2014). Using rats for vision research. *Neuroscience*; DOI: 10.1016/j.neuroscience.2014.12.025.

Reynolds JH & Chelazzi L (2004). Attentional modulation of visual processing. *Annu Rev Neurosci* **27,** 611–647.

Reynolds JH, Chelazzi L & Desimone R (1999). Competitive mechanisms subserve attention in macaque areas V2 and V4. *J Neurosci* **19,** 1730–1753.

Reynolds JH, Pasternak T & Desimone R (2000). Attention Increases Sensitivity of V4 Neurons. *Neuron* **26,** 703–714.

Ristic J & Kingstone A (2009). Rethinking attentional development: reflexive and volitional orienting in children and adults. *Dev Sci* **12,** 289–296.

Robbins TW & Arnsten AFT (2009). The neuropsychopharmacology of fronto-executive function: monoaminergic modulation. *Annu Rev Neurosci* **32,** 267–287.

Robinson DL & Petersen SE (1992). The pulvinar and visual salience. *Trends Neurosci* **15,** 127–132.

Rodgers CC & DeWeese MR (2014). Neural correlates of task switching in prefrontal cortex and primary auditory cortex in a novel stimulus selection task for rodents. *Neuron* **82,** 1157–1170.

Rodriguez M, Gomez C, Alonso J & Afonso D (1992). Laterality, alternation, and perseveration relationships on the T-maze test. *Behav Neurosci* **106,** 974–980.

Rosselli FB, Alemi A, Ansuini A & Zoccolan D (2015). Object similarity affects the perceptual strategy underlying invariant visual object recognition in rats. *Front Neural Circuits* **9,** 10.

Rowland BA, Quessy S, Stanford TR & Stein BE (2007*a*). Multisensory integration shortens physiological response latencies. *J Neurosci* **27,** 5879–5884.

Rowland BA, Stanford TR & Stein BE (2007*b*). A model of the neural mechanisms underlying multisensory integration in the superior colliculus. *Perception* **36,** 1431–1443.

Rowland BA & Stein BE (2008). Temporal profiles of response enhancement in multisensory integration. *Front Neurosci* **2,** 218.

Runyan C a, Schummers J, Van Wart A, Kuhlman SJ, Wilson NR, Huang ZJ & Sur M (2010). Response features of parvalbumin-expressing interneurons suggest precise roles for subtypes of inhibition in visual cortex. *Neuron* **67,** 847–857.

Sahibzada N, Dean P & Redgrave P (1986). Movements resembling orientation or avoidance elicited by electrical stimulation of the superior colliculus in rats. *J Neurosci* **6,** 723–733.

Samuel AG & Kat D (2003). Inhibition of return: a graphical meta-analysis of its time course and an empirical test of its temporal and spatial properties. *Psychon Bull Rev* **10,** 897–906.

Santangelo V, Olivetti Belardinelli M, Spence C & Macaluso E (2009). Interactions between voluntary and stimulus-driven spatial attention mechanisms across sensory modalities. *J Cogn Neurosci* **21,** 2384–2397.

Sathian K (2005). Visual cortical activity during tactile perception in the sighted and the visually deprived. *Dev Psychobiol* **46,** 279–286.

Sato TR & Schall JD (2003). Effects of Stimulus-Response Compatibility on Neural Selection in Frontal Eye Field. *Neuron* **38,** 637–648.

Sawinski J, Wallace DJ, Greenberg DS, Grossmann S, Denk W & Kerr JND (2009). Visually evoked activity in cortical cells imaged in freely moving animals. *Proc Natl Acad Sci U S A* **106,** 19557–19562.

Schiller PH (2011). The Superior Colliculus and Visual Function. In *Comprehensive Physiology*, ed. Terjung R. John Wiley & Sons, Inc., Hoboken, NJ, USA.

Schindel R, Rowlands J & Arnold DH (2011). The oddball effect: perceived duration and predictive coding. *J Vis* **11,** 17.

Schmidt M, Boller M, Özen G & Hall WC (2001). Disinhibition in rat superior colliculus mediated by GABAc receptors. *J Neurosci* **21,** 691–699.

Schroeder CE & Foxe J (2005). Multisensory contributions to low-level, "unisensory" processing. *Curr Opin Neurobiol* **15,** 454–458.

Schwarz C, Hentschke H, Butovas S, Haiss F, Stüttgen MC, Gerdjikov T V, Bergner CG & Waiblinger C (2010). The head-fixed behaving rat--procedures and pitfalls. *Somatosens Mot Res* **27,** 131–148.

Sefton AJ, Dreher B & Harvey A (2004). Visual System. In *The Rat Nervous System*, Third Edit., ed. Paxinos G, pp. 1083–1165. Elsevier.

Sefton AJ, Dreher B, Harvey AR & Martin PR (2015). Visual System. In *The Rat Nervous System*, Fourth Edi., pp. 945–981. Elsevier. Available at: http://dx.doi.org/10.1016/B978-0-12-374245-2.00030-9 [Accessed November 28, 2014].

Segal RL & Beckstead RM (1984). The lateral suprasylvian corticotectal projection in cats. *J Comp Neurol* **225,** 259–275.

Seymoure P & Juraska JM (1997). Vernier and grating acuity in adult hooded rats: The influence of sex. *Behav Neurosci*.

Shams L, Kamitani Y & Shimojo S (2000). Illusions. What you see is what you hear. *Nature* **408,** 788.

Sheppard JP, Raposo D & Churchland AK (2013). Dynamic weighting of multisensory stimuli shapes decision-making in rats and humans. *J Vis* **13,** 4.

Shipp S (2004). The brain circuitry of attention. *Trends Cogn Sci* **8,** 223–230.

Skaliora I, Doubell TP, Holmes NP, Nodal FR & King AJ (2004). Functional topography of converging visual and auditory inputs to neurons in the rat superior colliculus. *J Neurophysiol* **92,** 2933–2946.

Smear M, Shusterman R, O'Connor R, Bozza T & Rinberg D (2011). Perception of sniff phase in mouse olfaction. *Nature* **479,** 397–400.

Snipes M & Taylor DC (2014). Model selection and Akaike Information Criteria: An example from wine ratings and prices. *Wine Econ Policy* **3,** 3–9.

Sohya K, Kameyama K, Yanagawa Y, Obata K & Tsumoto T (2007). GABAergic neurons are

less selective to stimulus orientation than excitatory neurons in layer II/III of visual cortex, as revealed by in vivo functional Ca2+ imaging in transgenic mice. *J Neurosci* **27,** 2145–2149.

Sooksawate T & Isa T (2006). Properties of cholinergic responses in neurons in the intermediate grey layer of rat superior colliculus. *Eur J Neurosci* **24,** 3096–3108.

Sparks DL (1986). Translation of sensory signals into commands for control of saccadic eye movements: role of primate superior colliculus. *Physiol Rev* **66,** 118–171.

Sparks DL (1999). Conceptual issues related to the role of the superior colliculus in the control of gaze. *Curr Opin Neurobiol* **9,** 698–707.

Sparks DL & Hartwich-Young R (1989). The deep layers of the superior colliculus. *Rev Oculomot Res* **3,** 213–255.

Spence C, Nicholls MER & Driver J (2001). The cost of expecting events in the wrong sensory modality. *Percept Psychophys* **63,** 330–336.

Spence C & Parise C (2010). Prior-entry: a review. *Conscious Cogn* **19,** 364–379.

Sriram B & Reinagel P (2012). Strong surround antagonism in the dLGN of the awake rat. *Arxiv Prepr arXiv12043683*.

Stanford TR, Quessy S & Stein BE (2005). Evaluating the operations underlying multisensory integration in the cat superior colliculus. *J Neurosci* **25,** 6499–6508.

Stanford TR & Stein BE (2007). Superadditivity in multisensory integration: putting the computation in context. *Neuroreport* **18,** 787–792.

Stechison MT, Saint-Cyr JA & Spence SJ (1985). Projections from the nuclei prepositus hypoglossi and intercalatus to the superior colliculus in the cat: an anatomical study using WGA-HRP. *Exp Brain Res*; DOI: 10.1007/BF00237674.

Stein B, Magalhaes-Castro B & Kruger L (1975). Superior colliculus: visuotopic-somatotopic overlap. *Science (80-)* **189,** 224–226.

Stein BE (1981). Organization of the rodent superior colliculus: Some comparisons with other mammals. *Behav Brain Res* **3,** 175–188.

Stein BE (1984). Development of the Superior Colliculus. *Annu Rev Neurosci* **7,** 95–125.

Stein BE & Arigbede MO (1972). Unimodal and multimodal response properties of neurons in the cat's superior colliculus. *Exp Neurol* **36,** 179–196.

Stein BE & Dixon JP (1979). Properties of superior colliculus neurons in the golden hamster. *J Comp Neurol* **183,** 269–284.

Stein BE & Gallagher HL (1981). Maturation of cortical control over superior colliculus cells in cat. *Brain Res* **223,** 429–435.

Stein BE, Magalhaes-Castro B & Kruger L (1976). Relationship between visual and tactile representations in cat superior colliculus. *J Neurophysiol* **39,** 401–419.

Stein BE & Meredith MA (1993). *The merging of the senses. Cognitive neuroscience.* A Bradford Book.

Stein BE & Stanford TR (2008). Multisensory integration: current issues from the perspective of the single neuron. *Nat Rev Neurosci* **9,** 255–266.

Stein BE, Stanford TR, Ramachandran R, Perrault TJ & Rowland BA (2009*a*). Challenges in quantifying multisensory integration: alternative criteria, models, and inverse effectiveness. *Exp Brain Res* **198,** 113–126.

Stein BE, Stanford TR & Rowland BA (2009*b*). The neural basis of multisensory integration in the midbrain: its organization and maturation. *Hear Res* **258,** 4–15.

Stein BE, Stanford TR & Rowland BA (2014). Development of multisensory integration from the perspective of the individual neuron. *Nat Rev Neurosci* **15,** 520–535.

Sterling P & Wickelgren BG (1969). Visual receptive fields in the superior colliculus of the cat. *J Neurophysiol* **32,** 1–15.

Stubblefield EA, Costabile JD & Felsen G (2013). Optogenetic investigation of the role of the superior colliculus in orienting movements. *Behav Brain Res* **255,** 55–63.

Stuesse SL & Newman D. (1990). Projections from the medial agranular cortex to brain stem visuomotor centers in rats. *Exp Brain Res* **80,** 532–544.

Sugihara T, Diltz MD, Averbeck BB & Romanski LM (2006). Integration of auditory and visual communication information in the primate ventrolateral prefrontal cortex. *J Neurosci* **26,** 11138–11147.

Summerfield C, Trittschuh EH, Monti JM, Mesulam MM & Egner T (2008). Neural repetition suppression reflects fulfilled perceptual expectations. *Nat Neurosci* **11,** 1004–1006.

Tafazoli S, Di Filippo A & Zoccolan D (2012). Transformation-tolerant object recognition in rats revealed by visual priming. *J Neurosci* **32,** 21–34.

Takemoto I, Sasa M & Takaori S (1978). Role of the locus coeruleus in transmission onto anterior colliculus neurons. *Brain Res* **158,** 269–278.

Talsma D & Woldorff MG (2005). Selective attention and multisensory integration: multiple phases of effects on the evoked brain activity. *J Cogn Neurosci* **17,** 1098–1114.

Tan MML & Harvey AR (1989). The cholinergic innervation of normal and transplanted superior colliculus in the rat: An immunohistochemical study. *Neuroscience* **32,** 511–520.

Tanner WP & Swets J a (1954). A decision-making theory of visual detection. *Psychol Rev* **61,** 401–409.

Tees RC (1999). The effects of posterior parietal and posterior temporal cortical lesions on multimodal spatial and nonspatial competencies in rats. *Behav Brain Res* **106,** 55–73.

Terjung R ed. (2011). *Comprehensive Physiology*. John Wiley & Sons, Inc., Hoboken, NJ, USA.

Thompson KG, Biscoe KL & Sato TR (2005). Neuronal basis of covert spatial attention in the frontal eye field. *J Neurosci* **25,** 9479–9487.

Toldi J, Fehér O & Wolff JR (1986). Sensory interactive zones in the rat cerebral cortex. *Neuroscience* **18,** 461–465.

Treisman AM (1960). Contextual cues in selective listening. *Q J Exp Psychol* **12,** 242–248.

Treue S & Trujillo JCM (1999). Feature-based attention influences motion processing gain in macaque visual cortex. *Nature* **399,** 575–579.

Tse PU, Intriligator J, Rivest J & Cavanagh P (2004). Attention and the subjective expansion of time. *Percept Psychophys* **66,** 1171–1189.

Vachon-Presseau E, Martin A, Lepore F & Guillemot J-P (2009). Development of the representation of auditory space in the superior colliculus of the rat. *Eur J Neurosci* **29,** 652–660.

Vermaercke B & Op de Beeck HP (2012). A multivariate approach reveals the behavioral templates underlying visual discrimination in rats. *Curr Biol* **22,** 50–55.

Vidyasagar TR (1978). Possible plasticity in the rat superior colliculus. *Nature* **275,** 140–141.

Wagner U, Baker L & Rostron C (2014). Searching for inhibition of return in the rat using the covert orienting of attention task. *Anim Cogn* **17,** 1121–1135.

Wallace DJ, Greenberg DS, Sawinski J, Rulla S, Notaro G & Kerr JND (2013). Rats maintain an overhead binocular field at the expense of constant fusion. *Nature* **498,** 65–69.

Wallace MT, Meredith MA & Stein BE (1992). Integration of multiple sensory modalities in cat cortex. *Exp brain Res* **91,** 484–488.

Wallace MT, Meredith MA & Stein BE (1993). Converging influences from visual, auditory, and somatosensory cortices onto output neurons of the superior colliculus. *J Neurophysiol* **69,** 1797–1809.

Wallace MT, Ramachandran R & Stein BE (2004). A revised view of sensory cortical parcellation. *Proc Natl Acad Sci U S A* **101,** 2167–2172.

Wang Q & Burkhalter A (2013). Stream-related preferences of inputs to the superior colliculus from areas of dorsal and ventral streams of mouse visual cortex. *J Neurosci* **33,** 1696–1705.

Ward NM & Brown VJ (1996). Covert orienting of attention in the rat and the role of striatal dopamine. *J Neurosci* **16,** 3082–3088.

Watson GDR, Smith JB & Alloway KD (2015). The Zona Incerta Regulates Communication between the Superior Colliculus and the Posteromedial Thalamus: Implications for Thalamic Interactions with the Dorsolateral Striatum. *J Neurosci* **35,** 9463–9476.

Weese GD, Phillips JM & Brown VJ (1999). Attentional Orienting Is Impaired by Unilateral Lesions of the Thalamic Reticular Nucleus in the Rat. *J Neurosci* **19,** 10135–10139.

Wei P, Liu N, Zhang Z, Liu X, Tang Y, He X, Wu B, Zhou Z, Liu Y, Li J, Zhang Y, Zhou X, Xu L, Chen L, Bi G, Hu X, Xu F & Wang L (2015). Processing of visually evoked innate fear by a non-canonical thalamic pathway. *Nat Commun* **6,** 6756.

Weldon DA, DiNieri JA, Silver MR, Thomas AA & Wright RE (2007). Reward-related neuronal activity in the rat superior colliculus. *Behav Brain Res* **177,** 160–164.

Weliky M, Fiser J, Hunt RH & Wagner DN (2003). Coding of natural scenes in primary visual cortex. *Neuron* **37,** 703–718.

Werner-Reiss U, Kelly KA, Trause AS, Underhill AM & Groh JM (2003). Eye Position Affects Activity in Primary Auditory Cortex of Primates. *Curr Biol* **13,** 554–562.

Westby GWM, Keay KA, Redgrave P, Dean P & Bannister M (1990). Output pathways from the rat superior colliculus mediating approach and avoidance have different sensory properties. *Exp Brain Res* **81,** 626–638.

White BJ & Munoz DP (2011). The superior colliculus. Available at: http://www.oxfordhandbooks.com/view/10.1093/oxfordhb/9780199539789.001.0001/oxfordhb-9780199539789-e-011 [Accessed July 9, 2015].

Wiesenfeld Z & Branchek T (1976). Refractive state and visual acuity in the hooded rat. *Vision Res* **16,** 823–827.

Wilkinson LK, Meredith MA & Stein BE (1996). The role of anterior ectosylvian cortex in cross-modality orientation and approach behavior. *Exp brain Res* **112,** 1–10.

Williams PE & Shapley RM (2007). A dynamic nonlinearity and spatial phase specificity in macaque V1 neurons. *J Neurosci* **27,** 5706–5718.

Winters BD & Reid JM (2010). A distributed cortical representation underlies crossmodal object recognition in rats. *J Neurosci* **30,** 6253–6261.

Womelsdorf T, Anton-Erxleben K & Treue S (2008). Receptive field shift and shrinkage in macaque middle temporal area through attentional gain modulation. *J Neurosci* **28,** 8934–8944.

Worden MS, Foxe JJ, Wang N & Simpson G V. (2000). Anticipatory biasing of visuospatial attention indexed by retinotopically specific alpha-band electroencephalography increases over occipital cortex. *J Neurosci*. Available at: http://www.scopus.com/inward/record.url?eid=2-s2.0-4243692384&partnerID=tZOtx3y1.

Wurtz RH & Goldberg ME (1971). Superior colliculus cell responses related to eye movements in awake monkeys. *Science (80-)* **171,** 82–84.

Yamasaki DS, Krauthamer G & Rhoades RW (1984). Organization of the intercollicular pathway in rat. *Brain Res* **300,** 368–371.

Zénon A & Krauzlis RJ (2012). Attention deficits without cortical neuronal deficits. *Nature* **489,** 434–437.

Zhang S, Xu M, Kamigaki T, Phong Hoang Do J, Chang W-C, Jenvay S, Miyamichi K, Luo L & Dan Y (2014). Long-range and local circuits for top-down modulation of visual cortex processing. *Science (80-)* **345,** 660–665.

Zoccolan D, Graham BJ & Cox DD (2010). A self-calibrating, camera-based eye tracker for the recording of rodent eye movements. *Front Neurosci* **4,** 193.

Zoccolan D, Oertelt N, DiCarlo JJ & Cox DD (2009). A rodent model for the study of invariant visual object recognition. *Proc Natl Acad Sci U S A* **106,** 8748–8753.